LOW MOLECULAR WEIGHT PFAS ALTERNATIVES (C-6) RESULT IN FEWER

CELLULAR AND BEHAVIORAL ALTERATIONS THAN LONG CHAIN (C-8/C-9) PFASS

IN LARVAL ZEBRAFISH

by

KATE M. ANNUNZIATO

A dissertation submitted to the

School of Graduate Studies

Rutgers, The State University of New Jersey

In partial fulfillment of the requirements

For the degree of

Doctor of Philosophy

Graduate Program in Toxicology

Written under the direction of

Keith Cooper

And approved by

_____

_____

_____

_____

_____

New Brunswick, New Jersey

October 2018

ABSTRACT OF THE DISSERTATION

LOW MOLECULAR WEIGHT PFAS ALTERNATIVES (C-6) RESULT IN FEWER CELLULAR
AND BEHAVIORAL ALTERATIONS THAN LONG CHAIN (C-8/C-9) PFASS IN LARVAL
ZEBRAFISH

By: KATE ANNUNZIATO

Dissertation Director:

Keith Cooper, PhD

Perfluoroalkylated substances (PFASs) are a class of compounds with widespread occurrence in the environment, and long chain PFASs (C-8/C-9) are reported to cause developmental toxicities and alterations in lipid homeostasis. This has led companies that once relied on long chain PFASs to switch to alternatives, such as the (C-6) low molecular weight alternatives, PFHxA, PFHxS, and 6:2 FTOH. However, fewer toxicity assessments have been completed on these compounds. This dissertation addresses this data gap through developmental toxicity assessment in early (5 days post fertilization, dpf) and later (14 dpf) life stage larval zebrafish. Endpoints examined include effects at the cellular and whole organism level to assess different levels of biological organization, and develop specific adverse outcome pathways (AOPs) for each compound. Previous research from our lab examined these endpoints following exposures to long chain PFASs. This allowed for comparison of AOPs of long chain PFASs and the low molecular weight alternatives. In 5 dpf larvae, exposures to 0.2-20 µM resulted in few morphometric effects; however, gene expression endpoints were the most sensitive to exposures.

In 14 dpf larvae, behavioral effects were observed with exposure to 6:2 FTOH and PFHxS, but not PFHxA, suggesting that nervous tissue development AOPs may not apply to this PFAS. Similarly, lipid distribution in 14 dpf larvae was altered only with PFHxS and 6:2 FTOH exposures. The involvement of PFASs in the manifestation of dysregulation of lipid homeostasis was examined in larval zebrafish using the long chain PFASs as a proof of concept. These studies were completed using BODIPY-FL fatty acids which allowed for visualization of the packaging and uptake of yolk sac lipids, and expression analysis of genes related to lipid distribution. Alterations in the packaging and uptake of yolk sac lipids were observed with the long chain PFASs, and these compounds were each associated with a different gene expression profile. These same genes were examined with the low molecular weight PFAS alternatives, and while again, each PFAS resulted in a unique gene expression profile, some of the same pathways impacted by long chain PFAS exposures appeared to be affected by the low molecular weight alternatives. Overall, the low molecular weight alternatives, PFHxA, PFHxS, and 6:2 FTOH were found to be less toxic than long chain PFASs in zebrafish, and while different toxicity profiles exist, there is some overlap in growth, neural development, and lipid homeostasis AOPs impacted with PFAS exposures.

ACKNOWLEDGEMENTS

There are many people to thank for making this thesis possible. First and foremost is Dr. Cooper. His guidance and support were critical throughout my graduate school education. Whenever I started to veer off course, conversations with him were able to set me straight again. I am truly grateful for all that he has taught me.

I would also like to thank Dr. White. Her expertise in molecular techniques aided greatly to this project, and more than that her moral support was critical. Conversations with her brightened up the days, and with Dr. White as a driving force for events, like the mud runs and cookie decorating, she made sure we had fun in Lipman.

To my committee, Drs. Aleksunes, Cohick, and Roepke, thank you for your guidance and input, which has helped to make this project a success.

I would like to thank the JGPT and RATS for all their support. I am grateful to have been among an amazing group of young scientists in the program.

I must acknowledge everyone in Lipman Hall. I truly could not imagine working in a friendlier environment. There are many people to thank for making the teaching experience at Rutgers so enjoyable, and I have learned so much from each of them: Dr. Voloshchuk provided so much support for her TA's. Dr. Kahn's kindness and support of all of the students he encountered is something I will miss (Although, I will not be too far away to come to the occasional lunch). Dr. Murphy, thank you for all your guidance and support. Finally, Dr. Crane, your dedication to the lab is so inspiring, and your support while teaching has meant so much.

I would also like to thank the rest of the faculty and staff for all their help. I also have to thank the rest of the Lipman Hall graduate students, for being wonderful coworkers, fellow gym enthusiasts, and happy hour buddies.

I could not have made it through this without the support of my fellow graduate students. To Tiffany Kung, Carrie Jantzen, and Dan Millemann, thank you for showing me the ropes when I first started graduate school. Between the gym and beer sessions, thank you all for making this

TABLE OF CONTENTS

Chapter 4: Exposure to PFASs Impacts Lipid Mobilization and Distribution in Larval Zebrafish

Chapter 5: General Conclusions, Discussion, and Future Directions

LIST OF TABLES

LIST OF FIGURES

ABBREVIATIONS

actb	beta-actin (nomenclature, gene)
AOP	adverse outcome pathway
apo	apolipoprotein (nomenclature, gene)
ap1s1	adaptor related protein complex 1, σ1 (nomenclature, gene)
bdnf	brain-derived neurotrophic factor (nomenclature, gene)
dpf	days post fertilization
FTOH	fluorotelomer alcohol
hpf	hours post fertilization
kg	kilogram
LC_{50}	lethal concentration 50
lepa	leptin hormone (nomenclature, gene)
LOEL	lowest observed effect level
lpl	lipoprotein lipase (nomenclature, gene)
mg	milligram
MS222	tricaine methanesulfonate
mttp	microsomal triglyceride transfer protein (nomenclature, gene)
NOAEL	no observable adverse effect level
OATP	organic anion transporting polypeptides (nomenclature, human, protein)
oatp	organic anion transporting polypeptides (nomenclature, zebrafish, protein)
ORO	Oil Red O
PFAS	perfluoroalkylated substance
PFHxA	perfluorohexanoic acid
PFHxS	perfluorohexane sulfonate
PFNA	perfluorononanoic acid
PFOA	perfluorooctanoic acid
PFOS	perfluorooctane sulfonate
ppar	peroxisome proliferator-activated receptor (nomenclature, gene)

ppb	parts per billion
ppt	parts per trillion
qPCR	quantitative polymerase chain reaction
slco	organic anion transporting polypeptides (nomenclature, zebrafish, protein)
slc27a1	long chain fatty acid transport protein (nomenclature, gene)
tgfb1a	transforming growth factor β1a (nomenclature, gene)
YSL	yolk syncytial layer
µM	micromolar

CHAPTER 1

INTRODUCTION

1.1 General Introduction

My research described in this dissertation assessed the toxicity of low molecular weight perfluoroalkylated substance (PFAS) alternatives in the developing zebrafish and contributed to the determination of the mechanism by which PFASs and their alternatives disrupt lipid homeostasis. Low molecular weight alternatives selected for toxicity assessment were perfluorohexanoic aid (PFHxA), perfluorohexane sulfonate (PFHxS), and 6:2 fluorotelomer alcohol (6:2 FTOH). In Chapter 2, developmental exposures to PFHxA, PFHxS, and 6:2 FTOH examined effects on morphological and gene expression endpoints in 5 days post fertilization (dpf) sac fry larval zebrafish. Endpoints were selected to allow for direct comparison to toxicity profiles established for long chain PFASs: perfluorooctanoic acid (PFOA), perfluorooctane sulfonate (PFOS), and perfluorononanoic acid (PFNA). In Chapter 3, 14 dpf larvae were examined for morphological, behavioral, and lipid accumulation effects. Embryos were exposed to the same doses and time period as in Chapter 2 and received a 9 day depuration period. From these studies, behavioral and gene expression endpoints were identified to be the most sensitive to PFAS exposure. A novel endpoint, lipid stain accumulation was measured in larval fish with exposure to long chain PFASs and the low molecular weight alternatives. Chapter 4 examined alterations to lipid distribution during early develop with long chain PFAS exposures and identified potential molecular targets through gene expression analysis. These studies contributed to the toxicity profiles of these compounds in the zebrafish model. In Chapter 5, comparisons are made for the toxicity profiles for the 6 PFASs and alternatives discussed in this dissertation.

1.2 Introduction to Perfluoroalkylated Substances (PFASs)

1.2.1 Categorization and Industrial Uses of PFASs

The PFASs are a class of chemicals that are comprised of a fully-fluorinated chain of carbon atoms attached to a carboxylic acid or sulfonate group. Historically, these compounds were referred to as PFCs; however to eliminate the confusion with perfluorocarbons, the name perfluoroalkylated substances is preferred (Buck et al. 2011). The end group is one way in which these compounds can be classified, as either carboxylates or sulfonates. Another classification is through chain length. Long chain PFASs are comprised of carboxylates with greater than 7 carbon atoms in the fluorinated chain and sulfonates with greater than 6 carbon atoms (Buck et al. 2011). However, there is debate in the scientific community that the 6 carbon sulfonate has bioaccumulation potential more similar to the long chain PFASs and should be classified as such (Land et al. 2018).

PFASs have been historically used in a number of manufacturing processes. They have been used in fire-fighting foams, as well as in the production of stain and grease-resistant products, including cloths, carpets, papers, and Teflon coatings (Buck et al. 2011). Based on concerns of prevalence of long chain PFASs in human and wildlife samples and the toxicity associated with exposure, manufacturers have discontinued use of PFOS, PFOA, and other long chain PFASs (USEPA 2014). Alternatives have been used in their place in manufacturing processes, and indeed fluorotelomers, which served as precursors to long chain PFASs, have been used in both fire-fighting and stain-resistance applications (Gomis et al. 2015; Lehmler et al. 2007). Other alternatives, such as short chain PFASs, have been used as well (Wang et al. 2013b).

To follow the trends towards long chain PFAS alternatives, the scientific community has shifted focus to study the prevalence and toxicity of these alternate products. These compounds contain additional functional groups with the goal of aiding in breakdown of these products. For example, ether groups have been inserted into the carbon chain to provide a potential site of microbial degradation. This class is referred to as perfluoropolyethers (PFPEs) (Wang et al. 2013b). Other alternatives have non-fully fluorinated chains, with hydrogen atoms along the backbone, and these compounds are referred to as polyfluoroalkyl substances (Buck et al. 2011). Finally, fluorotelomer alcohols, which were used to produce PFASs, have also been introduced as

alternatives to long chain PFASs in manufacturing processes (Yuan et al. 2016). The fluorotelomer alcohols are similar to the PFASs in that they too contain a fluorinated backbone; however, the carboxylic acid or sulfonate terminal group is replaced with an alcohol group (Gomis et al. 2015). This means that there are hundreds of PFASs and alternatives to study (Xiao 2017).

Discussion in these studies will be limited to 5 PFASs and 1 fluorotelomer: perfluorooctanoic acid (PFOA), perfluorooctane sulfonate (PFOS), perfluorononanoic acid (PFNA), perfluorohexanoic acid (PFHxA), perfluorohexane sulfonate (PFHxS), and 6:2 fluorotelomer alcohol (6:2 FTOH). The structures of these compounds are depicted in Table 1.

1.2.2 Chemical Properties of PFASs

The chemical structure of the PFASs leads to unique properties that make them useful in various industrial processes. The hydrophobic fluorinated chain and hydrophilic terminal groups make these compounds useful surfactants (Lau 2012). These two groups in PFOS are in opposition, such that it is impossible to determine a water-octanol coefficient (K_{OW}) as it forms a distinct layer between the two phases (Lehmler et al. 2007). However, all PFASs are soluble in water due to the hydrophilic end group (Wang et al. 2015). Once in water, the end groups may exist in their protonated or deprotonated forms, which is determined by the pH of the environment and the pKa of the PFAS (Buck et al. 2011).

The solubility of the PFASs in water provides a potential route for them to enter the environment after point and non-point sources of exposure. Once in the environment, they are resistant to degradation due to the high energy bonds along the fluorinated backbone (Buck et al. 2011). This then poses a risk for long term exposure scenarios, as well as the possibility for these compounds to travel in the environment (Lau et al. 2007). This is of particular concern with the fluorotelomers which readily volatilize and are therefore able to travel longer distances in the environment than their sulfonate or carboxylate counterparts (Gomis et al. 2015; Lehmler et al. 2007).

1.2.3 Prevalence of PFASs in the Environment

PFOS and PFOA have been detected in water sources throughout the globe, ranging from ng/L (ppt) to mg/L, with higher concentrations reported at contaminated sites and waste-water treatment facilities (Ahrens 2011). In the United States some areas of concern are: the Tennessee River with up to 114 ng/L PFOS and 128 ng/L PFOA (Hansen et al. 2002), Cape Fear Basin in North Carolina with up to 132 ng/L PFOS, 287 ng/L PFOA, and 194 ng/L PFNA (Nakayama et al. 2007), and Great Lakes region with 21-70 ng/L PFOS and 27-50 ng/L PFOA (Boulanger et al. 2004). More recently, total PFAS concentrations in raw water supplies in New Jersey were reported to range from 5-174 ng/L (Post et al. 2013). Not only are these compounds present in water supplies, but they are also detected in the biota as well. They have been detected in a wide range of species including Baltic sea and freshwater fish (Koponen et al. 2014), fish in the Great Lakes as well as surrounding urban rivers (Stahl et al. 2014).

Locations in the United States with detectable PFAS in the water systems are not only near PFAS production sites and waste-water treatment facilities, but also military bases where ample fire training has occurred (Hu et al. 2016). In the United States, military bases have some of the highest reporting of PFAS concentrations in water supplies, up to 10,000,000 parts per trillion, ppt (Sullivan 2018). Therefore, there is still cause for concern of long chain PFAS exposure. Additionally, increasing concentrations of PFAS alternatives are reported in water supplies throughout the globe (Pan et al. 2018). Recently, in the median PFAS concentrations (ng/L) of 7.78 PFHxA, 1.72 PFHxS, 5.24 PFOA, 3.50 PFOS, and 2.36 PFNA were reported in the Delaware River (Pan et al. 2018). Other alternatives, such as GenX and ADONA, have been reported in water supplies, and these non-traditional PFASs pose their own unique health risks (Xiao 2017).

1.2.4 Detection of PFASs in Humans

Multiple datasets have examined the tissue and serum levels of PFASs in humans. One large undertaking was through the NHANES (National Health and Nutrition Examination Survey)

dataset, which provides serum levels of PFOS, PFOA, PFNA, and PFHxS. PFHxA was not monitored. In the 2007-2008 collection years, the mean serum concentrations (ng/mL) for males were 2.6 PFHxS, 17.1 PFOS, 4.7 PFOA, and 1.4 PFNA. The PFAS serum concentrations (ng/mL) in females were 1.4 PFHxS, 10.9 PFOS, 3.5 PFOA, and 2.0 PFNA (Webster et al. 2016). These concentrations tended to decrease over time. The collapsed mean serum PFAS concentrations (ng/mL) for the 2009-2014 collection years were 3.1 PFHxS, 15.1 PFOS, 4.1 PFOA, and 2.0 PFNA in males. In females, these values in ng/mL were 1.9 PFHxS, 10.3 PFOS, 3.3 PFOA, and 1.8 PFNA (Khalil et al. 2016).

While PFHxA was not monitored in the NHANES dataset, other datasets have included PFHxA. A small cohort at Duke University reported mean serum concentrations (ng/mL) of 0.14 ng/mL PFHxA, 1.57 ng/mL PFOA, 0.67 ng/mL PFNA, 3.12 ng/mL PFHxS, and 4.96 ng/mL PFOS (Siebenaler et al. 2017). In this study, PFHxA was detected in 83.8% of the cohort, while the other PFASs were detected in 100% of the cohort. Similarly, a study collected from American Red Cross blood donation reported a decrease in PFAS serum concentration from 2000 to 2015. The mean concentrations for 2000 and 2015, respectively, were 2.3 and 0.9 ng/mL PFHxS, 35.1 and 4.3 ng/mL PFOS, 4.7 and 1.1 ng/mL PFOA, and 0.6 and 0.4 ng/mL PFNA (Olsen et al. 2017). While these studies demonstrate a decrease PFAS over time, there is persistence in serum concentrations.

In addition to the serum concentrations of PFASs, tissue concentrations have also been reported from autopsy samples. From a small cohort in Spain, median liver PFAS concentrations (ng/g) were 1.8 PFHxS, 41.9 PFOS, 68.3 PFHxA, 4 PFOA, and 1.0 PFNA (Perez et al. 2013). PFHxA was also detected at a high concentration in the brain at a mean of 141 ng/g, and mean PFNA concentrations were also high in the brain at 13.5 ng/g.

1.2.5 PFAS Toxicokinetics

The toxicokinetic properties of the PFASs not only vary with each PFAS, but it also varies across species and sexes. This explains the wide variety in serum concentrations and half-lives reported

(Lau 2012; Lau et al. 2007). Exposure is most likely via oral pathways through contaminated water and food (Stahl 2011; USEPA 2017a). Once inside the body, these compounds tend to bind to proteins, and the affinity for organic carbon (log Koc) increases with chain length (Labadie and Chevreuil 2011). This increase is steeper with the sulfonates. More specifically, PFOS and PFOA have high affinities for albumin in the serum (Loccisano et al. 2011). In addition, the long chain PFASs are able to bioaccumulate in tissues. The bioaccumulation factor (log BAF) is about 2 for both PFNA and PFHxS, and the log BAFs increase with increasing chain length with both (Labadie and Chevreuil 2011). This is most likely related to the affinity for lipids and subsequent accumulation in adipocytes observed with the sulfonate (Sanchez Garcia et al. 2018).

There is also the potential for PFASs to reach a developing embryo, as PFOS and PFOA are able to cross the placental barrier (Loccisano et al. 2011). These compounds have also been reported in human milk samples, so these compounds may also elicit their effects during lactation (Loccisano et al. 2011). Human epidemiological data form a cohort of women with measureable serum PFAS supports this mechanism, as exclusive breastfeeding resulted in a 30% increase in children serum PFOS, PFOA, and PFNA (Mogensen et al. 2015).

It has been demonstrated that half-lives are sex- and species-specific. A single oral dose of PFOA was excreted quickly in female rats, male hamster, and rabbits, in both sexes; yet, excretion was much slower in male and female mice (Hundley et al. 2006). Half-life values vary across the other PFASs as well, but overall, carbon chain length tends to correlate with half-life (Conder et al. 2008; Lau 2012). Similarly, half-lives in humans appear to be sex and age-dependent. Estimated half-lives based on serum and urine concentrations in a cohort in China demonstrated striking differences between sexes. Young females (0.5 – 10 years old) had mean half-lives in years of 7.7 PFHxS, 6.2 PFOS, 2.1 PFOA, and 2.5 PFNA. In the same study, older females and all males were collapsed into a single group with reported half-lives in years of 35 PFHxS, 27 PFOS, 2.6 PFOA, and 4.3 PFNA (Zhang et al. 2013). In another study half-lives for both sexes were determined in years to be 5.3 PFHxS, 3.4 PFOS, and 2.7 PFOA (Li et al. 2018). The very long half-lives of years are striking when compared to other compounds and drugs that

are measured in hours or days. The long half-lives and resistance to metabolism, in part, explains the PFAS levels detected in populations around the world.

The fluorotelomers are unique in that unlike the PFASs, these compounds are biotransformed. It was first reported that one possible metabolite of 8:2 FTOH was PFOA, which raised concerns for other fluorotelomers to possibly produce PFASs in biological tissues (Hagen et al. 1981). Enzymes in primary rat hepatocytes were able to convert 6:2 FTOH to 6:2 FTCA (fluorotelomer carboxylic acid), 6:2 FTUCA (fluorotelomer unsaturated carboxylic acid), and PFHxA (Martin et al. 2005). However, conjugation appears to be the main pathway, producing sulfates, glucuronides, or glutathione conjugates. Following 4 µM 8:2 FTOH for 4 hours in hepatocytes, 78% was biotransformed, and of this only 8.5% formed the FTCA, FTUCA, and PFAS metabolites (Martin et al. 2005).

1.3 Overview of Long Chain PFAS Toxicity

1.3.1 Long Chain PFAS Toxicity in Model Organisms

This discussion will include a brief introduction to some of the observed toxicities of long chain (C-8/C-9) PFAS exposures. Complete reviews are reported in the following texts (Lau 2012; Lau et al. 2007; Post et al. 2012). One major organ of toxicity identified with PFAS exposures is the liver. PFOA can cause hepatomegaly and hypertrophy of hepatocytes, as well as induce hepatic cancer (Lau et al. 2004). The PFASs have been shown to activate PPARα, which is purported to be the mechanism of action of this cancer (Wolf et al. 2014; Wolf et al. 2008a). PFOS have been shown to increase lipid accumulation in the liver and cause steatosis (Butenhoff et al. 2009a; Butenhoff et al. 2009b). PPARα knock-out studies have demonstrated that this nuclear receptor is not necessary for PFOS and PFOA to elicit liver toxicity (Abbott et al. 2009; Albrecht et al. 2013; Das et al. 2017; Wolf et al. 2008b). These effects will be discussed in greater detail in Section 1.9.

PFOS and PFOA can cause a number of developmental and reproductive effects, including reduced litter size, offspring size, and offspring survivability (Lau et al. 2007; Luebker et al. 2005). Reproductive effects are observed with exposure to both PFOS and PFOA; however, strain and sex differences have been observed (Negri et al. 2017). These compounds can also disrupt normal testosterone and estrogen which may contribute to the observed reproductive effects (Jensen and Leffers 2008). Another major reproductive endpoint of PFAS toxicity is effect on mammary gland development. At very low doses (0.01-1 mg/kg/day oral gavage in dams from GD 1 -17) PFOA was demonstrated to decrease branching in the mammary gland and therefore decreased milk production (Tucker et al. 2015; White et al. 2007; White et al. 2011). Female offspring, exposed only *in utero* and during lactation, also displayed this altered morphology of mammary tissue (Tucker et al. 2015). Because this occurs at such low doses, this endpoint may serve as the point of departure for future risk assessments.

Other endpoints of concern are reported as well with PFAS exposures. Immunotoxicity has also been associated with PFOS and PFOS exposure, specifically these compounds caused a decreased antibody response to stimuli and potentially interfere with vaccine efficiency (NTP 2016). These compounds have also been studied for their potential impacts on thyroid tissue (Melzer et al. 2010; Weiss et al. 2009). Neurotoxicity has also been associated, particularly with PFOS exposure, where hyperactivity and lack of habituation has been noted in rodent models (Johansson et al. 2008; Ribes et al. 2010). Further discussion of behavioral effects is in Section 1.7.

1.3.2 Epidemiological Findings of Long Chain PFASs

Through NHANES and other data sets examining serum concentrations of PFASs, a number of associations have been established between PFAS exposures and adverse outcomes. For example, serum PFOS, PFHxS, and PFNA in postmenopausal women was associated with osteoporosis and decreased bone density (Khalil et al. 2016). Similarly, osteoarthritis was associated with serum PFOA in females (Uhl et al. 2013). Elevated serum PFOS and PFOA was

also reported in breast cancer patients (Bonefeld-Jorgensen et al. 2011). Serum PFOA has been associated with thyroid disease as well (Melzer et al. 2010). Taken together these studies demonstrate that the PFASs may target the same systems as has been demonstrated in the model organisms.

Epidemiological studies have also focused on children which highlights the impact of developmental PFAS exposures. Effects from exposure have been noted at birth, where cord serum PFOA and PFOS has been associated with decreased birth weight and size (Apelberg et al. 2007). In children, PFAS exposures have been associated with a variety of adverse outcomes. From a cohort of Taiwanese children, PFAS exposure has been positively correlated with asthma, total cholesterol, total triglycerides, estrogen levels, and negatively correlated with testosterone (Zeng et al. 2015; Zhou et al. 2016; Zhu et al. 2016). An additional study demonstrated serum concentrations of PFOS, PFOA, and PFHxS positively correlated with ADHD in children 12-15 years old (Hoffman et al. 2010), and in a separate study, serum PFOS was associated with poor executive functioning in children (Vuong et al. 2016). These compounds have also been reported to elicit immunotoxic effects, where serum PFAS was associated with decreased antibody response to common vaccinations (Grandjean et al. 2012; Stein et al. 2016).These studies highlight that PFAS exposures might pose unique risks to children.

1.4 PFAS Risk Assessment

The US EPA has set health advisory levels at 70 parts per trillion (ng/L) for a combination of PFOS and PFOA in water supplies (USEPA 2017a). This was based on the combination of studies that showed that rat pup weight and ossification during puberty was impacted at a developmental exposure of 0.07 µg/L PFOS, and a similar cancer slope factor at 0.07 mg/kg/day was observed with PFOA. In addition, PFOA was recognized as "possibly carcinogenic to humans" (USEPA 2017a). However, a number of states have promoted maximum concentration levels (MCLs) in drinking water for individual PFASs (ranging from 10-30 ng/L) which are much lower than the current EPA guidance, summarized in (CDPHE 2017).

Based on the prevalence and toxicity associated with exposure to long chain PFASs, the EPA established the stewardship program which sought to phase out the use of PFOS and PFOA by 2015 (USEPA 2014). This was a voluntary program, but there was high compliance amongst companies that had used these compounds (USEPA 2017b). Since the phase out, there has been a decrease in serum PFAS, up to 61% PFHxS, 88% PFOS, 77% PFOA, and 33% PFNA from 2000 to 2015 data collected at American Red Cross centers (Olsen et al. 2017). There still remains measurable amount of PFASs, most likely due to their long half-lives, continued use of products manufactured with PFASs, and persistence in the environment. In the United States, some of the areas with the highest PFAS contamination are military bases with a recent report stating 126 bases have PFAS in water supplies above the EPA limit of 70 ppt (Sullivan 2018). While the present study focuses on short chain PFAS alternatives, reference will be made to long chain PFASs at concentrations of 0.2 and 2 µM, which translates to approximately 100,000 and 1,000,000 ppt, respectively. Of 126 military bases, 31 had PFAS levels above 0.2 µM and 11 above 2 µM (Sullivan 2018).

1.5 Overview of Low Molecular Weight PFAS Alternatives

In order to comply with the Stewardship program, companies have switched to chemical alternatives to meet their manufacturing needs (Wang et al. 2013b). There are hundreds of alternatives (Xiao 2017), but the 3 selected for this dissertation were simple C-6 fluorinated compounds with either a terminal carboxylic acid (PFHxA), sulfonate (PFHxS), or alcohol group (6:2 FTOH). These low molecular weight alternatives were incorporated into industrial uses because they were deemed safer than PFOS/PFOA, based on *in vitro* findings and their shorter half-lives than long chain PFASs (Conder et al. 2008; Wang et al. 2015). However, with the increase in use, these compounds have been detected in waterways around the globe (Pan et al. 2018). Additionally, there is increased detection of these compounds in food packaging (Rice 2015; Yuan et al. 2016). The C-6 also may arise from microbiological metabolism in the environment. For instance, 8:2 FTOH, a precursor to PFOA, can be metabolized to PFHxA by microbial communities (Zhang et al. 2017). However, despite the increase in the environment and

multiple possible routes of exposure, there is very limited toxicity data of the low molecular weight alternatives that are being used.

1.5.1 Perfluorohexanoic Acid (PFHxA) Toxicity

Mammalian models dominate in the toxicity data available for PFHxA exposures. An early study of a 90 day oral gavage of up to 200 mg/kg/day in rats identified the liver as a target organ of toxicity (Chengelis et al. 2009b). In these animals, liver hypertrophy was observed, but this was recoverable after a 28 day depuration period. In addition, serum ALT and ALP were elevated and an increase in peroxisomal beta oxidation was observed. In males only, there was a decrease in total serum cholesterol. Another study followed a similar oral gavage paradigm up to 200 mg/kg/day during a chronic 2 year treatment period. In addition to effects in the liver, they observed a dose-dependent decrease in the survival rate of the female rats (Klaunig et al. 2014). A functional battery of behavioral tests was also completed; however, this revealed no changes in the endpoints examined with PFHxA exposure. PFHxA exposures can also impact development, where dam exposures of 175 mg/kg/day caused a decrease in pup survivability; however, the developmental response curve as the NOAEL, no observable adverse effect level, was established at 100 mg/kg/day (Iwai and Hoberman 2014). These studies not only reveal that the liver is a target organ of PFHxA toxicity, as was observed with PFOA exposure, but also that sex-specific responses exist with this compound as well.

In general, the half-lives of PFHxA are shorter than that of PFOS; however, there are slight species and sex-specific differences that may explain the sexually dimorphic response observed with exposure. A comparison toxicokinetic study in rats and monkeys reported a single IV dose of 10 mg/kg PFHxA in monkeys to be cleared by 24 hours post injection in females and 48 hours post injection in males (Chengelis et al. 2009a). In rats administered a single IV dose of 10 mg/kg PFHxA, the half-life was shorter in males at 2.1 days and 2.5 days in females. Similar clearance rates have been verified in other studies (Ohmori et al. 2003; Wilhelm et al. 2010). Also, despite these shortened half-lives compared to some long chain PFASs, there is still the potential for

PFHxA to accumulate in tissues as it has been observed in liver and brain tissues collected from autopsies (Perez et al. 2013).

Very few studies have been completed in lower vertebrate and cell models assessing toxicity of PFHxA. The *in vitro* studies tend to find PFHxA to be less toxic than its long chain counterpart, PFOA (Mulkiewicz et al. 2007). For example, PFHxA had a limited ability to cause ROS in HepG cells, compared to the dramatic increase observed with PFOS exposure (Eriksen et al. 2010). A single study in *Xenopus* reported an LD_{50} during developmental exposures of 1523.5 µM PFHxA and identified the liver as a target organ of toxicity, where hepatomegaly was reported at 130 µM (Kim et al. 2015). There is the potential for this compound to induce reproductive effects in aquatic models as it has been observed that PFHxA has similar affinity for trout estrogen receptor as PFOA and PFNA, although this is still 5 orders of magnitudes less than an estradiol control (Benninghoff et al. 2011). These few studies have identified specific liver, reproductive, and developmental responses as potential outcomes with PFHxA exposure, which will be examined in the larval zebrafish in the current dissertation.

1.5.2 Perfluorohexane Sulfonate (PFHxS) Toxicity

The toxicokinetic models have demonstrated that PFHxS, like PFOS, has the highest tissue-plasma coefficient in the liver, suggesting that this might be a target organ of toxicity (Kim et al. 2017). This has been observed where chronic 3 mg/kg/day PFHxS led to increased liver weight in rats and mice (Butenhoff et al. 2009a; Chang et al. 2018). Additionally, the male rats also had liver hypertrophy and increased cholesterol (Butenhoff et al. 2009a). Similarly, in transgenic mice with a humanized lipoprotein profile, PFHxS exposure at 3 mg/kg/day increased liver weight and liver triglyceride levels, but decreased serum triglycerides (Bijland et al. 2011). These effects on the liver and lipid metabolism are very similar to those effects elicited from PFOS exposure, as will be discussed in Section 1.9.

There is also concern for the potential interaction between PFASs with thyroid hormones, as a weak negative correlation has been reported in epidemiological studies (Lewis et al. 2015), and

PFHxS has a greater affinity than PFOS or PFOA for the T4 binding site on its transport protein, albeit much lower than T4 (Weiss et al. 2009). This has been demonstrated *in vivo*, where exposure to PFOS caused changes in genes related to thyroid function (Du et al. 2013). This may be related to the transporter discussion in Section 1.8.2.

Particular attention has been paid towards the nervous system with PFHxS exposure. From a single oral exposure ranging from 0.61 to 9.2 mg/kg PFHxS at post-natal day 10 in mice, behavioral effects were observed at 2 months (Viberg et al. 2013). While the behavioral phenotype was consistent between the sexes, the activity levels were significantly different, suggesting a sexually dimorphic behavioral response. The behavioral effects correspond with what is reported in the *in vitro* literature as well. PFHxS exposure (100 µM) was shown to cause apoptosis of primary cerebellar granule neurons and PC12 neuronal cells (Lee et al. 2014a; Lee et al. 2014b) and accumulate in the membranes of primary cerebellar granule neurons at concentrations of 10 µM PFHxS (Berntsen et al. 2017). However, additional studies up to 250 mg/kg PFHxS have reported no impacts on behavior with PFHxS exposures (Butenhoff et al. 2009a; Chang et al. 2018).

Another important consideration for the toxicity profile of PFHxS is its toxicokinetics. While tissue concentrations, half-lives, and bioaccumulation factors vary across sexes and species with all PFASs, variability is highest with PFHxS. Following a single IV dose of 10 mg/kg, serum half-lives in male and female monkeys after 24 weeks were 141 and 87 days, respectively (Sundstrom et al. 2012). In mice following 23 weeks of exposure, the measured half-lives were 30.5 and 27.97 days in males and females, and in rats following 10 weeks, the half-lives were 0.96 and 1.64 days in males and females. This most likely relates to the sex-specific behavioral and lipid-related responses observed (Butenhoff et al. 2009a; Viberg et al. 2013). Therefore sex and species should be given thorough consideration when assessing this toxicological data.

1.5.3 6:2 Fluorotelomer Alcohol (6:2 FTOH) Toxicity

DuPont, one of the companies that manufacture PFASs, provided detailed toxicity assessment of 6:2 FTOH in mammalian models (O'Connor et al. 2014; Serex et al. 2014). From these studies, a LD_{50} of 1750 mg/kg for an acute oral exposure was identified in rats, and following a 90 day oral dose of 50 and 125 mg/kg/day, there was an increase in mortality, determined to be due to kidney necrosis (Serex et al. 2014). In female rats, there was also increased cholesterol and hyperplasia and necrosis in the liver that persisted after 3 months recovery. Dams exposed to these same concentrations had decreased weight, but no effects on fertility or offspring survivability (O'Connor et al. 2014). When exposure was lengthened to begin 70 days prior to mating and continued through lactation, additional reproductive effects were observed, including increased parental mortality, reduced parental body weight, increased pup mortality, and pups in the 250 mg/kg treatment groups were not nursing, which resulted in dehydration. Similar effects on pups have been reported with PFOA exposures, due to altered female breast development (Tucker et al. 2015; White et al. 2007; White et al. 2011). While this has yet to be examined with 6:2 FTOH, it emphasizes that there might be sex-specific responses with this compound as well that may target females and reproductive endpoints. There is the potential for 6:2 FTOH to elicit reproductive outcomes; however, these effects were observed at very high doses. In addition, this compound is readily metabolized for excretion (Martin et al. 2005).

There are also a few studies that have examined reproductive effects of 6:2 FTOH in aquatic species, specifically focused on the potential estrogenic effects of this compound. In male medaka following a 3 day exposure, 100 µM 6:2 FTOH induced estrogen receptor (ERα) protein expression, and 1 µM induced vitellogenin levels, which is and ER-driven outcome (Ishibashi et al. 2008). Both endpoints were not observed with exposure to PFOS or PFOA. Similar observations were made in zebrafish, where 7 day exposures of 0.03 – 0.3 mg/L increased serum testosterone in males and serum estradiol in females (Liu et al. 2009). Exposure of primary tilapia hepatocytes to 6:2 FTOH was also able to induce production of vitellogenin (Liu et al. 2007). Cell culture studies have also demonstrated the estrogenic properties of 6:2 FTOH in breast cancer models (Maras et al. 2006; Vanparys et al. 2006). These data suggest that estrogen pathways may also be a target of 6:2 FTOH toxicity, mediating the reproductive effects.

1.6 Zebrafish Model

1.6.1 Introduction to the Zebrafish Model

The zebrafish is an advantageous toxicological model because of the high homology of pathways to other aquatic species and humans (Howe et al. 2013). Early development of zebrafish can be monitored through the clear chorion encasing the developing embryo. These early life stages have been well-categorized (Kimmel et al. 1995), and the genome has been sequenced allowing for studies to examine the genes regulating development (Amsterdam et al. 2004). This model is also attractive for its high fecundity allowing this to be a high-throughput screening tool. In addition, development occurs quickly, which makes generational studies possible in a shortened time frame compared to rodents and other salmonid species.

Within the first day of development, rapid cellular division occurs, through formation of the blastula and gastrulation. The developing cell mass forms on top of the maternally-deposited yolk sac (Kimmel et al. 1995). Unlike species that develop inside the mother, zebrafish are lecithotrophs, which means that they must rely on the yolk for nutrients and energy during development (Miyares et al. 2014). Organogenesis occurs throughout the next few days of development, with hatching occurring at roughly 72 hours post fertilization (hpf). By 120 hpf, hatched larvae have reached the sac fry stage. This is a critical stage, when the larvae must begin feeding from external sources (Kimmel et al. 1995). During the larval stages, zebrafish undergo rapid growth from a few millimeters to centimeters in length. At 3 months, zebrafish typically reach a juvenile stage, with full sexual maturity reached at roughly 5 months, although this time frame may vary due to the temperature sensitivity of development (Parichy et al. 2009).

1.6.2 PFAS Toxicity in the Zebrafish Model

The zebrafish model has been used in toxicological assessment of PFAS exposures, specifically long chain PFASs. Following early developmental exposures, PFOS and PFOA were shown to cause reduced length, effects on heart rate, pericardial edema, and malformations (Chen et al.

2014; Hagenaars et al. 2011). PFOA showed additional effects in terms of yolk sac edema and delayed hatch, yet the reported LC_{50} of PFOA was much higher than PFOS. Studies from our lab have also demonstrated the developmental effects of PFOS, PFOA, and PFNA on these endpoints, where there was an observed reduction in larval length and effects on yolk sac area with all 3 compounds (Jantzen et al. 2016a). It has also been demonstrated that larval behavior is altered with PFAS exposures (Huang et al. 2010; Jantzen et al. 2016a; Ulhaq et al. 2013b)

Adult zebrafish have also been utilized to demonstrate effects at later life stages through acute and chronic exposures. Studies from our lab have demonstrated that changes in behavior and gene expression persist into adulthood following acute developmental exposures of PFOS, PFOA, and PFNA (Jantzen et al. 2016b). Additionally chronic exposures to PFOA elicited reproductive effects including fecundity and developmental delays in offspring (Jantzen et al. 2017). Other chronic studies have demonstrated lipid effects with PFNA (Zhang et al. 2012) and PFOA (Hagenaars et al. 2013). However, PFOS seems to cause the most drastic effects on the liver, causing steatosis (Cheng et al. 2016; Cui et al. 2017; Du et al. 2009). Bioconcentration factors and half-lives for PFASs have been determined in adult female zebrafish as summarized in Table 1.1, modified from (Chen et al. 2016). These values demonstrate that half-lives do vary across the PFASs, with the sulfonates tending to last longer in tissues. Overall, the similarity to humans demonstrates that this model is suitable for studying PFASs.

1.7 Behavioral Studies

1.7.1 Behavioral Effects with PFAS Exposure

The PFASs have been linked to a number of behavioral effects in rodent models (Mariussen 2012). Both maternal exposures during F1 development and single exposures during early post-natal development have shown that PFOS causes increased activity and lack of habituation at later life stages (Fuentes et al. 2007; Johansson et al. 2008; Ribes et al. 2010). Similar effects were demonstrated in mice following gestational PFOA exposures, where locomotion and habituation were impacted (Johansson et al. 2008). PFOS exposure has also been reported to

alter the outcome of water maze tests in rats (Fuentes et al. 2007; Long et al. 2013). There is also evidence in the literature that PFASs may target neurons at a cellular level, where PFOS was shown to impact neurotransmitter release, and PFOS, PFOA and PFHxS impacted post-synaptic current and decreased neurite length (Liao et al. 2009; Long et al. 2013). These impacts on neuronal growth and function may explain some of the observed behavioral effects.

1.7.1 Behavioral Studies in the Zebrafish Model

In larval and adult zebrafish, multiple assays have been developed to study the effects of stressors on different behavioral endpoints. An open field test was utilized in the present study. This allows for examination of exploratory behaviors in fish and the balance between predator avoidance and foraging (Champagne et al. 2010). In the open field test, fish are placed into a novel tank where the fish must either explore and seek out potential prey or hide from predators. This can be measured by a number of endpoints, such as velocity, distance, and proportion of time spent in different regions of the arena. This last endpoint can indicate thigmotaxis, which is a wall-hugging behavior, beneficial for predator avoidance, but if elevated can indicate an anxiety-like phenotype (Champagne et al. 2010). In addition, zebrafish display phototaxis response, and a quick transition from light to dark stimulates several minutes of increased activity, but this will decrease back to baseline levels (Hurd and Cahill 2002; Kristofco et al. 2016). Unlike rodents, zebrafish are more active during the day under normal conditions (Hurd and Cahill 2002). Studies have been completed to determine the baseline behavior profile of zebrafish at specific stages of development. From 5-10 dpf, zebrafish larvae move in simple circuits, but behavior at the 14 day time point examined in this study is not limited to these simple patterns and behavioral patterns reach adult levels between 3 and 6 weeks of age (Orger and de Polavieja 2017). Taken together, larval zebrafish behavioral assays lend themselves for high-throughput analysis of effects on complex pathways (Reif et al. 2016).

In zebrafish, behavioral effects similar to those reported in rodent models were reported with exposure to PFASs. Increased activity has been observed in larval zebrafish following low dose

exposures to PFOS (Jantzen et al. 2016b; Ulhaq et al. 2013b). However, low PFOS

concentrations appear to be critical in eliciting this response as increased activity was not

observed at higher concentrations in the 3-10 mg/L range (Ulhaq et al. 2013b). PFOA exposure

also increased activity, although these studies identified different impacted endpoints (Jantzen et

al. 2016a; Ulhaq et al. 2013b). Additionally, in these studies, both increased and decreased

activity were observed following PFNA exposures. However, later time points may be more

impacted by PFNA treatment, as adult males exposed only during early development showed

decreased activity and time spent on the edges of the arena, indicating thigmotaxis (Jantzen et al.

2016b). The present study utilizes the framework of these studies to determine if similar

behavioral effects are observed with exposure to PFHxA, PFHxS, and 6:2 FTOH.

1.8 Genes Examined in Growth and Neural Pathways

1.8.1 Brain-Derived Neurotrophic Factor (BDNF)

Brain-derived neurotrophic factor (BDNF) is critical in development, specifically in axonal growth,

arborization, complexity, and synaptic formation and maintenance (McAllister 2001). There is high

homology in *bdnf* across species, with 91% amino acid homology between humans and zebrafish

(Hashimoto and Heinrich 1997). Bdnf binds to the tyrosine kinase receptor, trk, and other

receptors and elicits effects on downstream targets. In zebrafish, there are 3 trk proteins active

during development, but trkB is the main isoform in neurons (Hashimoto and Heinrich 1997).

Expression of bdnf has been detected as soon as the 256-cell stage and steadily increases

through 12 dpf (De Felice et al. 2014). Gradient levels of bdnf are important in development, as it

has been shown to have both stimulatory and inhibitory effects on neuronal and dendrite

development (McAllister 2001). It is also critical in lateral line development in zebrafish (Germana

et al. 2010a). The lateral line is similar to the hairy cells of the inner ears of mammal; however,

the neuromast cells of the lateral line exist in clusters along the body of the fish (Froehlicher et al.

2009). These cells function to aid in movement of the fish, orientation in the water column, and

detection of stimuli. Bdnf expression is 7-fold higher in neuromast cells during lateral line

development than in adult (Germana et al. 2010a). Bdnf expression has also been observed during the development of the retina and gonads, suggesting bdnf plays a role in the development of these organ systems as well (Cacialli et al. 2018; Germana et al. 2010b). Following developmental exposure to PFOS, PFOA, and PFNA lead to a 10-fold increase in *bdnf* expression in male adult zebrafish, and this may be related to a significant effect on behavior in the male PFNA-exposed fish (Jantzen et al. 2016b). The present study will examine bdnf expression levels following exposure to the low molecular weight PFAS alternatives.

1.8.2 Organic Anion Transporting Polypeptide (OATP) Transporters

(A note on protein formatting: Human transporters are written as OATP, rodent as Oatp, and zebrafish as oatp. Gene nomenclature follows the same capitalization formatting using the acronym *slco*, solute carrier organic anion transporter.)

Multiple families belong to the oatp transporters, but this discussion will be limited to members of the oatp1b/1a families, oatp2b1, and oatp1d1. OATP transporters are transmembrane proteins responsible for the movement of various endogenous compounds, such as steroid conjugates, bilirubin, bile acids, thyroxine, and prostaglandins (Klaassen and Aleksunes 2010). These transporters overlap in substrate binding; however, affinities for specific substrates vary between them (Hagenbuch and Gui 2008) . OATP2B1 in humans is found in high concentrations in the liver, kidneys, placenta, and to a lesser extent in lungs, heart, and gonads (Klaassen and Aleksunes 2010). OATP1B1 and 1B3, which are very similar, are found in highest concentrations in the liver, kidneys, ovaries, and to a lesser extent in other tissues. In humans, OATP1A2 is expressed at high levels in the brain and liver, and is present in other tissues as well (Klaassen and Aleksunes 2010).

The oatp transporters have been identified in zebrafish, and homology between zebrafish and humans for key motifs has been reported. In zebrafish, oatp2b1 is phylogenically most similar to human OATP2B1, and the similar tissue distribution suggests an overlap in function (Popovic et al. 2010). The transporter oatp1d1 is unique to teleost fish and first discovered in skate (Meier-

Abt et al. 2007). This transporter is a functional ortholog to OATP1B1, OATP1B3 and OATP1A2, and shares amino acid similarity with OATP1C1 (Popovic et al. 2013). However, expression patterns of oatp1d1 are ubiquitous across all tissues. Zebrafish oatp1d1 is critical in the movement of conjugated steroids in the liver, which is similar to OATP1B1/1B3 in humans, and in the brain, which is similar to OATP1A2, suggesting its role in the excretion of these metabolites (Popovic et al. 2013).

Expression patterns of these oatps vary between the sexes, especially in rodent models (Klaassen and Aleksunes 2010), which is postulated to explain the differences in PFAS clearance and therefore, the sexual dimorphic responses to PFAS toxicity (Lau 2012; Li et al. 2018). The PFASs have also been shown to directly interact with oatp transporters. Both PFOA and PFNA were shown to have the ability to inhibit the normal function of OATP1A2/Oatp1a1 and block uptake of the endogenous substrate, estrone-3-sulfate (Weaver et al. 2010; Yang et al. 2010). These transporters are functional orthologs to zebrafish oatp1d1 (Klaassen and Aleksunes 2010; Popovic et al. 2013). This finding is translational to zebrafish where PFOA was found to inhibit oatp1d1, and PFOS was a substrate to oatp1d1 (Popovic et al. 2014). Studies of OATP2B1/1B1/1B3 have shown that PFOS is a substrate for these transporters, as well as their homologs in rodents (Zhao et al. 2017). The transport of PFASs as substrates provides a means of uptake of these compounds, and potentially explains their unique toxicokinetics. The ability of these PFASs to inhibit transporters function and endogenous ligand movement likely contributes to the species and sex-specific toxicodynamic profile of these compounds and the observed effects.

In addition, gene expression patterns can be altered with PFAS exposures. PFOA exposure caused a decrease in expression of *Slco1a1* and *1b2* , the gene nomenclature of the oatp proteins, in mouse liver (Cheng and Klaassen 2008). Additionally, larval zebrafish exposed to PFOA had increased *slco2b1* expression, yet decreased expression following PFNA exposure (Jantzen et al. 2016a). The expression changes persisted into adult life stages. Following developmental PFOS and PFNA exposures adults had decreased *slco2b1* gene expression and

decreased *slco1d1* expression following exposure to PFOs, PFOA, and PFNA (Jantzen et al. 2016b). These changes may relate to the kinetic interactions between the PFASs and oatp transporters.

1.8.3 Transforming Growth Factor β1A (TGFB1A)

The transforming growth factor superfamily consists of many factors involved in a large number of signaling pathways, and the TGF-β factors are a small subset of that family (Lawrence 1996). In zebrafish, tgf-β is critical for early development including left-right axis determination (Vonica et al. 2011), through organogenesis of the gonads and vasculature (Hsu et al. 2018; Jadrich et al. 2006), and possibly even playing a role in regeneration (Liu et al. 2018a). This discussion will be limited to tgfb1, which functions in muscle development and regulation of immune responses (Kim and Ingham 2009; Letterio and Roberts 1998; Vonica et al. 2011). It was demonstrated in a zebrafish tgfb1 knockout model that there was reduced growth of muscle fibers and an altered morphology of the fiber bundles, which formed a wavy pattern (Kim and Ingham 2009). Tgfb1a may also play a critical role in lateral line formation, similar to BDNF (Germana et al. 2010a). Tgfb1a is the only member of this family expressed during the development of the lateral line, and knockout studies have demonstrated that the loss of this factor leads to decreased neuromast number and altered neuromast morphology (Xing et al. 2015). These studies show the various organ systems that rely on proper expression of tgfb1a during development. PFASs may also target this system as larvae developmentally exposed to PFOS and PFNA had significant reduction in *tgfb1a* gene expression (Jantzen et al. 2016a). Additionally, larvae that followed the same developmental exposure paradigm had significant up-regulation of *tgfb1a* as adults following PFOS and PFNA exposures, but this was only observed in the males (Jantzen et al. 2016b).

1.8.4 Adaptor-Related Protein Complex 1σ1 (AP1S1)

The AP-1 complexes are ubiquitously expressed proteins that aid in the formation of protein- and lipid-containing vesicles (Nakatsu et al. 2014). There are a variety of these complexes, each

made up of a unique combination of subunits to form a heterotetrameric protein. AP-1 is critical in the functionality of the Golgi network and formation of endosomes (Nakatsu et al. 2014). Complete knockout of the Ap-1 complex was embryonic lethal in mice (Zizioli et al. 1999). Mutations in the AP-1 proteins have been associated with a number of human disease states, including Crohn's Disease and colorectal cancer (Nakatsu et al. 2014). This discussion will focus on the role of the sigma subunit, σ1, as the small functional subunit that can join the AP-1 complexes. Mutations in the sigma subunit have been associated with MEDNIK (mental retardation, enteropathy, deafness, neuropathy, ichthyosis, and keratodermia), supporting that ap1s1 is critical in neural and neural-derived tissue development (Montpetit et al. 2008).

In zebrafish, there are 3 AP-1 complexes: 1A and 1C function in neural system development, moderating Golgi and endosome function and 1B which functions in kidney development (Gariano et al. 2014). Kidney-related function is unique to zebrafish and has not been observed in rodent models. Knockout studies have also been completed to examine the roles of specific subunits and their expression patterns during development (Gariano et al. 2014; Zizioli et al. 2010). Zebrafish knockdown of ap1s1 led to reduced number of interneurons, reduced number of axonal processes in the spinal cord, and delayed behavioral response to stimuli early in development (Montpetit et al. 2008). This suggests ap1s1 regulates nervous system development similar to bdnf, and it has been reported that expression of these two factors are interrelated (Gaiddon et al. 1996; Huynh and Heinrich 2001; Tuvikene et al. 2016). There is evidence that PFAS exposures may interact with ap1s1, as larval zebrafish developmentally exposed to PFOA, PFOS and PFNA has *ap1s1* expression levels at roughly half that of control larvae (Jantzen et al. 2016a). Additionally, levels of *ap1s1* were significantly increased in F1 embryos from a chronically PFOA-exposed parental zebrafish population (Jantzen et al. 2017).

1.9 Lipid Metabolism

1.9.1 PFASs and the Dysregulation of Lipids

PFAS exposures target the liver specifically inducing β-oxidation of fatty acids and other alterations on lipid metabolism, reviewed in (Lau 2012). Some of these hallmarks include increased liver weight, triglyceride accumulation, cholesterol accumulation, and varied degrees of histological change, ranging from increased lipid accumulation to hypertrophy and steatosis (Abbott et al. 2009; Albrecht et al. 2013; Das et al. 2017; Rosen et al. 2010). The elevated lipid accumulation in the liver is typically associated with decreased serum triglyceride and cholesterol, suggesting that these lipids are being selectively shuttled to the liver. This was strongly demonstrated in two studies pairing PFOS and PFOA exposure with high fat diet (HFD) (Wang et al. 2013a; Wang et al. 2014). In both cases the HFD with PFAS exposure elicited more severe hepatoxicity, and these effects were not mitigated following a recovery period.

As discussed previously, there are species differences in half-lives and severity of response to PFAS exposure (Lau 2012; Lau et al. 2007). One potential explanation is the species differences in PPARα activity and expression levels (Choudhury et al. 2000). In order to address this potential issue scientists have utilized more humanized models. A large number of these studies have utilized PPARα-null mice (full discussion in Section 1.10.1). Additionally, it has been demonstrated that subchronic exposures to PFHxS (6 mg/kg/day) and PFOS (3 mg/kg/day) in APOE*3-Leiden.CETP mice, which have similar lipoprotein metabolism patterns to humans, had increased liver weight and increased triglyceride accumulation in the liver (Bijland et al. 2011). Alternate mechanisms have yet to be established, but studies in cell models have demonstrated changes in lipid distribution and profiles with PFAS exposures (Gorrochategui et al. 2015; Watkins et al. 2015).

These findings align with what is reported in the epidemiological literature. In men, serum PFOA is correlated with diabetes, but not in females (He et al. 2017). Another study found a positive correlation with serum PFOA and risk of being overweight and obese in both sexes (Barry et al. 2014). Additionally, in a weight loss study, it was found that serum PFOS, PFOA, PFNA, and PFHxS correlated with increased weight gain after the diet restriction ended in women only (Liu et

al. 2018b). Together these studies demonstrate that lipid dysregulation exists in humans exposed to PFASs.

Studies in aquatic models have also highlighted the potential effects of PFAS on lipid metabolism. Salmon exposed to PFOS and PFOA had altered fatty acid profiles, many of which were decreased, compared to controls (Arukwe et al. 2013). In zebrafish, PFOS induced fatty liver (Fai Tse et al. 2016), hepatic steatosis (Cheng et al. 2016), and liver fatty degeneration (Cui et al. 2017). Gene expression analysis in zebrafish has identified some potential targets (Cheng et al. 2016; Cui et al. 2017; Du et al. 2009; Hagenaars et al. 2011; Krovel et al. 2008; Lee et al. 2017; Liu et al. 2007; Sant et al. 2018; Zhang et al. 2012). Some genes of interest will be discussed in Section 1.10.

1.9.2 Lipid Metabolism in the Zebrafish Model

There is high homology of many factors that regulate lipid metabolism in zebrafish and mammals, reviewed in (Quinlivan and Farber 2017; Wallace and Pack 2003). However, there are some unique aspects of lipid utilization early in development, which will be discussed in this section. Zebrafish rely on a large maternal deposition of yolk nutrient for energy to sustain early growth before feeding begins (Fraher et al. 2016). Mammals have much smaller yolk sacs and many rely on nutrient and waste removal during development through a maternal placenta, reviewed in (Freyer and Renfree 2009). This critical difference in early nutritional status provides some unique structures to examine in zebrafish development.

The yolk cell is a dynamic structure that plays a role in more than simply providing nutrients (Carvalho and Heisenberg 2010; Fraher et al. 2016). It contains maternal mRNAs and proteins that allow for metabolism of the lipids and other yolk nutrients. It is also active in mediating the movement of the developing cells over the yolk cell during epiboly (Bruce 2016). As to be expected, removal of 50-70% of the yolk sac cell early in development is lethal, but survival rates increase as stage at which the yolk is removed increases (Liu et al. 1999). A unique structure, the yolk syncytial layer (YSL), forms between the yolk cell and developing embryo. While yolk

syncytia across species vary in evolutionary origin, functions remain similar (Carvalho and Heisenberg 2010; Freyer and Renfree 2009). This is a layer of cells that form a barrier, as well as performing a number of vital functions along this critical border (Carvalho and Heisenberg 2010). Early in division, cells along the yolk form the YSL and undergo a few rounds of division prior to epiboly (Kondakova and Efremov 2014). During the epiboly stages, the YSL nuclei change size and shape, nuclei are transcriptionally active, and areas along the embryo vary in thickness (Kondakova and Efremov 2014).

Homology also exists between humans and zebrafish with regards to both the digestive system and lipid metabolism (Wallace and Pack 2003). Digestive organs form at the mid-somite stage of development, which is prior to 24 hpf (Wallace and Pack 2003). By 5 dpf, the intestinal lumen is open and functional, including the regulation by digestive hormones, cholecystokinin and serotonin, and a flourishing microbiota (Quinlivan and Farber 2017).

The development of BODIPY-FL fatty acids has allowed for the study of lipid metabolism in zebrafish. BODIPY-FL fatty acids come in many chain lengths attached to a stable fluorescent molecule, and for the present study C12 fatty acids were selected. It has been reported that the shorter fatty acids are not actively metabolized and the longer alternatives are unable to cross the YSL in zebrafish (Anderson and Stahl 2013; Carten et al. 2011). It has been demonstrated that tagged fatty acids utilize the same uptake mechanisms as endogenous lipids (Stahl et al. 1999). Upon injection, the BODIPY-FL fatty acids are quickly dispersed throughout the yolk, and yolk cell enzymes metabolize the fatty acids into new lipids, predominantly triglycerides (Fraher et al. 2016; Miyares et al. 2014). These tagged fatty acids have also been utilized in studies focused on later stages of development. Following liposomal feedings of BODIPY-FL C12 fatty acids, sac fry larvae had absorbed and transported the fatty acids into the intestinal lumen and the cytoplasm of enterocytes (Carten et al. 2011). Zebrafish will also metabolize these fatty acids into triglycerides and phosphatidylcholine in the intestines and breaks down these fatty acids via β-oxidation in the liver (Carten et al. 2011).

In addition, many of the enzymes that function in the uptake and metabolism of yolk lipids along the YSL are utilized in the digestive organs (Flynn et al. 2009; Quinlivan and Farber 2017; Salmeron 2018). Table 1.2 summarizes the genes discussed in this dissertation in terms of their homology to human genes and location of expression. Full discussion of each gene's function follows. While these genes are critical in zebrafish yolk uptake, there is also homology in the importance of yolk uptake in the rodent model as well, where knockout of one transporter, mttp, was embryonic lethal (Terasawa et al. 1999).

1.10 Genes Examined in Related Pathways

1.10.1 Peroxisome Proliferator Activating Receptors (PPARα and PPARγ)

PPARs are nuclear receptors, which when activated heterodimerize with RXR and bind to the promoter region of a number of genes related to lipid metabolism (Ahmadian et al. 2013; Mandard et al. 2004). A number of lipids act as endogenous ligands for this receptor, including polyunsaturated fatty acids which have a high affinity for PPAR (Dreyer et al. 1993). Activation leads to a phenotypic change in the cell, increasing the size and number of peroxisomes. PPARα and PPARγ are similar in that they play a role in mediating lipid homeostasis, and regulate many of the same downstream targets (Ahmadian et al. 2013; Mandard et al. 2004). PPARα is typically associated with response to fasting, so genes related to fatty acid uptake, transport, and fatty acid β-oxidation are increased transcriptionally after receptor activation (Mandard et al. 2004). It is expressed highly in the liver in rodents, as well as in zebrafish at larval and adult stages (Ibabe et al. 2005a). PPARγ is localized in adipocytes and is typically associated with activating genes that promote adipogenesis (Ahmadian et al. 2013). Zebrafish are similar in that pparγ localizes in adipocytes, and this occurs along with the first appearance of precursor adipocytes at 8 dpf (Flynn et al. 2009), although white adipose tissue does not appear until 14 dpf (Quinlivan and Farber 2017). In addition, pparγ is localized in the liver of zebrafish as well (Ibabe et al. 2005a). Some specific and overlapping downstream targets of pparα and pparγ are *slc27a*, *mttp*, *lpl*, and *apoa1*, which will be discussed further in this section.

Based on early work with the PFASs, demonstrating elevated β-oxidation of fatty acids, it was proposed that Pparα activation may be mediating these effects (Sohlenius et al. 1992). *In vitro* studies have verified that all PFASs discussed in this study have the ability to activate Pparα, and in combination, the PFASs have an additive effect on Pparα activation (Wolf et al. 2014; Wolf et al. 2008a). While PPARα activation may contribute to PFAS toxicity, it is not the only targeted mechanism. Chronic PFOA of up to 20 mg/kg/day caused monkeys to develop hepatotoxicity, but β-oxidation was not observed (Butenhoff et al. 2002). Additionally, a number of studies in PPARα-null animals have noted hepatoxicity with PFAS exposures (Das et al. 2017; Rosen et al. 2010; Yang et al. 2002). These differences in Ppar activation are most likely related to species differences in response to pparα agonism and expression levels of the receptor (Choudhury et al. 2000). One study comparing wild-type (WT), PPARα-null, and humanized-PPARα mice revealed that the species from which pparα was derived influenced the toxicity (Albrecht et al. 2013). There was decreased pup survival and increased liver weight with PFOA exposure in only the WT mice. However, markers of Pparα activation, specifically *acox1* and *cyp4a10* which are two genes regulated by Pparα, were altered in both the WT and humanized-PPARα mice.

It is unknown to what extent pparα activation drives the toxicity associated with PFAS exposure in zebrafish. To begin to tease out the mechanism, gene expression analysis was completed in larvae in the present study for both *pparα* and *pparγ*. In addition, genes that serve as downstream targets, including *slc27a*, *mttp*, *lpl*, and *apoa1,* were analyzed. These genes were selected from a transcriptomics study examining lipid metabolism with PFAS exposure in PPARα-null mice (Das et al. 2017). Activation of Pparα may also relate to expression levels of Oatp transporters (Cheng and Klaassen 2008), which may provide a link to the transporter-related effects discussed in Section 1.8.2.

1.10.2 Leptin Hormone (LEPA)

Mammalian leptin regulates satiety and weight gain, reviewed in (Pan and Myers 2018). This hormone is produced by adipocytes, and the brain has a high concentration of leptin receptors.

Knockout models of leptin and its receptor in rodents exhibit increased body weight, adipogenesis, and hunger, which lead to hyperphagia (Yen et al. 1976). Zebrafish contain 2 paralogs of the mammalian leptin hormone, leptin-a and leptin-b (Gorissen et al. 2009). Discussion will be limited to leptin-a, which is more highly expressed than leptin-b and localized to the liver. Leptin-a has only 23% sequence homology with human leptin; however, there is conservation of critical binding sites, quaternary structure, and expression patterns (Gorissen et al. 2009). The leptin receptor is expressed in high concentrations in the notochord early in development, and adults have high expression levels in the muscle, gills, testes, and relatively low but isolated expression in the hindbrain (Liu et al. 2010b).

Leptin's function in zebrafish appears to differ slightly from that of rodents. Zebrafish with mutant leptin have no effect on weight gain (Michel et al. 2016), which is very different from the rodent knockout models (Yen et al. 1976). However, it does appear to play a role in regulating lipid homeostasis (Salmeron et al. 2015). Rainbow trout fed a high fat diet are unable to regulate leptin response to an insulin stimulus (Salmeron et al. 2015). Leptin is also critical in the maintenance of a proper metabolic rate in zebrafish, where knockdown models have demonstrated that larvae utilize less oxygen and produce less acid during metabolism (Dalman et al. 2013).

1.10.3 Solute Carrier 27A1 (SLC27A1)

SLC27a1 is a long chain fatty acid transporter, belonging to the solute carrier family 27 (Anderson and Stahl 2013). These transporters are also referred to as fatty acid transport proteins (FATP) and function in the uptake of long chain fatty acids. Additionally, it is associated with acyl coA synthetase activity (Coe et al. 1999). From rodent knock-out studies, it has been shown Slc27a1 is critical for distribution of lipids into fat deposits, and its lack of function in these studies can protect from obesity (Kim et al. 2004). Similar functions have been observed in zebrafish, and additionally, slc27a1 has been shown to have some regulative properties in zebrafish, as it can be involved in the selective uptake of some fatty acids (Quinlivan and Farber 2017).

In rodents, Slc27a1 is predominantly localized in skeletal muscle heart, brown adipose tissue, and white adipose tissue (Anderson and Stahl 2013). In lower levels, Slc27a1 can be found in the skin, kidney, brain, and endothelial cells. Similarly, it is localized to adipocyte membranes in trout (Salmeron et al. 2015), and enterocytes in zebrafish (Quinlivan and Farber 2017). While slc27a1 has not been studied in the YSL, other acyl coA synthetases have been identified in YSL (Quinlivan and Farber 2017), so it is possible slc27a1 functions here as well. Expression of *slc27a1* is regulated by both pparα and pparγ (Frohnert et al. 1999; Mandard et al. 2004)

1.10.4 Microsomal Triglyceride Transfer Protein (MTTP)

The microsomal triglyceride transfer protein, mttp, functions in the packing of triglycerides in lipoproteins (Hussain et al. 2003). Lipoproteins, as the name implies, are vesicles containing both lipids and proteins (German et al. 2006). These structures are classified into categories such as HDL, LDL, and chylomicrons, based on lipid content, lipid density, and lipoprotein diameter. Mttp is responsible for packaging triglycerides into lipoproteins containing apolipoprotein b, apob (Hussain et al. 2003).

This protein is especially critical early in development, functioning in the uptake of yolk lipids. This has been demonstrated in the rodent model, where mice with knockout of mttp function do not survive gestation (Raabe et al. 1998; Terasawa et al. 1999). This has been demonstrated in zebrafish as well, where morpholinos showed reduced growth, yolk uptake, and mortality by 6 dpf (Schlegel and Stainier 2006). These studies demonstrate the importance of this protein in early development. Additionally, *mttp* expression is highest in the zebrafish is highest 5-9 dpf, where expression is found in the YSL, liver and intestines (Marza et al. 2005). Expression in the liver and intestines persists into adulthood, emphasizing the conservation in mttp function throughout life stages (Marza et al. 2005). Following a high fat diet in zebrafish, there was increased gene expression of mttp (Schlegel and Stainier 2006).

1.10.5 Apolipoproteins (APOA1 and APOC2)

The apolipoproteins are a class of protein involved in the packing of lipids into lipoprotein vesicles (Dominiczak and Caslake 2011). Specific apolipoproteins are associated with each lipoprotein category. This discussion will be limited to 2 apolipoproteins, APOA1 and APOC2. APOA1 is involved in the formation of HDL and chylomicrons, and therefore, is the major apolipoprotein in the high density portion of serum (Schonfeld and Pfleger 1974). In fact, following a high fat diet in zebrafish, *apoa1* levels increase (Carten et al. 2011). Similarly, apoc2 is associated with HDL and VLDL formation (Dominiczak and Caslake 2011). Both apoa1 and apoc2 paralogs in zebrafish have similar function, and are critical to lipid metabolism in the digestive organs of larval fish (Cheng et al. 2006; Otis et al. 2015).

In zebrafish, apolipoproteins also play a role in mediating the uptake of lipids across the YSL (Quinlivan and Farber 2017). While the YSL has formed before epiboly commences (Bruce 2016), the first apolipoprotein, apoa1, does not appear in the YSL until the embryos have reached the 80-100% epiboly stage (Otis et al. 2015). However, both are present and necessary for a functional YSL (Otis et al. 2015; Pickart et al. 2006). Zebrafish apoc2 morpholinos were unable to uptake yolk lipids into the developing embryo, and metabolism of C12 fatty acids into phosphatidylcholine and lysophosphatidylcholine was reduced (Pickart et al. 2006). This highlights the role of apolipoproteins in transport and metabolism of yolk lipids.

Genetic regulation of *apoa1* and *apoc2* is mediated through the PPAR pathways. There is a PPARα response element in the promoter region of *apoa1* (Mandard et al. 2004). Apoc2 is also involved in this pathway as it plays a critical role in activating lipoprotein lipase, lpl, which is regulated by PPARα (Avraham-Davidi et al. 2012; Kersten 2014; Mandard et al. 2004).

1.10.6 Lipoprotein Lipase (LPL)

Lipoprotein lipase, lpl, is involved in the degradation of lipoproteins, specifically degrading triglycerides into their constituent fatty acids (Kersten 2014). Lpl in zebrafish differs from that of humans because an additional exon, not translated in humans, exists in fish (Arnault et al. 1996). Despite this sequence difference, human and zebrafish lpl have similar function (Feng et al.

2014). This breakdown of triglycerides into fatty acid chains is critical in lipid uptake, and therefore, lpl expression is high in YSL and ubiquitous throughout the embryo early in development (Feng et al. 2014). In later stages, lpl expression is high in the liver, head, and lateral line.

This gene is a downstream target of each of the nuclear receptors in this discussion: pparα, pparγ, and leptin, reviewed in (Ahmadian et al. 2013; Mandard et al. 2004; Salmeron 2018). Therefore, changes in expression would likely change if these pathways are targeted. Additionally, apoc2 plays a critical role in lpl activation (Avraham-Davidi et al. 2012).

1.11 Research Objectives and Hypothesis

The main hypothesis of this dissertation was that despite the general classification of the PFAS group, each PFAS would produce different adverse outcomes in larval zebrafish following developmental exposures. This was examined in the context of low molecular weight PFAS alternatives (C-6). Three alternatives with different terminal groups were selected, PFHxA, PFHxS, and 6:2 FTOH, to examine the effect of end group on outcomes. These outcomes were then compared to previous data from our lab on long chain PFASs, PFOA (C-8), PFOS (C-8), and PFNA (C-9), to make comparisons across PFAS chain length. To examine exposure effects in the developing zebrafish, a number of cellular, morphological, and behavioral endpoints were selected for analysis at early (5 dpf, sac fry) and later (14 dpf) larval life stages. These endpoints were selected to cover multiple levels of biological organization and complexity in attempts to determine critical points along AOPs related to growth, nervous tissue development, and lipid homeostasis.

This work was divided into 3 specific aims:

1. The first aim was to determine effects on developmental exposures in early life stage larvae (5 dpf), including establishment of LC50 values, morphometric effects, and alterations in gene expression with the low molecular weight PFAS alternatives.

2.   The second aim sought to examine more complex outcomes following exposures to low molecular weight PFAS alternatives in later life stage larvae (14 dpf) through analysis of behavioral effects and lipid distribution alterations.

3.   The final aim examined alterations in lipid distribution with PFAS exposure, using the long chain PFASs as a proof of concept. Effects of C-6 and C-8/9 exposures on expression of genes related to lipid mobilization and distribution were examined to compare possible pathways for all PFASs in these studies.

Table 1.1. Zebrafish bioconcentration parameters following 24 day exposures to PFASs, modified from (Chen et al. 2016). Dose and bioconcentration factor (BCF) are reported as mean ± standard deviation. The rate of uptake and half-lives are reported as mean ± standard error. Data collected from adult female zebrafish. N=36.

Compound	Mean Dose (µg/L) N=36	Rate of Uptake Plasma (L/kg/d)	Half-life Plasma (d)	Log BCF$_{SS}$ Plasma (L/kg, ww)	Rate of Uptake Liver (L/kg/d)	Half-life Liver (d)	Log BCF$_{SS}$ Liver (L/kg, ww)
PFHxA	1.22 ± 0.084	26.6 ± 18.9	9.6 ± 1.3	1.78 ± 0.03	8.9 ± 3.2	NA	1.73 ± 0.06
	7.02 ± 0.207	29.1 ± 13.6	3.2 ± 1.3	1.61 ± 0.02	9.5 ± 5.5	14.7 ± 6.0	1.70 ± 0.09
PFHxS	0.69 ± 0.06	186.1 ± 60.7	6.4 ± 0.2	2.94 ± 0.10	94.5 ± 3.4	4.6 ± 0.2	2.56 ± 0.09
	8.59 ± 1.53	123.3 ± 31.1	14.7 ± 0.9	2.58 ± 0.10	33.0 ± 10.3	10.2 ± 0.3	2.39 ± 0.10
PFOA	0.86 ± 0.22	252.5 ± 142.4	5.3 ± 0.5	2.79 ± 0.12	94.4 ± 35.0	6.5 ± 1.9	2.39 ± 0.12
	6.64 ± 1.20	237.6 ± 153.9	2.8 ± 0.6	2.45 ± 0.08	133.4 ± 111.3	3.7 ± 0.5	2.43 ± 0.08
PFOS	1.12 ± 0.31	1917.0 ± 546.6	34.7 ±5.20	4.12 ± 0.15	1194.0 ± 331.3	30.1 ± 13.1	3.64 ± 0.12
	15.2 ± 5.06	774.3 ± 180.2	27.7 ±3.32	3.77 ± 0.15	301.1 ± 89.4	3.9 ± 0.1	3.55 ± 0.15
PFNA	0.69 ± 0.17	1653.4 ± 459.8	21.7 ± 4.7	4.07 ± 0.11	351.1 ± 86.7	19.3 ± 5.3	3.18 ± 0.12
	3.63 ± 0.806	3543.3 ± 1483.2	11.6 ± 4.6	3.97 ± 0.14	309.0 ± 111.7	7.5 ± 1.4	3.45 ± 0.10

Table 1.2. Genes related to lipid metabolism examined in the present study (Chapter 4). Listed are the gene name, orthologs in zebrafish, human paralogs and the percent homology to humans, and tissue distribution.

GENE	GENE ID	ZEBRAFISH ORTHOLOGS	HUMAN PARALOGS AND % HOMOLOGY	TISSUE DISTRIBUTION	RELEVANT CITATIONS
lepa	NM_001128576	*lepb*	*Leptin* 23% DNA	Liver	(Gorissen et al. 2009)
pparα	NM_001161333	*pparab*	*PPARα* 67% amino acid	Liver Intestines Kidneys Adipose Gonads Skeletal muscle	(Den Broeder et al. 2015; Ibabe et al. 2005a)
pparγ	NM_131467	---	*PPARγ* 67% amino acid	Liver Intestines Kidneys Adipose Gonads Skeletal muscle	(Den Broeder et al. 2015; Ibabe et al. 2005a)
apoa1	NM_131128	*apoa1b*	*APOA1* 48.3% DNA	YSL Intestines Liver	(Otis et al. 2015)
apoc2	NM_001326448	---	APOC2	YSL Liver	(Cheng et al. 2006; Pickart et al. 2006)
lpl	NM_131127	---	*LPL* 62% amino acid	YSL Liver Nervous tissue	(Feng et al. 2014)
mttp	NM_212970	---	*MTTP* 54% amino acid	YSL Intestines Liver	(Marza et al. 2005; Quinlivan and Farber 2017)
slc27 a1a	NM_001013537	*slc27a1b*	*SLC27A1/FATP1* 65% amino acid	Skeletal muscle Adipose	(Quinlivan and Farber 2017; Salmeron et al. 2015)

*Molecular Initiating Event (MIE)   *Key Events (KE)   *Adverse Outcomes (AO)
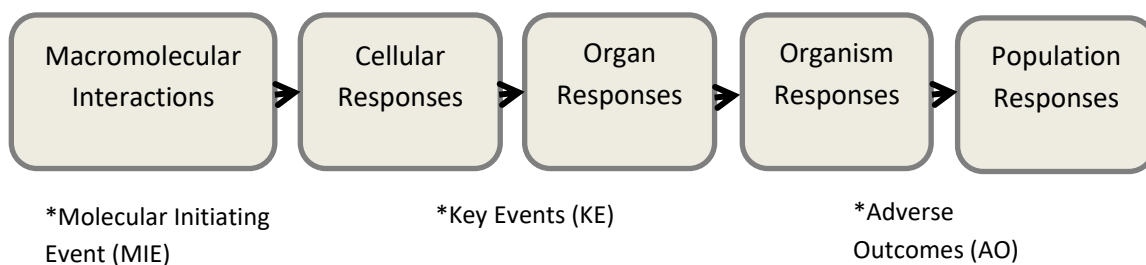
Figure 1.1. General outline of an adverse outcome pathway (AOP). Exposure of a compound results in a macromolecular interaction, referred to as a molecular initiating event, MIE, which triggers a cascade of outcomes. The outcomes include key events, KE, at the cellular and organ level. The ultimate adverse outcome (AO) of the pathway is observed at the organism or population level.

CHAPTER 2

Morphometric and Gene Expression Alterations in 5 dpf Larvae Exposed to Low Molecular

Weight PFAS Alternatives

2.1 Introduction

Perfluoroalkylated substances (PFASs) continue to be a class of chemicals that raise

environmental and health concerns worldwide. Their extensive use and structural variations in

commercial products for manufacturing, their persistence in the environment, and the lack of

toxicological data pose a serious data gap. Long chain PFASs in particular PFOS,

perfluorooctane sulfonate, and PFOA, perfluorooctanoic acid, have been demonstrated to cause

toxicity in a variety of model organisms, including hepatic, developmental, reproductive, and

behavioral effects (Lau 2012; Post et al. 2012).

Due to safety concerns, companies have voluntarily switched to other compounds, including low

molecular weight alternatives (Lehmler et al. 2007; Wang et al. 2013b). These compounds have

shorter serum half-lives than the long chain PFASs and are therefore deemed safer (Conder et al.

2008; Lau 2012). However, with increased use the low molecular weight PFASs have been

detected in human samples in the ng/mL range, like that of PFOS and PFOA (Lewis et al. 2015;

Olsen et al. 2017; Siebenaler et al. 2017). Serum levels of PFOS and PFOA have decreased over

the past few years, and due to recent increasing concerns of the bioaccumulation and toxicity

associated with PFHxS, serum levels of this compound have plateaued (Land et al. 2018).

Additionally, PFHxA, PFHxS, and 6:2 FTOH have been detected in ground and surface water

supplies across the world (Ahrens 2011). PFHxS was detected in low concentrations in a variety

of species; however, PFHxA levels are often below the limit of detection in tissue samples

(Kannan et al. 2005; Sedlak et al. 2017).

The present study focuses on 3 low molecular weight alternatives: PFHxA, perfluorohexanoic

acid, PFHxS, perfluorohexane sulfonate, and 6:2 FTOH, 6:2 fluorotelomer alcohol (Table 2.1).

Each contains 6 fluorinated carbons, which will allow for comparison to the toxicities associated with the 8 carbon PFASs. Fewer studies exist for the low molecular weight alterntives. Subchronic and chronic exposures up to 200 mg/kg/day PFHxA in rats identified the liver to be a target organ of toxicity, where hypertrophy of hepatocytes and increased beta-oxidation was observed (Chengelis et al. 2009b; Klaunig et al. 2014). In addition, chronic PFHxA caused a significant decrease in the survival rate of the exposed females, suggesting that there might be sex-specific toxicities (Klaunig 2014). The livers of rats were also enlarged when exposed to doses as low as 3 mg/kg/day PFHxS for 1-2 months (Bijland et al. 2011; Butenhoff et al. 2009a; Chang et al. 2018).

Rodent studies with 6:2 FTOH have demonstrated kidney necrosis at 125 mg/kg/day, but at lower doses serum albumin, bilirubin, and proteins levels were increased (Serex et al. 2014). Studies in cell culture identified possible estrogenic agonism by 6:2 FTOH and other fluorotelomers (Maras et al. 2006; Vanparys et al. 2006). This has been observed *in vivo* in aquatic models as 6:2 FTOH was reported to induce ERα and vitellogenin in medaka, zebrafish, and tilapia (Ishibashi et al. 2008; Liu et al. 2010a; Liu et al. 2007; Liu et al. 2009). This suggests 6:2 FTOH may play a unique endocrine disrupting role.

The zebrafish model is useful for its ability to provide toxicity screening and therefore, it reduces reliance on mammalian studies. There is high homology in early developmental processes, and there is 70-80% genetic homology to humans (Howe et al. 2013). Toxicity testing for the long chain PFASs has been completed in the zebrafish model, establishing the doses at which PFOS and PFOA affect early embryonic development (Hagenaars et al. 2011; Ulhaq et al. 2013a). PFOA exposure has been demonstrated to cause developmental abnormalities, yolk sac edema, and delayed hatching (Zheng et al. 2011). A variety of exposure paradigms have demonstrated PFOS can alter early organogenesis and development of the swim bladder, pancreas, muscle fibers, and liver in adults, suggesting multiple targets for PFOS exposures (Chen et al. 2014; Cheng et al. 2016; Huang et al. 2010; Sant et al. 2017).

Studies from our lab have demonstrated morphological and gene expression effects in both larvae and adult zebrafish following developmental exposure to PFOS and PFOA (Jantzen et al. 2016a; Jantzen et al. 2016b; Jantzen et al. 2017). Exposure to 2 µM PFOA caused a significant reduction in larval size and yolk sac edema (Jantzen et al. 2016a). PFOS exposure of the same dose caused a significant reduction in size and decreased yolk sac area. Additionally, the gene expression results identified possible unique pathway targets for each compound. These studies demonstrated that exposure to each PFAS can lead to the development of different morphometric and behavioral phenotypes in zebrafish.

Candidates for gene expression analysis in this study of low molecular weight alternatives were selected based on findings from the larval exposure to PFOS and PFOA (Jantzen et al. 2016a). Organic anion transporters, oatpb1 (gene name: *slco2b1*) and oatp1d1 (gene name: *slco1d1*), are responsible for the transfer of endogenous ligands, such as bile acids, steroid conjugates thyroxine, bilirubin, and prostaglandins, across membranes throughout the body, but expression for these transporters is high in the liver (Klaassen and Aleksunes 2010; Popovic et al. 2010). In zebrafish, oatp2b1, has high homology to human OATP2B1, and both PFOS and PFHxS are substrates for human OATP2B1 (Popovic et al. 2010; Zhao et al. 2017). Oatp1d1 is unique to fish; however, it has been demonstrated that PFOS is a substrate and PFOA is an inhibitor of Oatp1d1 function (Popovic et al. 2014).

The remaining genes are related to central nervous, muscle, and lateral line development. Brain-derived neurotrophic factor, bdnf, is necessary for axonal growth and arborization, as well as synaptic formation (McAllister 2001). This factor is critical not only in the developing zebrafish brain, but also the formation of the lateral line, which functions similar to the inner ear hairy cells in mammals regulating orientation and balance (De Felice et al. 2014; Germana et al. 2010a; Hashimoto and Heinrich 1997). Similarly, transforming growth factor beta, tgfb1a, is linked to the development of the lateral line, as well as the formation of proper skeletal muscle bundles (Kim and Ingham 2009; Xing et al. 2015). The adaptor protein complex -1, ap1s1, is responsible for vesicle formation, critical for shuttling proteins in the Golgi network (Nakatsu et al. 2014).

Knockout of the entire complex is embryonic lethal (Zizioli et al. 1999); however, knockdown studies of the ap1s1 subunit have demonstrated its role in central nervous system development (Montpetit et al. 2008). Additionally, ap-1 binding sites are located near bdnf promoters and this complex forms a positive feedback loop with bdnf expression (Gaiddon et al. 1996; Huynh and Heinrich 2001; Tuvikene et al. 2016).

A comparison of these low molecular weight PFAS alternatives, PFHxA, PFHxS and 6:2 FTOH, has not yet been assessed in the zebrafish model. The present study aims to determine the toxicity profiles of PFHxA, PFHxS, and 6:2 FTOH in zebrafish following low dose developmental exposure. Exposure to PFOS and PFOA caused unique morphological phenotypes and gene expression profiles in zebrafish (Jantzen et al. 2016a). The goal of the present study was to compare these findings to low molecular weight alternatives, and possibly identify similarities across chain length and terminal groups. This information will contribute to the development of novel adverse outcome pathways (AOPs) for these compounds.

2.2 Methods

2.2.1 Zebrafish Husbandry:

Zebrafish, strain AB (Zebrafish International Resource Center, Eugene, OR) were housed in Aquatic Habitat (Apopka, FL) recirculating systems. Municipal water supplies following sand and carbon filtration filled the systems. Water quality was monitored monthly to ensure water was maintained at <0.05 ppm nitrite, <0.2 ppm ammonia, DO, and 7.2-7.7 pH. The temperature was monitored twice daily to ensure that tank water was held between 26 and 28 °C. Fish were maintained on a 14:10 hour light: dark cycle, and fed twice daily a diet of artemia in the mornings and aquatox/tetramin flake mix in the evenings. All experiments were conducted following Rutgers University Animal Care and Facilities Committee guidelines under the zebrafish husbandry and embryonic exposure protocol (08-025).

2.2.2 Experimental Setup

Stock solutions of PFHxA (perfluorohexanoic acid, Oakwood Chemical, Estill, SC), 6:2 FTOH
(1H,1H,2H,2H-perfluorooctan-1-ol, Sigma Aldrich, St. Louis MO), and PFHxS
(trideafluorohexane-1-sulfonic acid potassium salt, Sigma Aldrich) were prepared at
concentrations of 2000 µM in egg water. Table 2.1 outlines the chemical structure of these
compounds. Embryos were exposed to static, non-renewed, nominal concentrations of each
compound. Figure 2.1 outlines the exposure paradigm, modified from OECD 212 (OECD 1998).
For each treatment, healthy embryos were selected at approximately 3 hpf (hours post
fertilization) where staging ranged from the 1000 cell to high stage (Kimmel et al. 1995).
Exposures were continued to 120 hpf, or 5 days post fertilization (dpf), when hatched larvae were
in the sac fry stage. All experiments had >85% control survival.

2.2.3 LC_{50} Determination

Embryos at 3 hpf were placed into individual glass vials containing 1 mL of nominal
concentrations of PFHxA, PFHxS, and 6:2 FTOH ranging from 0-1000 µM. Fifteen embryos were
selected per treatment group, and embryos were monitored daily with total mortality established
at 5 dpf. Experimental replicates were completed with all doses of one compound, and each
experiment was independently replicated 3 times. Determination of LC_{50} values was completed
as outlined in the following (Litchfield and Wilcoxon 1948).

2.2.4 Morphometric Analysis

Low doses of 0, 0.02, 0.2, and 2 µM PFAS were selected to remain below the LC_{50} determined in
the present study and align with low doses of long chain PFASs tested in the zebrafish model
(Jantzen et al. 2016a). A high dose (20 µM) study was carried out after the initial low dose study.
For both studies fifteen embryos were individually reared in glass vials and exposed to 1 mL of
treated or control egg water. Static, non-renewed exposures were continued until 120 hpf (Figure
2.1), at which point egg water was removed and replaced with 10% buffered formalin to fix the
larvae for further analysis. The fixed larvae were stained following an acid-free alcian blue-

alizarin red protocol, which allows for visualization of the cartilage and yolk membranes of the larvae (Walker and Kimmel 2007).

Photographs of each sample were collected using an Olympus SZ-PT dissecting microscope mounted with a Scion digital camera (CFW-1310C). Measurements were taken using Photoshop CS2 for the following endpoints: total body length, yolk sac area, and pericardial sac area. Measurements in pixels were normalized to ruler length in Photoshop. Three independent experiments were completed which each consisted of 15 animals per dose. Mean and standard error were calculated for each endpoint in each treatment group.

2.2.5 Gene Expression Analysis

Twenty-five embryos were group housed in 20 mL glass vials and exposed to 8 mL of treated 0, 0.2, 2, or 20 µM PFAS in egg water. Each experiment contained 4-5 vials per treatment. At 24 hpf, dead embryos were removed from the vials to prevent fungal growth. Static, non-renewed exposures were continued until 120 hpf, at which point larvae were snap frozen in liquid nitrogen. RNA was isolated following Sigma's RNAzol protocol. Purity was assessed using a NanoDrop 1000 Spectrophotometer (ThermoScientific), RNA with A260/280 below 1.7 were excluded from analysis. RNA concentrations were diluted to 200 ng/µL in RNase-free water. RNA was converted into cDNA using the High Capacity Reverse Transcription Kit (Applied Biosystems, ThermoFisher). Gene expression was quantified via qPCR using iQ^{TM} SYBR® Green Supermix (Biorad, Hercules CA) in a Biorad iCylcer iQ machine. The qPCR protocol used was 35 cycles of 95°C for 15 seconds and 60°C for 60 seconds. The primers used in this study are outlined in Table 2. Standard curves were used to generate transcript numbers, which were normalized to *actb* as a housekeeping gene. Outliers were determined as values exceeding 2 standard deviations from the mean. All experiments were independently replicated three times, and the transcript numbers were combined to determine the mean and standard error (SEM) for each treatment.

2.2.6 Statistical Analyses

Statistical analysis was completed using SigmaPlot[TM] 11.0 software. One-way analysis of

variance (ANOVA) were completed to compare across concentrations for each compound,

followed by either a Bonferroni post hoc test or Student T test, when data passed normality and

variance tests. High dose morphometrics were analyzed via Mann-Whitney rank sum T test.

Significance was set at $p < 0.05$.

2.3 Results

2.3.1 Lethality and Morphometric Effects of PFAS Exposures at 5 dpf Sac Fry Larvae

Within Table 2.3 are summarized the dose response data for PFHxA, PFHxS, and 6:2 FTOH at 5

dpf. PFHxA was determined to be the most toxic to the developing zebrafish with an LC_{50} of 290

µM. The LC_{50} values for PFHxS and 6:2 FTOH were 340 and 830 µM, respectively. The full dose

response curves of mortality are depicted in Figure A1. It was observed during this study that

there was a delayed onset of death with exposure to PFHxS, which occurred post-hatch between

4 and 5 dpf.

Morphometric analysis was carried out on 5 dpf sac fry larvae following low dose PFAS

exposures (0, 0.02, 0.2, and 2 µM), and the results are summarized in Table 2.4A. Following

exposure to 0.2 µM PFHxA, sac fry larvae had significantly decreased total body length and yolk

sac area compared to controls. However, these effects were not dose-dependent and not

observed at other doses examined. PFHxS exposure at 2 µM caused a significant increase in

total body length. There was a significant decrease in total body length of larvae exposed to 0.02

µM 6:2 FTOH, but this same effect was not observed at higher concentrations. In addition,

PFHxS and 6:2 FTOH did not have any significant effect on yolk sac area. Pericardial sac area

was measured, and no edema or significant increases in pericardial area were observed (data not

shown).

A high dose exposure of 20 µM was also completed to determine if higher concentrations were

necessary to elicit morphological effects because these compounds have been reported to be

less toxic than their long chain PFAS counterparts (Wang et al. 2015). Significant morphometric effects were observed following exposure to 20 µM PFHxS (Table 2.4B), where larvae were significantly larger and had significantly increased yolk sac areas compared to controls. No significant effects in total length or yolk sac area were observed following exposure to 20 µM PFHxA or 6:2 FTOH. Pericardial area was also not significantly increased with any of the experimental compounds (data not shown).

2.3.2 Changes in Gene Expression with PFAS Exposures at 5 dpf

Gene expression was completed after a 5 day developmental exposure of 0, 0.2, 2, and 20 µM PFHxA, PFHxS, and 6:2 FTOH. Slight changes in expression of oatp transporters, *slco2b1* and *slco1d1*, were observed in 5 dpf sac fry larvae (Figure 2.2). There was a small, approximately 25%, but significant decrease in expression of *slco2b1* with exposure to 2 µM PFHxA; however, at 20 µM PFHxA this trend was not observed (Figure 2.2A). Expression of *slco2b1* was significantly increased in the 2 µM 6:2 FTOH treatment group. Fold change gene expression of *slco1d1* did not vary significantly from controls at all concentrations of PFHxA and PFHxS (Figure 2.2B). There was a small significant increase in expression following exposure of 20 µM 6:2 FTOH. Overall, dose-dependent changes in *slco2b1* and *slco1d1* gene expression were not observed with exposures to these compounds.

The other genes examined, *tgfb1a*, *bdnf*, and *ap1s1,* were more sensitive to PFAS exposures (Figure 2.3). Transforming growth factor beta 1a, *tgfb1a,* expression was significantly increased at all 3 doses of PFHxA examined (Figure 2.3A). Similarly, there was a significant dose-dependent increase in *tgfb1a* expression, at all doses of 6:2 FTOH. This was not observed with exposure to PFHxS, where a trend of decreased *tgfb1a* was observed. At 20 µM 6:2 FTOH, there was an increase in *tgfb1a* transcript levels. Expression of brain-derived neurotrophic factor, *bdnf,* trended towards an increase with developmental exposures to all PFASs (Figures 2.3B). Significant increases were observed at 20 µM PFHxA, 2 µM PFHxS, and 20 µM 6:2 FTOH. Adaptor related protein complex, *ap1s1,* expression followed a dose-dependent increase with

PFHxA exposure (Figure 2.3C). There was a large increase in expression at 2 and 20 µM PFHxA, 3.63- and 13.2-fold, respectively. Exposure to 6:2 FTOH caused a smaller increase in *ap1s1* expression at 20 µM 6:2 FTOH. In contrast, there was a significant decrease in *ap1s1* expression at 0.2 µM PFHxS.

2.4 Discussion

2.4.1 General Conclusions

There are fewer studies examining the toxicity of low molecular weight PFASs, but this work suggests that each of these alternatives poses unique health risks. The morphological endpoints following exposure to the low molecular weight PFASs are not the most sensitive adverse outcome related impacts. Significant increases in body length and yolk sac at 2 and 20 µM PFHxS were the only monotonic morphological response observed (Table 2.4). These doses are reported to be above typical environmentally-relevant concentrations (Ahrens 2011; Sullivan 2018). Changes in gene expression, however, were observed at the environmentally-relevant doses of these compounds. Significant changes in *bdnf*, *tgfb1a*, and *ap1s1* transcript levels were observed with 0.2 µM concentrations of PFHxA, PFHxS, and 6:2 FTOH (Figure 2.3). Therefore, these compounds may be eliciting effects at low doses on critical biochemical pathways through altered gene expression. The question remains as to whether these alterations in gene expression will be manifested at protein and higher levels of organization.

This study identifies some genetic targets for PFHxA, PFHxS, and 6:2 FTOH: *slco2b1*, *slco1d1*, *bdnf*, *tgfb1a*, and *ap1s1*. These genes were selected based on previous data from our lab with similar developmental exposure to long chain PFASs (Jantzen et al. 2016a; Jantzen et al. 2016b; Jantzen et al. 2017). The effects observed following the low molecular weight PFAS exposures would support the premise that shared molecular pathways exist for the long chain PFASs and low molecular weight alternatives. In addition, *bdnf*, *tgfb1a,* and *ap1s1* exist in interrelated pathways, and can be related to the morphological effects observed at higher doses. These gene candidates may be related to molecular initiation events and associated pathways that lead to

phenotypic outcomes, related to the AOPs of these compounds (OECD 2016). From these gene expression findings, it is possible that neural AOPs are impacted by low molecular weight PFAS alternatives, and other outcomes related to these pathways will be examined in later chapters of this dissertation.

There were few changes in expression of the transporters, *slco2b1* and *slco1d1*, with exposure to these compounds. While interaction with long chain PFASs is reported in the literature, fewer studies have examined these low molecular weight alternatives (Cheng and Klaassen 2008; Kudo et al. 2002; Popovic et al. 2014; Weaver et al. 2010; Yang et al. 2010). In the present study, small and non-dose-dependent fold changes of gene expression were observed. This differed from the gene expression of 5 dpf larvae exposed to long chain PFASs. For example, developmental exposure to 2 µM PFOA caused a 2-fold induction of *slco2b1* and PFOS caused an 8-fold induction (Jantzen et al. 2016a). Effects on the transcription level of both transporters persisted into adulthood where a significant down-regulation were observed with exposure to PFOS (*slco1d1* and *slco1d1*) and PFOA (*slco1d1*) (Jantzen et al. 2016b). A contributing factor to the lack of response in gene expression in this study may be that RNA was collected from whole body larvae as opposed to organ systems. This whole-body approach disregards the tissue-specific expression pattern of these transporters (Popovic et al. 2010) and may explain the lack of change observed in transporter gene expression. Additionally, there is overlap of substrates, which might offset any effects to a specific transporter (Klaassen and Aleksunes 2010). While the protein and functional status of these transporters were not studied, these compounds do not target *slco2b1* or *slco1d1* gene expression levels in this developmental model at the whole body larval level.

2.4.2 Toxicity Profile for PFHxA Exposure in Zebrafish

At the 0.2 µM PFHxA dose, there was a significant reduction in the overall length and yolk sac size of the 5 dpf larvae; however, this observation was not observed at higher doses (Table 2.4A). Due to the nonmonotonic response for these endpoints, it may be that the doses examined

in this study are below the LOEL. In *Xenopus*, the lowest concentration of PFHxA where reduced body length was observed was 1000 µM (Kim et al. 2015). Similarly, studies in adult rats of up to 200 mg/kg/day for subchronic and chronic periods of exposure had no effects on growth (Chengelis et al. 2009b; Klaunig et al. 2014).

The endpoints most affected by PFHxA exposure were the gene expression findings (Figure 2.3). While gene expression changes were observed, these changes did not translate to morphological effects in any of the endpoints examined with PFHxA exposure. The changes in gene expression might reflect biomolecular targets, revealing potential AOPs. All doses examined caused a significant induction in *tgfb1a* transcript expression, which is involved in the formation of muscle bundles in zebrafish (Kim and Ingham 2009). Therefore, there was the potential to target morphometric development, but this was not observed. Induction of *tgfb1a* was reported in a zebrafish non-alcoholic steatohepatitis and was also linked to the development of hepatocellular cancer (Yan et al. 2017). Taking into account the liver toxicity associated with the long chain carboxylate, PFOA, (Lau et al. 2007) and the liver toxicity noted at high doses of PFHxA (Chengelis et al. 2009b; Klaunig et al. 2014), the potential role of *tgfb1a* in these effects warrant further study.

There was also a dose-dependent increase in adaptor-related protein, *ap1s1,* expression with PFHxA exposure and a 13-fold induction of expression at 20 µM PFHxA (Figure 2.3C). This protein is responsible for vesicle formation and protein movement at a subcellular level, and ap1s1 has been found to be especially critical in development of the spinal cord, transporting acetylcholine (Montpetit et al. 2008; Nakatsu et al. 2014). The expression of *ap1s1* is related to that of *bdnf*, with *bdnf* able to promote expression of ap-1, the entire complex, and stimulates its activity (Gaiddon et al. 1996; Huynh and Heinrich 2001). Ap-1 may also be involved in a positive feedback loop with *bdnf* (Tuvikene et al. 2016), which would explain the increased *bdnf* expression observed in the present study at 20 µM PFHxA (Figure 2.3B). In addition, it has been reported in the literature that PFHxA accumulates in human brain tissue (Perez et al. 2013).

Together, this suggests that neural AOPs may be impacted with PFHxA exposure, and that the regulation of these two factors may be interrelated in this model.

One goal of this study was to compare the toxicity profile of PFHxA to PFOA in the developing zebrafish model, summarized in Table 2.5 (Jantzen et al. 2016a). The same endpoints in the present study are summarized in Table 2.6. There is evidence to suggest that PFHxA is less toxic than its long chain counterpart (Wang et al. 2015), but we anticipated a similar response due to the shared carboxylic acid moiety. Developmental exposure to 2 µM PFOA caused a decreased total body length and yolk sac edema at 5dpf (Jantzen et al. 2016a). However, no morphometric effects were observed at this time point in our studies with 2 or 20 µM PFHxA exposures. While gene expression of *ap1s1* and *slco2b1* were altered at 5 dpf for both compounds, the direction and level of change was not consistent, suggesting different AOPs are targeted by each compound.

2.4.3 Toxicity Profile for PFHxS Exposure in Zebrafish

In the present study, there was a post hatch delay in mortality with PFHxS exposure that was not observed with PFHxA or 6:2 FTOH. To our knowledge this endpoint has not been reported in *in vivo* studies with PFHxS. This may suggest that events later in development are targeted by PFHxS exposure and warrant further study. Additionally, there was a significant increase in total length observed at 2 and 20 µM PFHxS, and a significant increase in yolk sac area in the 20 µM treatment group (Table 2.4). This corresponds to the literature where increased weight was observed in male mice exposed for 42 days to 0.3 and 1 mg/kg/day PFHxS (Chang et al. 2018). However, similar studies in rats have reported no effect on body weight (Butenhoff et al. 2009a). The effects may be explained by the longer half-lives observed in mice than rats (Lau et al. 2007). In the zebrafish larvae, PFHxS exposure may be triggering or stimulating a pathway resulting in this observed increased growth.

PFHxS and PFOS differed in the phenotypes induced in the developing zebrafish. Data from PFOS exposures in Jantzen et al. 2016a are summarized in Table 2.5, and results from the

present study in Table 2.6. Following a 5 day exposure to 2 μM PFOS, the sac fry larvae were significantly smaller in length and yolk sac area compared to controls. The opposite effects were observed in the present study, where PFHxS caused a significant increase in length, at 2 and 20 μM, and a significant increase in yolk sac area at 20 μM (Table 2.4).

The gene expression data provides support that nervous system AOPs might be targeted following PFHxS exposure. There was an increase in neuronal growth factor *bdnf* at 2 μM PFHxS and decrease in *ap1s1* at 0.2 μM PFHxS (Figure 2.3B and C). Both factors are related to nervous system growth and development, as well as interrelated in expression (Germana et al. 2010a; Nakatsu et al. 2014; Tuvikene et al. 2016). Additionally, knockdown of ap1s1 early in zebrafish development led to disorganized fin morphology, decreased axonal processes, and a reduction in the number of interneurons (Montpetit et al. 2008). These endpoints were not evaluated in the present study but may manifest in behavioral effects and could be assessed as biomarkers in future studies.

2.4.4 Toxicity Profile for 6:2 FTOH Exposure in Zebrafish

In terms of LC_{50} values calculated in this study, 6:2 FTOH was the least toxic of the 3 compounds examined in 5 dpf zebrafish (Table 2.3). This was also reflected in the morphological data, where the only significant effect was a decrease in total body length observed at 0.02 μM 6:2 FTOH (Table 2.4). LC_{50} values have not been previously reported in zebrafish; however LOELs were established at 0.82 μM for effects on the gonadal somatic index in zebrafish and 10 μM for effects on the hepatosomatic index in medaka (Ishibashi et al. 2008; Liu et al. 2009). It is possible that the early stages of zebrafish development and morphological endpoints are less sensitive to 6:2 FTOH exposures.

Gene expression changes were observed following low dose exposures to 6:2 FTOH. There was a significant dose-dependent increase in *tgfb1a* transcript expression with 6:2 FTOH exposure (Figure 2.3A). Tgfb1a is necessary for proper muscle and lateral line development (Kim and Ingham 2009; Xing et al. 2015). An increase in gene expression of *ap1s1* and *bdnf* were

observed with exposure to 20 µM 6:2 FTOH. Bdnf is also involved in lateral line development (Germana et al. 2010a). Additionally, both *bdnf* and *ap1s1* are also related to central nervous system development and function (De Felice et al. 2014; Montpetit et al. 2008). Taken together, these data might suggest that, like PFHxS, the nervous system development is a target AOP.

Endpoints related to endocrine disruption were not examined in the present study; however, alterations to the endocrine system may explain the observed effects. One hallmark of endocrine disruptor toxicity is non-monotonic low dose effects (Vandenberg et al. 2012), and this might explain the decreased length in the 5 dpf larvae at 0.02 µM 6:2 FTOH. It is possible that endocrine function is related to the change in gene expression as well; 6:2 FTOH is reported to change expression patterns of reproductive hormones and receptors in tissues along the HPG, hippocampal-pituitary-gonadal, axis (Ishibashi et al. 2008; Liu et al. 2009).

2.4.5 Conclusions

The present study is the first demonstrating the LC_{50} values for the developing zebrafish model at 5dpf. These values were comparable for PFHxA and PFHxS at 290 and 340 µM, respectively. However, the LC_{50} of 6:2 FTOH was higher at 830 µM. Following 0.02-20 µM exposures to these C-6 alternatives, few morphological effects were observed in 5 dpf larvae. Gene expression of *bdnf*, *tgfb1a*, and *ap1s1* were altered at concentrations as low as 0.2 µM, proving to be the most sensitive endpoints and determining the LOEL in this study. These outcomes are summarized in Table 2.6.

In developmental studies of mice, PFHxA had an adverse effect on pup survivability with dam exposures of 175 mg/kg/day, which was the developmental LOEL (Iwai and Hoberman 2014). In similar studies of PFHxS, up to 10 mg/kg/day elicited effects in the parental mice, but no adverse developmental outcomes were observed (Butenhoff et al. 2009a; Chang et al. 2018). Exposures of 125 mg/kg/day 6:2 FTOH impacted both F_0 and F_1 endpoints (Serex et al. 2014). Together, these studies demonstrate a LOEL of 125-175 mg/kg/day for developmental exposures to the low

molecular weight PFASs, and these values are roughly ten-fold higher than the high dose in the present study.

Finally, each low molecular weight alternative elicited a different pattern of effects at the cellular and tissue levels in a growth AOP. This suggests that PFAS chain length does not drive toxicity. Similarly, in comparison with long chain PFASs, there does not appear to be consistent profiles within terminal groups (Jantzen et al. 2016a). In addition, morphometric and gene expression alterations following C-8/C-9 PFAS exposures were observed at lower concentrations than the C-6 compounds in the present study. Therefore, the low molecular weight alternatives are less toxic than long chain PFASs in the developing zebrafish.

Table 2.1. Chemical structures of perfluorohexanoic acid (PFHxA), perfluorohexane sulfonate (PFHxS), and 6:2 fluorotelomer alcohol (6:2 FTOH).

Figure 2.1. Exposure paradigm of all experiments. Waterborne PFAS exposures began at 3 hours post fertilization (hpf) and continued until 120 hpf. Endpoint examined in the sac fry larvae include LC$_{50}$ determination, morphometrics, and gene expression.

Table 2.2. Gene name, ID, function, and primers (5'-3') utilized in this study.

GENE		GENE ID	FORWARD PRIMER	REVERSE PRIMER	FUNCTION
actb	beta-actin	NM_131031	CGAGCAGG AGATGGGA ACC	CAACGGAA ACGCTCATT GC	House-keeping gene
slco2b1	Solute carrier organic anion transporter family member 2b1	NM_001037678	TTGCCCTG CCTCACTTC ATT	AGGCTGGA GTTGAGTC TGGT	Organic anion transporter
slco1d1	Solute carrier organic anion transporter family member 1d1	NM_001348086	GCCGCATT TCTTCCAAG GAC	TGTAAGGC ACGGCAGA ACAT	Organic anion transporter
tgfb1a	Transforming growth factor beta 1a	NM_182873	CCAGCAGA GCACGGAT AAGT	TCATATCTG CCAGACCA GCG	Muscle development
ap1s1	Adaptor related protein complex 1 sigma 1 subunit	NM_200309	CCGTCGAA ATGATGCG CTTT	GTACTTATC CAGCACCA CCTG	Vesicle formation
bdnf	Brain-derived neurotrophic factor	NM_131595	AGGTCCCC GTGACTAAT GGT	CGCTTGTC TATTCCTCG GCA	Neuron development

Table 2.3. Calculated LC$_{50}$ and 95% confidence intervals for PFHxA, PFHxS, and 6:2 FTOH at 5 dpf.

	LC$_{50}$ (µM)	95% Confidence Interval
PFHxA	290	266.4 – 315.6
PFHxS	340	316.3 – 365.5
6:2 FTOH	830	808.1 – 852.5

Table 2.4. Measurements of total body length (mm) and yolk sac area (mm^2) at 5 dpf following exposure to PFHxA, PFHxS and 6:2 FTOH. (A) Values indicate mean and standard error of measurements. An asterisk (*) indicates $p<0.05$, one-way ANOVA on ranks, N=36-40. (B) Morphometric measurement at 5 dpf following exposure to 20 µM PFHxA, PFHxS and 6:2 FTOH. Values indicate mean and standard deviation of measurements. An asterisk (*) indicates $p<0.05$, Mann Whitney Rank Sum test, N=38-45.

A.

	CONCENTRATION (µM)			
Compound	**0**	**0.02**	**0.2**	**2**
	TOTAL BODY LENGTH (mm)			
PFHxA	4.15 ± 0.023	4.23 ± 0.027	**3.96 ± 0.032***	4.21 ± 0.029
PFHxS	4.08 ± 0.027	4.02 ± 0.022	4.04 ± 0.019	**4.24 ± 0.024***
6:2 FTOH	4.44 ± 0.027	**4.34 ± 0.029***	4.39 ± 0.025	4.48 ± 0.025
	YOLK SAC AREA (mm^2)			
PFHxA	0.294 ± 0.0058	0.300 ± 0.0073	**0.242 ± 0.0094***	0.303 ± 0.0065
PFHxS	0.299 ± 0.0051	0.286 ± 0.0093	0.304 ± 0.0066	0.285 ± 0.0057
6:2 FTOH	0.306 ± 0.0096	0.298 ± 0.0074	0.291 ± 0.0062	0.302 ± 0.0061

B.

	20 µM			
	Control	**PFHxA**	**PFHxS**	**6:2 FTOH**
Total Body Length (mm)	3.97 ± 0.026	4.00 ± 0.034	**4.11 ± 0.050***	3.98 ± 0.044
Yolk Sac Area (mm^2)	0.293 ± 0.0064	0.287 ± 0.0064	**0.323 ± 0.0078***	0.303 ± 0.0062
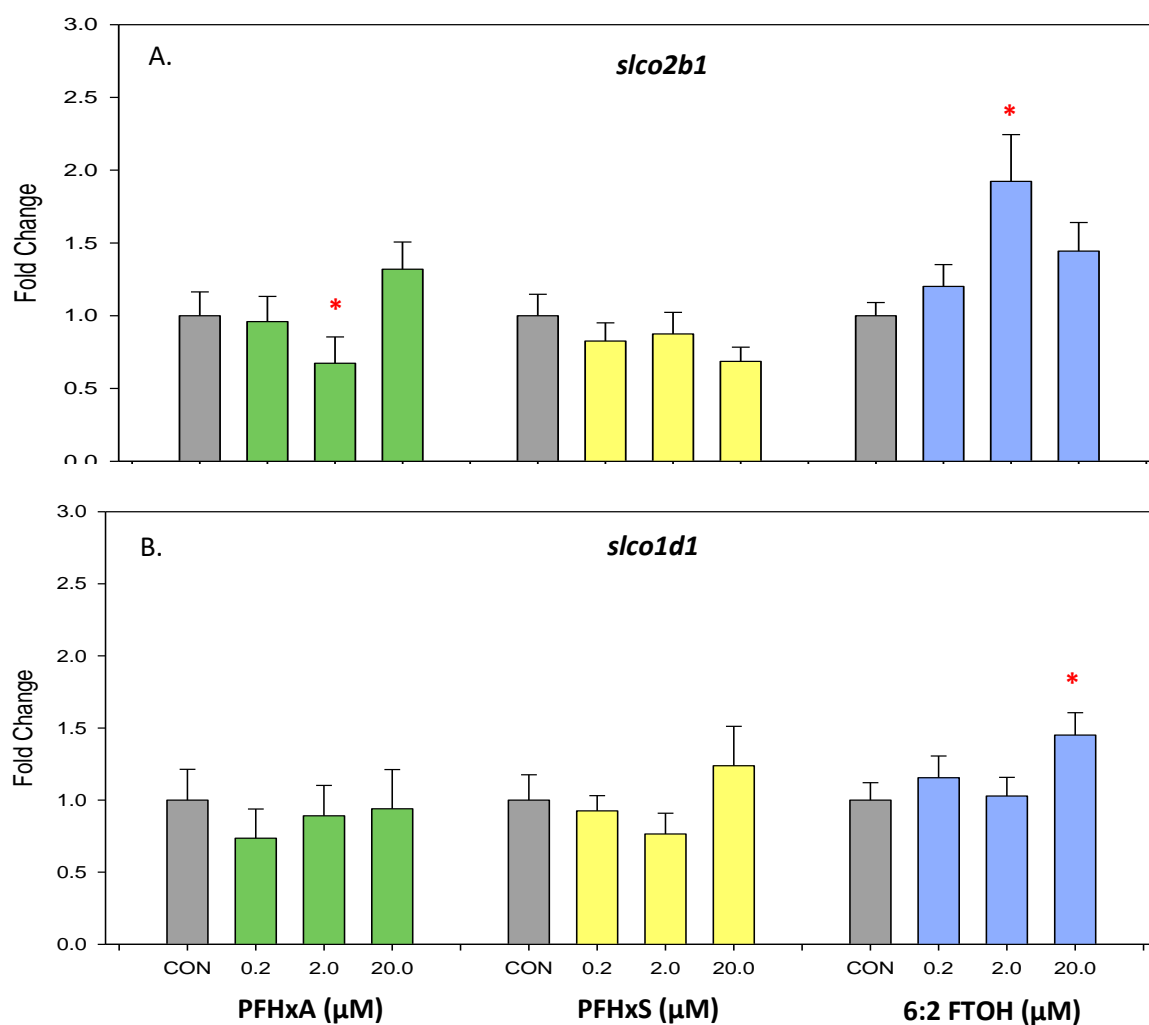
Figure 2.2. Gene expression of slco transporters at 5 dpf following exposure to 0, 0.2, 2, and 20 µM PFHxA, PFHxS, or 6:2 FTOH. Gene expression represented as mean and standard error (SEM) fold change of (A) *slco2b1* (B) *slco1d1*. An asterisk (*) indicates $p < 0.05$, one-way ANOVA, N=8-14.
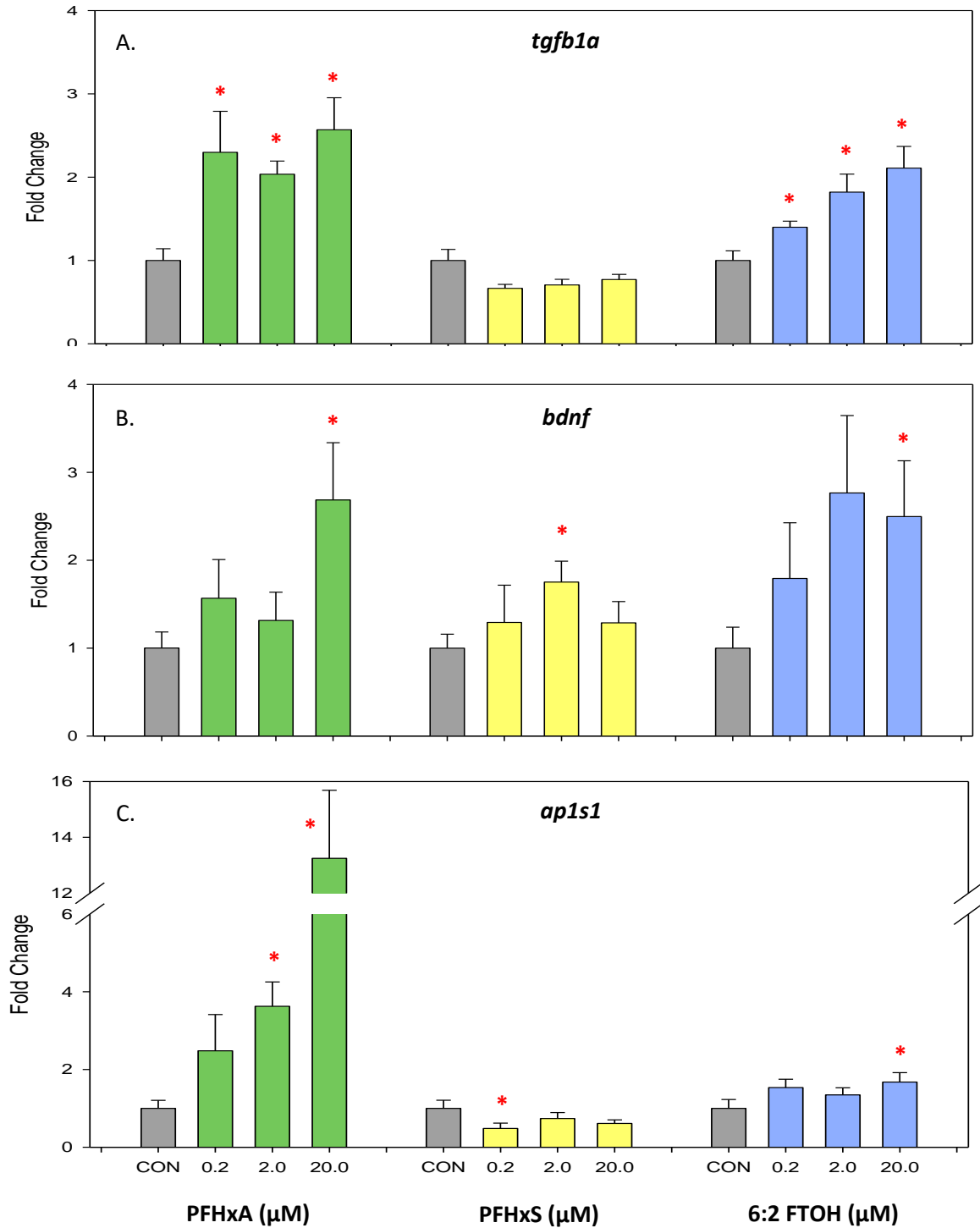
Figure 2.3. Gene expression of *tgfb1a*, *bdnf*, and *ap1s1* at 5 dpf following exposure to 0, 0.2, 2, and 20 µM PFHxA, PFHxS, or 6:2 FTOH. Gene expression represented as mean and standard error (SEM) fold change of (A) *tgfb1a,* transforming growth factor (B) *bdnf*, brain-derived neurotrophic factor (C) *ap1s1,* adaptor related protein complex. An asterisk (*) indicates $p < 0.05$, one-way ANOVA, N=8-14.

Table 2.5. Summary of findings in 5 dpf zebrafish following 2 µM PFOA, PFOS, and PFNA exposures during the same developmental window as the present study (Jantzen et al. 2016a). Up arrows indicate a significant increase, down arrows indicate a significant decrease, and "N.S." indicates no significance difference from controls.

	2 µM PFOA	2 µM PFOS	2 µM PFNA
MORPHOMETRICS			
Total Body Length	⬇	⬇	⬇
Yolk Sac area	⬆	⬇	⬆
GENE EXPRESSION			
slco2b1	⬆	⬆	⬇
tgfb1a	**N.S.**	⬇	⬇
ap1s1	⬇	⬇	⬇

Table 2.6. Summary of morphometric and gene expression findings in the present study following 2 and 20 µM PFHxA, PFHxS, and 6:2 FTOH in 5 dpf larvae. Up arrows indicate a significant increase, down arrows indicate a significant decrease, and "N.S." indicates no significance difference from controls.

	PFHxA		PFHxS		6:2 FTOH	
	2 µM	20 µM	2 µM	20 µM	2 µM	20 µM
MORPHOMETRICS						
Length	N.S.	N.S.	↑	↑	N.S.	N.S.
Yolk Sac Area	N.S.	N.S.	N.S.	↑	N.S.	N.S.
GENE EXPRESSION CHAPTER 2						
slco2b1	↓	N.S.	N.S.	N.S.	↑	N.S.
slco1d1	N.S.	N.S.	N.S.	N.S.	N.S.	↑
tgfb1a	↑	↑	N.S.	N.S.	↑	↑
bdnf	N.S.	↑	↑	N.S.	N.S.	↑
ap1s1	↑	↑	N.S.	N.S.	N.S.	↑

CHAPTER 3

Morphological and Behavioral Effects in 14 dpf Larval Zebrafish Following a Developmental

Exposure to PFHxA, PFHxS, and 6:2 FTOH

3.1 Introduction

Perfluoroalkylated substances (PFASs), such as PFOS and PFOA, have been associated with a

number of developmental effects (Lau 2012; Lau et al. 2007; Tsuda 2016). These outcomes

coupled with their prevalence in the water supplies and human serum samples have raised

concern over potential exposures (Hu et al. 2016; Khalil et al. 2016; Pan et al. 2018; Post et al.

2013). The EPA has established a combined limit for PFOS and PFOA at 70 ppt (ng/L) (USEPA

2014; USEPA 2017a). This has led to the use of PFAS alternatives, such as the C-6 compounds,

in manufacturing processes, and subsequently, a greater number of these alternatives have

appeared in water supplies (Pan et al. 2018; Wang et al. 2013b). Short chain PFASs, including

PFHxA and PFHxS, have been used as long chain PFAS alternatives because they have shorter

half-lives and are generally assumed to be safe (Conder et al. 2008; Wang et al. 2015). However,

few studies to date have been completed to assess the toxicity of these compounds. The C-6

fluorotelomer, 6:2 FTOH has been used as an alternative to long chain PFASs and as a precursor

in the manufacturing of C-6 PFASs (Gomis et al. 2015; Rice 2015; Wang et al. 2013b). Due to the

rapid metabolism and few toxic outcomes observed with 6:2 FTOH (Martin et al. 2005; O'Connor

et al. 2014; Serex et al. 2014), this compound was selected as a negative control of fluorinated

chain length in this study.

The zebrafish model is well-established for its use for screening potential developmental toxicants

and its high homology to human genes and pathways (Howe et al. 2013). In addition, behavioral

patterns in larval fish have been studied so that high throughput behavioral assays are possible,

with outcomes that translate to rodent work (Champagne et al. 2010; Orger and de Polavieja

2017; Reif et al. 2016). The effects of developmental long chain PFAS exposures on behavioral

outcomes have been examined in the zebrafish model (Hagenaars et al. 2014; Jantzen et al.

2016a; Ulhaq et al. 2013b). However, this has not been examined with PFHxA, PFHxS, or 6:2 FTOH exposures. One study in mice identified that a single developmental dose of PFHxS was able to impact behavioral effects in the adults (Viberg et al. 2013). Therefore, the current study will address this gap in the toxicological literature.

Hepatotoxicity, specifically lipid accumulation in the liver, is a well-reported outcome of PFAS exposures (Lau 2012; Lau et al. 2007). Originally proposed to be a consequence of PPARα activation (Sohlenius et al. 1992), markers of liver toxicity have been observed in pparα-null models demonstrating that other pathways are targeted (Abbott et al. 2009; Albrecht et al. 2013; Das et al. 2017; Rosen et al. 2010). Pparα activity and expression profiles vary across species (Choudhury et al. 2000). This coupled with the species-specific half-lives of the PFASs raises concern for use of rodent models examining PFAS toxicity (Lau et al. 2007; Stahl 2011). The zebrafish model has been recognized for its similarities to human responses to pparα agonists (Den Broeder et al. 2015; Ibabe et al. 2005a; Ibabe et al. 2005b). Additionally, a number of studies have verified the presence of liver steatosis in adult zebrafish with PFOS exposures (Cheng et al. 2016; Cui et al. 2017; Fai Tse et al. 2016) . The lipid staining experiment in this study aimed to determine if larval zebrafish responded similarly and to compare the results of the low molecular weight PFAS alternatives with the results from long chain PFASs.

In the present study, behavioral, morphometric, and lipid staining endpoints were assessed at varying concentrations of PFHxA, PFHxS, and 6:2 FTOH in 14 dpf zebrafish larvae. Larvae were exposed to waterborne concentrations of these compounds from 3 to 120 hpf and a 9 day depuration, or washout, period. Endpoints were assessed in 14 dpf larvae, demonstrating the persistence of responses to these compounds. The behavioral endpoints chosen for assessment were based on previous work from our lab examining developmental exposures of long chain PFASs (Jantzen et al. 2016a). Therefore, the results from this study will not only contribute to the toxicity profiles of the C-6 compounds, but also allow for a direct comparison to the C-8/C-9 PFASs using similar paradigms.

3.2 Methods

3.2.1 Zebrafish Husbandry:

Zebrafish, strain AB (Zebrafish International Resource Center, Eugene, OR) were housed in Aquatic Habitat (Apopka, FL) recirculating systems. Municipal water supplies following sand and carbon filtration filled the systems. Water quality was monitored monthly to ensure water was maintained at <0.05 ppm nitrite, <0.2 ppm ammonia, DO, and 7.2-7.7 pH. The temperature was monitored twice daily to ensure that tank water was held between 26 and 28 °C. Fish were maintained on a 14:10 hour light: dark cycle, and fed twice daily a diet of artemia in the mornings and aquatox/tetramin flake mix in the evenings. All experiments were conducted following Rutgers University Animal Care and Facilities Committee guidelines under the zebrafish husbandry and embryonic exposure protocol (08-025).

3.2.2 Experimental Setup

Stock solutions of PFOA (perfluorooctanoic acid, Sigma Aldrich, St. Louis MO), PFOS (perfluorooctane sulfonate, Sigma Aldrich), PFNA (perfluorononanoic acid, Sigma Aldrich), PFHxA (perfluorohexanoic acid, Oakwood Chemical, Estill, SC), PFHxS (trideafluorohexane-1-sulfonic acid potassium salt, Sigma Aldrich), and 6:2 FTOH (1H,1H,2H,2H-perfluorooctan-1-ol, Sigma Aldrich) were prepared at concentrations of 2000 μM in egg water. Table 3.1 contains the chemical structure of these compounds. Embryos were exposed to static, non-renewed, nominal concentrations of each compound. Figure 3.1 outlines the exposure paradigm, modified from OECD 212 (OECD 1998). For each treatment, healthy embryos were selected at approximately 3 hpf (hours post fertilization) where staging ranged from the 1000 cell to high stage (Kimmel et al. 1995). Exposures were continued through hatch until larvae reached the sac fry stage at 5 days post fertilization (dpf), at which point larvae were transferred into treatment-free water and reared until analysis was completed on larvae at 14 dpf. All experiments had >85% control survival.

3.2.3 Behavioral Analysis

Twenty-five embryos were selected and exposed 3-120 hpf (Figure 3.1) to 8 mL of 0, 0.2, 2, or 20 µM PFHxA, PFHxS or 6:2 FTOH. Three to four vials were established per treatment per experiment. At 120 hpf, larvae were removed from the vials into beakers containing treatment-free system water. Larvae were reared in an incubator held between 26-27°C with 14:10 hour light: dark cycle. At 120 hpf, a feeding regiment was established, twice daily Ziegler Larval AP50 (Aquatic Habitats). At 14 dpf, the larvae were assessed for behavioral endpoints. The larvae were individually transferred into 1.5 mL system water per well in a clear-bottomed 24 well plate. The treatments were randomized throughout the plate.

Plates were placed in the behavior room 1hour prior to recording with all lights on to allow for the larvae to acclimate to the novel surroundings (Metz et al. 2006). After 1 hour, the lights were turned off and recording under infrared filter began using Noldus Ethovision (Leesburg, VA) tracking software. All experimentation was restricted to 1-4 pm, when variability due to larval circadian rhythm is minimized (MacPhail et al. 2009). Four cameras were set to record 4 plates for a 30 minute period. Two recordings were completed each afternoon. Therefore, each experimental setup was recorded on 8 plates and videos. The experimental replicate was independently repeated.

Videos were analyzed through Ethovision XT Software. The parameters analyzed were total distance traveled, cross frequency (the number of crosses through the center of the arena), and mean velocity over the 30 minute assay. Each plate was considered a plate replicate with 7-8 plates in total analyzed per compound. Outliers were defined as points outside of 3 standard deviations of the mean for all control data for each endpoint. Mean values were then determined per compound concentration per plate replicate. Statistical analysis was completed on these values. Values were separated into 10 minute time bins to differentiate initial startle response from delayed responses. Total distance, number of crosses, and mean velocity are reported for each time bin, 0-10, 10-20, or 20-30 minutes, and cumulative across the assay 30 minute assay. The data from individual larval was utilized to generate the figures in the supplemental data.

3.2.4 Morphometric Analysis

Following behavioral analysis, twenty larvae from each treatment were randomly selected for lipid

staining, using an Oil Red O (ORO) dye for neutral lipids. Samples were fixed in 10% buffered

formalin in individual vials. The staining protocol utilized was described in the following (Mehlem

et al. 2013). Exposures of 0.02, 0.2, and 2 μM PFOS, PFOA, and PFNA were completed

following the same exposure paradigm (Figure 3.1). These samples were also stained with ORO.

Photographs of each sample were collected using an Olympus SZ-PT dissecting microscope

mounted with a Scion digital camera (CFW-1310C). ImageJ software was used to measure total

length, liver area, and stained neural area, as outlined in Figure 3.5. Stain intensity was

measured in the liver and neural regions by normalizing mean pixel intensity in these regions to

background levels. Two independent experiments were completed which each consisted of 20

animals per dose. Mean and standard error of the mean were calculated for each endpoint in

each treatment group.

3.2.5 Statistical Analyses

Statistical analysis was completed using SigmaPlot^{TM} 11.0 software. One-way analysis of

variance (ANOVA) were completed to compare across concentrations for each compound,

followed by either a Bonferroni post hoc test or Student T test, when data passed normality and

variance tests. Regression analysis was completed on behavioral endpoints in supplemental

figure S1. Significance was set at $p < 0.05$.

3.3 Results

3.3.1 Changes in Larval Locomotor Behavior with PFAS Exposures at 14 dpf

A locomotion assay was completed in larvae at 14 dpf following a 5 day developmental exposure

to 0, 0.2, 2, and 20 μM PFHxA, PFHxS, or 6:2 FTOH and 9 days in treatment-free water. The 30

minute assay was divided into 10 minute time bins to differentiate between the initial startle

response from the change in light stimulus and the following effects on acclimation. Figure 3.2 shows the mean distance traveled within each time bin as well as cumulative over the entire assay. PFHxA exposure did not affect distance traveled (Figure 3.2A). Following 20 µM PFHxS exposure, there was a significant decrease in total distance traveled during the behavioral assay, as a cumulative distance, as well as in the 0-10 and 10-20 minute time bins (Figure 3.2B). Exposure to 6:2 FTOH increased distance traveled, where a significant increase in distance was observed at 2 µM in the 0-10 minute time bin and cumulatively (Figure 3.2C). Increased travel in young larvae allows for increased possibility of predation.

Figure 3.3 contains the cross frequency throughout the assay. Exposure to PFHxA at all doses did not cause effects on cross frequency (Figure 3.3A). Exposure to 20 µM PFHxS caused a significant decrease in larval crossing over the course of the assay; however, this was not significant within any of the individual time bins (Figure 3.3B). There were no observed changes in cross frequency with exposure to 6:2 FTOH at any dose (Figure 3.3C).

Velocity was also recorded in the locomotion assay, and these values are represented as the mean for each 10 minute time bin (Figure 3.4). PFHxA exposure caused no significant effects on larval velocity (Figure 3.4A). Similarly, no significant changes in velocity were observed with exposure to PFHxS (Figure 3.4B). In this assay, velocity typically decreases over time (Emran et al. 2008; Kristofco et al. 2016; MacPhail et al. 2009), and this is evident in the controls and PFHxA- and PFHxS-exposed larvae. However, this decrease in velocity is absent with exposure to 20 µM 6:2 FTOH (Figure 3.4C). Exposure to 6:2 FTOH caused a significant increase in mean velocity compared to controls in the 10-20 and 20-30 minute time bins. Velocity typically decreases over time following the initial startle response with the change in photostimulus at the startle of the assay (MacPhail et al. 2009). However, the 6:2 FTOH-exposed larvae lack assimilation, and velocity remained increased over the course of the assay.

Data from individual larvae was utilized to generate the figures in the supplemental data. Figure A2 contains the control data from each treatment group in terms of the total distance traveled and

cross frequency over the course of the assay. Sigmaplot curve fitting software selected linear regression as the best fitting model, and there was a significant linear relationship between total distance and cross frequency. Neither variable produced a significant relationship with velocity (data not shown). Scatterplots of all 3 behavioral endpoints were generated for control and the two highest concentrations of each compound to determine if any subpopulation behavioral phenotypes were apparent, but none were observed (Supplemental Figures A3-5).

3.3.2 Alterations in Morphometrics and Lipid Staining: PFHxA, PFHxS, and 6:2 FTOH

Total body length was measured for each larva, and results are summarized in Table 3.2. There was a significant increase in length following exposure to 0.2 and 2 μM PFHxS compared to controls. No effects on length were observed with exposure to any concentration of PFHxA or 6:2 FTOH.

As liver toxicity and altered lipid metabolism are often associated with PFAS exposures (Lau 2012), liver area and lipid stain accumulation were measured in ORO-stained larvae at 14 dpf. A representative image of an ORO-stained control larva and identification of the liver is depicted in Figure 3.5. There were no changes in normalized liver ORO staining with exposure to any of the low molecular weight alternatives (Figure 3.6). However, there were significant increases in liver area at 0.2 and 2 μM PFHxS exposures (Figure 3.6C), and 20 μM 6:2 FTOH caused a significant decrease in liver area (Figure 3.6E).

ORO stain accumulation was also measured in the neural region of the larvae, as outlined in Figure 3.5. The C-6 compounds caused effects on the neural area stained with the ORO dye (Figure 3.7). There was a significant decrease in stained neural area at all doses of PFHxA examined (Figure 3.7A). However, there was a significant increase in ORO-stained neural area in the 0.2 and 2 μM PFHxS-exposed larvae (Figure 3.7C). Neither PFHxA nor PFHxS caused significant effects on the normalized stain intensity in this region (Figure 3.7B, D). Exposure to 6:2 FTOH caused a significant increase in ORO-stained neural area at the 2 μM concentration, but a

significant decrease in normalized stain intensity was measured with exposure to 20 µM 6:2 FTOH (Figure 3.7E, F).

3.3.3 Alterations in Morphometrics and Lipid Staining: PFOA, PFOS, and PFNA

Liver and neural region area and ORO stain accumulation were also measured in larvae developmentally exposed to 0.02-2 µM PFOA, PFOS, and PFNA. There were no significant alterations in liver area with exposure to PFOA, but there was a significant increase in normalized liver ORO staining with exposure to 2 µM concentration (Figure 3.8A, B). PFOS-exposed larvae had significantly smaller liver areas at 0.02 and 2 µM concentrations compared to controls; however, no changes in lipid stain intensity were measured (Figure 3.8C, D). PFNA exposure induced an increase in liver area at 0.02 and 2 µM concentrations, but again no changes in normalized lipid staining were observed (Figure 3.8E, F).

Exposure to PFOA caused a significant decrease in the neural region stained with ORO dye at the 0.2 and 2 µM, and at these same concentrations PFOA, there was a significant increase in the amount of stain within this region (Figure 3.9A, B). In contrast, exposure to 2 µM PFOS caused a significant increase in stained neural area and increased normalized stain intensity within that region (Figure 3.9C, D). The only alteration in the neural region of the PFNA-exposed larvae was a significant decrease in stained area in the 0.2 µM treatment group (Figure 3.9E, F).

3.4 Discussion

3.4.1 General Conclusions

The results of this study demonstrate the ability of developmental exposures to PFASs and low molecular weight alternatives to impart lasting effects on larval zebrafish. Behavioral, morphometric, and lipid distribution effects were observed in 14 dpf larvae following a 5 day developmental exposure and a 9 day depuration period. This study is the first to report effects in 14 dpf larvae with PFHxA, PFHxS, and 6:2 FTOH exposures. Lasting effects following

developmental exposures to long chain PFASs have been previously reported in both larval (Jantzen et al. 2016a) and adult zebrafish (Jantzen et al. 2016b).

The larvae in this study received a 9 day depuration period prior to the behavioral assay, which may indicate that morphology or biochemistry could be permanently altered. It is also possible that internal doses of these compounds were still present. In adult female zebrafish, plasma half-life of PFHxA ranged between 3.2-9.6 days, and the half-life for PFHxS was measured between 6.4-14.7 days (Chen et al. 2016). Similarly, plasma half-lives in zebrafish were 2.8-5.3 days PFOA, 27.7-34.7 days PFOS, and 11.6-21.7 days PFNA (Chen et al. 2016). The excretory mechanisms, such as the kidneys, for these compounds were in development during the exposure period, so it is possible that serum doses were measurable when these endpoints were assessed.

Behavioral effects were observed in larvae exposed to PFHxS and 6:2 FTOH. With the exception of the effect on length with PFHxS, these compounds did not elicit morphological effects at 14 dpf (Table 3.2), or 5 dpf (Table 2.4). It has been reported that behavioral responses in zebrafish larvae are more sensitive to low dose exposures to classical toxicants (Reif et al. 2016). In addition, behavioral endpoints can be predictive of morphological effects that may appear at higher concentrations. Behavioral biomarkers are a result of complex interactions that involve the integration of multiple systems, and minor effects may only be manifested when these systems are impacted.

3.4.2 Toxicity Profile for PFHxA Exposure

PFHxA exposure caused no changes in 14 dpf larval zebrafish behavior (Figures 3.2-3.4). This suggests either that PFHxA does not impact zebrafish behavior or that the doses examined in this study were below the LOEL for behavioral effects. There was also increased variability in these assays which may contribute. These findings correlated with the rodent literature as no changes in either a locomotor assay or functional observational battery have been observed in rats treated with PFHxA (Chengelis et al. 2009b; Klaunig et al. 2014).

There were some changes on lipid distribution in 14 dpf larvae, where a significant decrease in the neural area stained with ORO was observed (Figure 3.7A). This may reflect a change in lipid distribution in these fish. However, no alterations in stain intensity were observed, and changes did not occur with liver stain or area (Figures 3.7, 3.8). This contrasts with results in the literature as the liver has been demonstrated to be a target organ of toxicity in rodents (Chengelis et al. 2009a; Chengelis et al. 2009b; Klaunig et al. 2014) and *Xenopus* (Kim et al. 2015). However, the doses in these experiments were much higher than those examined in the present study.

In this study, PFHxA did not impact total length in 14 dpf larvae at the doses examined. Similarly, these doses at 5 dpf caused no impact on length or other morphometric endpoints (Chapter 2, Figure 2.4). Again, it is possible that the doses examined are below the LOEL for morphological effects. Therefore, these compounds are less toxic than the long chain PFASs.

One goal of this study was to compare toxicity profiles across the perfluorinated carboxylates. In Jantzen et al. 2016a, the same developmental exposures and endpoints were examined following PFOA and PFNA exposures. Morphometric and behavioral results from Jantzen et al. study are summarized in Table 3.3, and for comparison, the results from the C-6 compounds are in Table 3.4. PFNA and PFOA exposure led to different morphological and behavioral phenotypes in 14 dpf larvae. Exposure to 2 µM PFOA caused a decrease in length and an increase in swim distance during the locomotor assay. Exposure to 2 µM PFNA caused a significant increase in length and a decrease in velocity in the behavioral assay. In comparison, 2 and 20 µM PFHxA caused no effects on total length or any behavioral endpoints. This demonstrates that despite the shared carboxylic acid moiety of these compounds each PFAS not only elicits different effects, but the concentrations at which effects will be visible are also altered.

3.4.3 Toxicity Profile for PFHxS Exposure

Following 20 µM PFHxS exposure, there was a decrease in both total distance across time bins and cumulative number of crosses (Figures 3.2B, 3.3B). This reflects a decrease in activity and exploratory behavior in the larval fish, as demonstrated by the decrease in number of crosses

through the center of the well. In an open field test, larvae with stimulated stress response will exhibit increased travel, more crosses through the center of the arena, and increased swim speed (Champagne et al. 2010). However, the PFHxS-exposed larvae exhibited a suppression of these stress systems and hypoactivity. Similar effects were observed with PFHxS exposures in rodent models. Following a single 1.4-21 μmol/kg PFHxS dose at 10 days old, mice at 2 months displayed decreased activity compared to controls during the first 20 minutes of the locomotor assay (Viberg et al. 2013). The mouse study differed from the zebrafish larvae in that the mice displayed a significant increase in activity during the last 10 minutes of the assay.

It is possible that the behavioral effects with PFHxS exposure in the present study are due to direct effects on the nervous systems of these fish. There is a reported elevated risk to notochord distortion with hypoactivity behavioral response (Reif et al. 2016). Studies have also reported PFHxS to induce apoptosis in primary neuronal cells of the cerebellum in rat pups, as well as in cell lines (Lee et al. 2014a; Lee et al. 2014b). At 50 μM PFHxS, cultured rat hippocampal cells displayed decreased neurite length (Liao et al. 2009). From the observed suppression of the stress systems, it is possible that cortisol levels might be impacted with PFHxS exposure. The long chain sulfonate, PFOS, can cause effects on cortisol levels, specifically increased levels were observed in PFOS-exposed salmon (Arukwe et al. 2013), and PFOS treatment is associated with increased activity (Jantzen et al. 2016a; Mariussen 2012). Since there is the potential for PFASs to impact cortisol levels, it is possible that PFHxS targets the same systems as PFOS, but elicits a decrease in cortisol leading to suppression in activity. Taken together, these might be potential targets of PFHxS toxicity and contribute to the decrease in larval activity.

These behavioral findings emphasis that early developmental exposures to PFHxS may have lasting behavioral effects on exposed populations. However, it is unknown what this impact will have on fish in wild populations. The decrease in activity and exploratory behaviors could be harmful if it means that a fish will not be in the search for prey or mates as it reaches sexual maturity (Champagne et al. 2010). Conversely, reduced stress responses are beneficial and evolutionarily adaptive for fish populations in areas of high predation (Brown et al. 2005).

The larvae exposed to PFHxS were significantly longer at 14 dpf (Table 3.2) and 5 dpf (Figure 2.4), which suggests that this is a persistent effect. It is possible that this increase in length relates to the behavioral effects observed, resulting in a difficulty for movement to occur. The increase in larval size was accompanied by an increase in liver and stained neural area (Figures 3.6, 3.7). However, with normalization of these areas to length, there is still an increase in both endpoints compared to controls (data not shown). Therefore, the lipid distribution and morphometrics of PFHxS-exposed larvae are both altered.

There were no changes in lipid accumulation in either the liver or neural region of the PFHxS-exposed larvae. This varies from the literature where mice with humanized apolipoprotein profiles had increased liver triglyceride content with PFHxS exposure (Bijland et al. 2011). In addition, this study along with other rodent models, have confirmed the increase in liver weight (Butenhoff et al. 2009a; Chang et al. 2018), similar to the increased liver area observed in this study.

3.4.4 Toxicity Profile for 6:2 FTOH Exposure

Similar to the outcomes of 6:2 FTOH in 5 dpf fish (Chapter 2), effects were observed at 14 dpf following exposure to this compound intended to serve as a negative control (summarized in Table 3.4). Behavioral endpoints were sensitive to 6:2 FTOH exposure, particularly at the higher doses of 2 and 20 µM (Figures 3.2, 3.4). Total distance traveled during the assay was significantly increased with exposure to 2 µM 6:2 FTOH in the first time bin (Figure 3.2C). This trend persisted over the remaining time bins, leading to a significant increase in cumulative distance at 2 µM. Additionally, 6:2 FTOH was the only compound to impact the mean velocity of the larvae, where a significant increase was observed compared to controls in the 10-20 and 20-30 minute time bins (Figure 3.4C). In this type of assay, there is an initial photoresponse and increased activity following the change in light at the start of the assay that diminishes over time as the larvae assimilate to change in environment (Champagne et al. 2010; Orger and de Polavieja 2017). However, the 6:2 FTOH-exposed larvae maintained elevated velocity throughout the study, which may suggest either a decreased ability to habituate to the dark stimulus or an

increase in basal speeds. Together, the increased swim speed and distance traveled support an elevated anxiety phenotype (Champagne et al. 2010). Increased activity also presents a threat in young larvae, as it increases the possibility of predation. These behavioral effects are the first reported with 6:2 FTOH exposures in zebrafish, despite the lack of behavioral responses observed in mice (Serex et al. 2014).

Exposure to 6:2 FTOH had no effect on larval length (Table 3.2); however, other morphometric effects were observed. There was a significant decrease in liver area with exposure to 20 µM 6:2 FTOH, but no effects on liver lipid staining were observed (Figure 3.6E, F). Effects were also observed in the neural region of the larvae, with a significant increase in stained area at 2 µM and decreased stain intensity at 20 µM (Figure 3.7E, F). This suggests that there is an alteration in lipid distribution in the nervous system, which may relate to the behavioral effects.

The effects of 6:2 FTOH treatment on liver and neural development have not yet been examined in the zebrafish model, and very few studies have been completed in rodent models. From a 90 day exposure of 125 mg/kg/day 6:2 FTOH in rats, increased liver weight was observed in males and females (Serex et al. 2014). Additionally, the female rats displayed histological changes in their livers, although these findings, which included necrosis, inflammation, vacuolization, and hypertrophy (Serex et al. 2014), were less specific to lipid metabolism compared to the histological changes observed with long chain PFASs (Abbott et al. 2009; Albrecht et al. 2013; Rosen et al. 2010).

Other factors not examined in this study may contribute to these findings. Unlike the other PFASs, fluorotelomers are metabolized (Stahl 2011). In hepatocytes, up to 78% of an initial exposure of 8:2 FTOH was conjugated with mostly sulfates or glucuronides, but transformation into PFASs was also measurable (Martin et al. 2005). Similar metabolism pathways have been reported with 6:2 FTOH, so it is possible that exposure to the metabolites contributes to the observed effects in these larval zebrafish with functional livers. Additionally, studies in aquatic models have focused on the estrogenic potential of 6:2 FTOH (Ishibashi et al. 2008; Liu et al.

2009), and it may be stimulation of the hypothalamic-pituitary-gonadal (HPG) axis that mediates the observed behavioral effects. There was dose-dependent reduction in 5 dpf larvae activity with increasing 17α-ethinylestradiol exposures (Fraser et al. 2017), so it is possible that alterations of the estrogen pathway lead to altered behavior at early life stages.

3.4.5 Lipid Accumulation with Long Chain PFASs

The ORO staining studies were replicated in the larval zebrafish following exposure to long chain PFASs: PFOA, PFOS, and PFNA. Increased liver weight is associated with PFOA exposure (Lau et al. 2007); however, this was not reflected in the liver area measurements in this study (Figure 3.8A). The lack of effect may be an artifact of attempting to use a 2D measurement for a 3D effect, suggesting that measuring larval liver weight may have been more appropriate. It is also possible that the time frame of exposure contributed to this lack of response, and that larval liver might not be sensitive to developmental exposures. Therefore, this warrants further study.

There was an increase in ORO lipid stain in 2 µM PFOA-exposed larvae suggesting an increase in lipids in the livers of these larvae, which aligns with the rodent literature (Figure 3.8B). Additionally, there was a decrease in the ORO-stained area in the neural regions of these larvae coupled with an increase in stain intensity at 0.2 and 2 µM PFOA concentrations (Figure 3.9A, B). This suggests that the neural lipids are more concentrated in a smaller region of the larvae. Additional effects have been previously reported in Jantzen et al. 2016a, summarized in Table 3.3. At 2 µM PFOA, there was a significant decrease in length of the larvae, and increase in distance swam over the behavioral assay. It is possible that these effects are related to the observed effects on lipid homeostasis.

Multiple studies have reported the development of hepatic enlargement, lipid accumulation, and steatosis in adult zebrafish following PFOS exposures at doses similar to the ones in this study (Cheng et al. 2016; Cui et al. 2017; Fai Tse et al. 2016). However, similar findings were not observed in the larval zebrafish of this study. PFOS treatment had no effect on fatty acid accumulation in the liver, and there was a significant decrease in liver size (Figure 3.8 C, D). It is

possible that this too relates to the timing of these studies and that liver effects are not visible in the embryo or larval stages. The decrease in liver area is not a reflection of the size of the larvae as there is no treatment effect on size with PFOS (Jantzen et al. 2016a). Within the neural region of these larvae, there was a significant increase in stained area and an increase in stain intensity with 2 µM PFOS exposure (Figure 3.9 C, D). It is possible that these changes in neural lipids relates to the hyperactivity reported with PFOS exposure, summarized in Table 3.3 (Jantzen et al. 2016a).
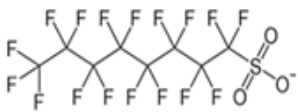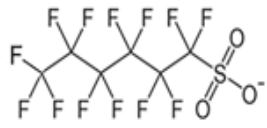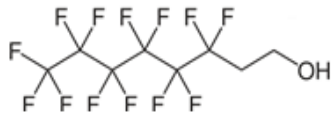
Similarly, PFNA has been demonstrated to induce lipid accumulation in the livers of rodents (Das et al. 2017) and zebrafish (Zhang et al. 2012). In this study, liver area was significantly increased, but no changes in lipid staining were observed (Figure 3.8E, F). The significant increase in liver area at 2 µM PFNA was accompanied by a similar increase in total length at this dose (Jantzen et al. 2016a). In the neural area of these fish, there were no changes in lipid stain intensity, and a significant decrease in stained area observed at 0.2 µM PFNA, that was not observed at higher doses (Figure 3.9E, F), suggesting this is not a critical endpoint with PFNA exposure.

3.5.5 Conclusions

In conclusion, exposures to low molecular weight PFAS alternatives, PFHxA, PFHxS, and 6:2 FTOH caused different morphometric, behavioral, and lipid distribution effects in 14 dpf larvae. This not only builds upon the profiles described in 5 dpf larvae, outlined in Chapter 2, but also emphasizes that persistent effects are observable following a 9 day depuration period. These studies demonstrated limited outcomes following PFHxA exposure. However, both PFHxS and 6:2 FTOH caused behavioral effects as well as alterations in the lipid staining in exposed larvae. Lipid staining was also completed in larvae exposed to PFOA, PFOS, and PFNA to test if the liver effects detected later in development are apparent in larval livers. This preliminary data suggests that ORO stain measurement may serve as an additional method for measuring lipid dysregulation in larval zebrafish; however, this needs to be confirmed through future studies. This study confirms that PFASs and alternatives alter lipid distribution in larval fish as well as altering

behavior endpoints, which prove to be more sensitive than morphological endpoints as described in Chapter 4.

Table 3.1. Chemical structures of perfluorooctanoic acid (PFOA), perfluorooctane sulfonate (PFOS), perfluorononanoic acid (PFNA), perfluorohexanoic acid (PFHxA), perfluorohexane sulfonate (PFHxS), and 6:2 fluorotelomer alcohol (6:2 FTOH).

Figure 3.1. Exposure paradigm of experiments. Waterborne PFAS exposures began at 3 hours post fertilization (hpf) and continued until 120 hpf. Larvae at 14 days post fertilization (dpf) were reared in treatment-free water until behavioral and morphometric endpoints were assessed.
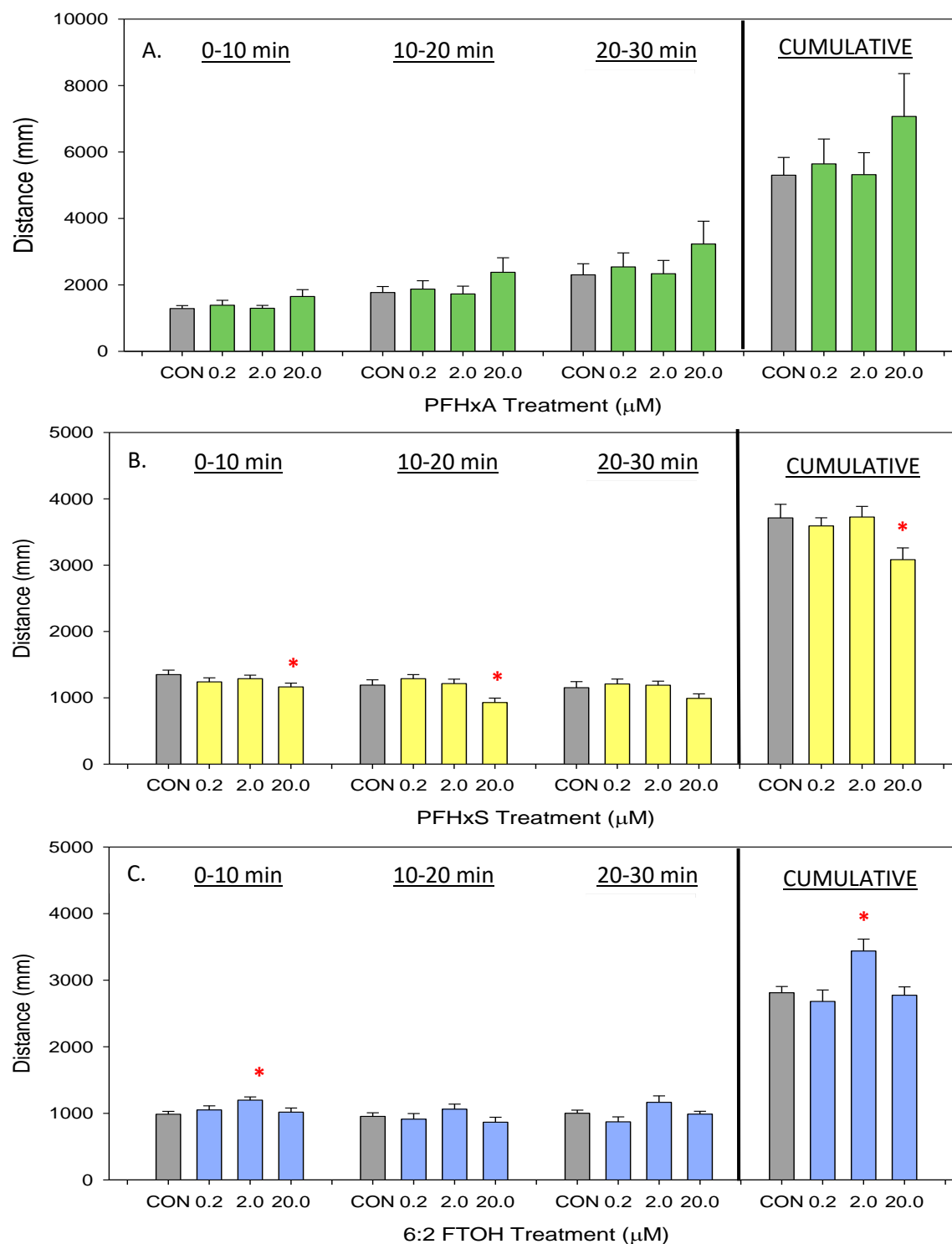
Figure 3.2. Distance travelled (mm) by developmentally PFHxA-, PFHxS-, or 6:2 FTOH-exposed larvae at 14 dpf. Data collected over a 30 minute period are divided into 10 minute time bins. Cumulative distance over the 30 minute assay is shown in the last column set. Values are reported as mean and SEM for each time bin with (A) PFHxA treatment (B) PFHxS treatment (C) 6:2 FTOH treatment. An asterisk (*) indicates $p<0.05$, one-way ANOVA, N=7-8.
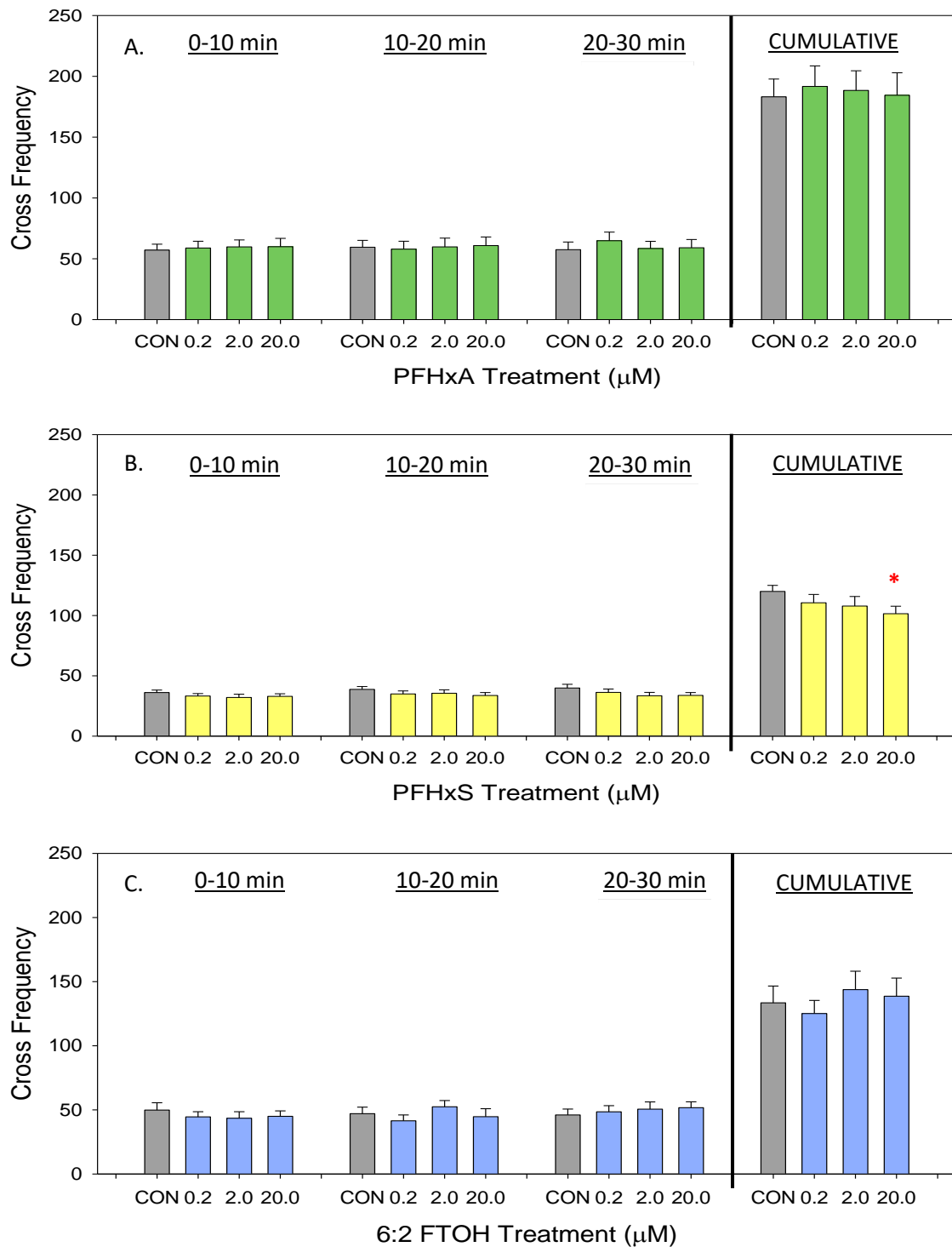
Figure 3.3. Cross frequency, or number of times the larvae swam through the center of the arena, of developmentally PFHxA-, PFHxS-, or 6:2 FTOH-exposed larvae at 14 dpf. Data collected over a 30 minute period are divided into 10 minute time bins. Cumulative distance over the 30 minute assay is shown in the last column set. Values are reported as mean and SEM for each time bin with (A) PFHxA treatment (B) PFHxS treatment (C) 6:2 FTOH treatment. An asterisk (*) indicates $p < 0.05$, one-way ANOVA, N=7-8.
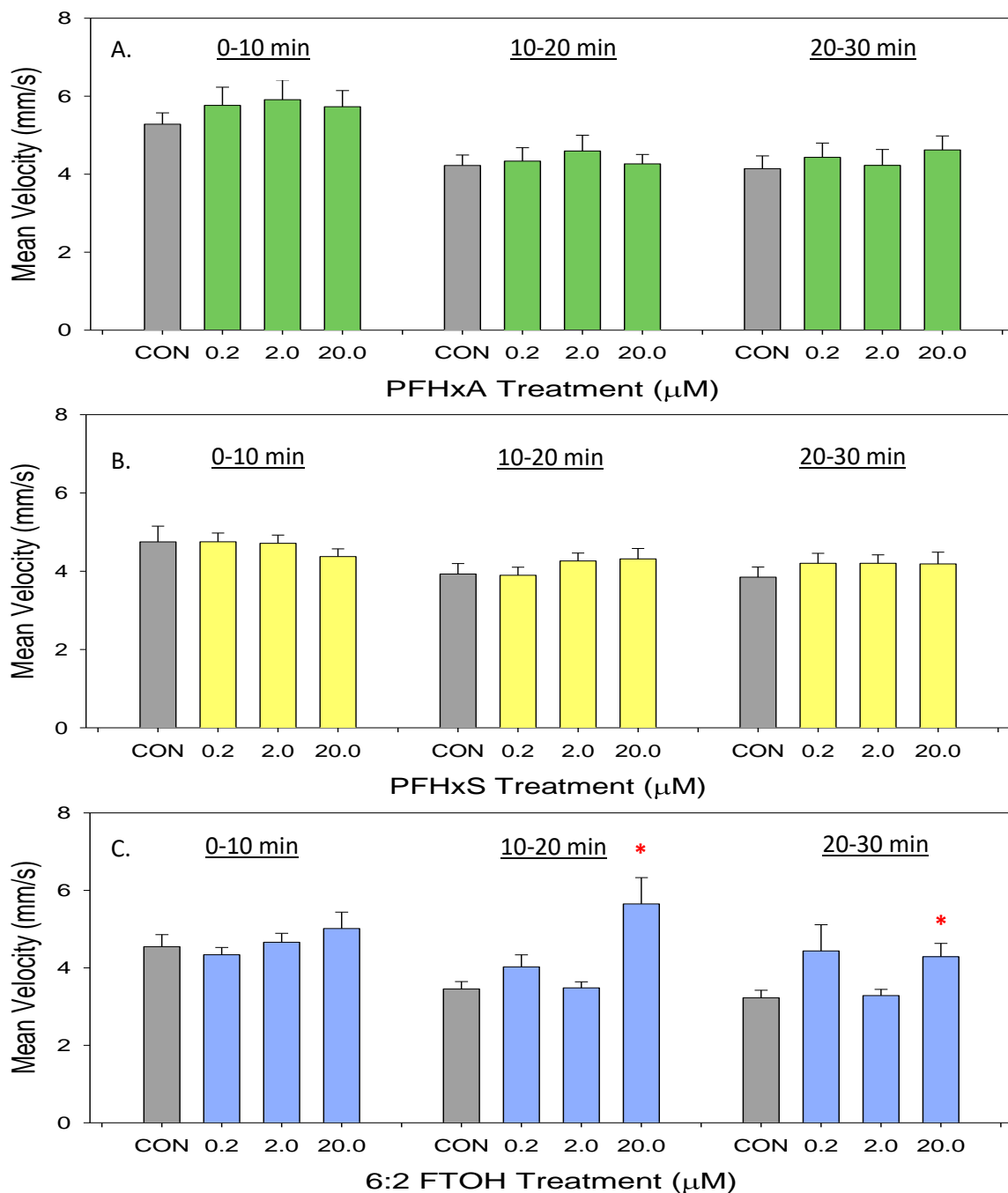
Figure 3.4. Mean velocity of developmentally PFHxA-, PFHxS-, or 6:2 FTOH-exposed larvae at 14 dpf. Data collected over a 30 minute period are divided into 10 minute time bins. Values are reported as non-cumulative mean and SEM for each time bin with (A) PFHxA treatment (B) PFHxS treatment (C) 6:2 FTOH treatment. An asterisk (*) indicates $p < 0.05$, one-way ANOVA, N=7-8.

Table 3.2. Measurements of total body length (mean ± standard deviation, in mm) at 14 dpf following developmental exposure to PFHxA, PFHxS and 6:2 FTOH. An asterisk (*) indicates $p<0.05$, one-way ANOVA, N=35-40.

Compound	CONCENTRATION (µM)			
	0	0.2	2	20
PFHxA	4.60 ± 0.18	4.60 ± 0.27	4.54 ± 0.20	4.66 ± 0.22
PFHxS	4.74 ± 0.25	**4.91 ± 0.26***	**4.91 ± 0.20***	4.85 ± 0.27
6:2 FTOH	4.76 ± 0.24	4.81 ± 0.23	4.85 ± 0.20	4.74 ± 0.26

Table 3.3. Summary of findings in 14 dpf zebrafish following 2 µM PFOA, PFOS, and PFNA exposures during the same developmental window as the present study (Jantzen et al. 2016a). Up arrows indicate a significant increase, down arrows indicate a significant decrease, and "N.S." indicates no significance difference compared to controls.

	2 µM PFOA	2 µM PFOS	2 µM PFNA
MORPHOMETRICS			
Total Body Length	⬇	N.S.	⬆
BEHAVIORAL EFFECTS			
Total Distance	⬆	⬆	N.S.
Cross Frequency	N.S.	⬆	N.S.
Velocity	N.S.	⬆	⬇

Table 3.4. Summary of findings in 14 dpf zebrafish following 2 and 20 µM PFHxA, PFHxS, and 6:2 FTOH exposures. Up arrows indicate a significant increase, down arrows indicate a significant decrease, and "N.S." indicates no significance difference compared to controls.

	PFHxA		PFHxS		6:2 FTOH	
	2 µM	20 µM	2 µM	20 µM	2 µM	20 µM
BEHAVIOR						
Total Distance	N.S.	N.S.	N.S.	⬇	⬆	N.S.
Cross Frequency	N.S.	N.S.	N.S.	⬇	N.S.	N.S.
Velocity	N.S.	N.S.	N.S.	N.S.	N.S.	⬆
MORPHOMETRICS AND LIPID STAINING						
Total Length	N.S.	N.S.	⬆	N.S.	N.S.	N.S.
Liver Area	N.S.	N.S.	⬆	N.S.	N.S.	⬇
Liver Stain	N.S.	N.S.	N.S.	N.S.	N.S.	N.S.
Neural Area	⬇	⬇	⬆	N.S.	⬆	N.S.
Neural Stain	N.S.	N.S.	N.S.	N.S.	N.S.	⬇

Figure 3.5. Representative example of Oil Red O (ORO) stained larvae reared in control media. Images taken under (A) bright light and (B) labeled. The liver is labeled in yellow, and the stained neural area is labeled in blue.
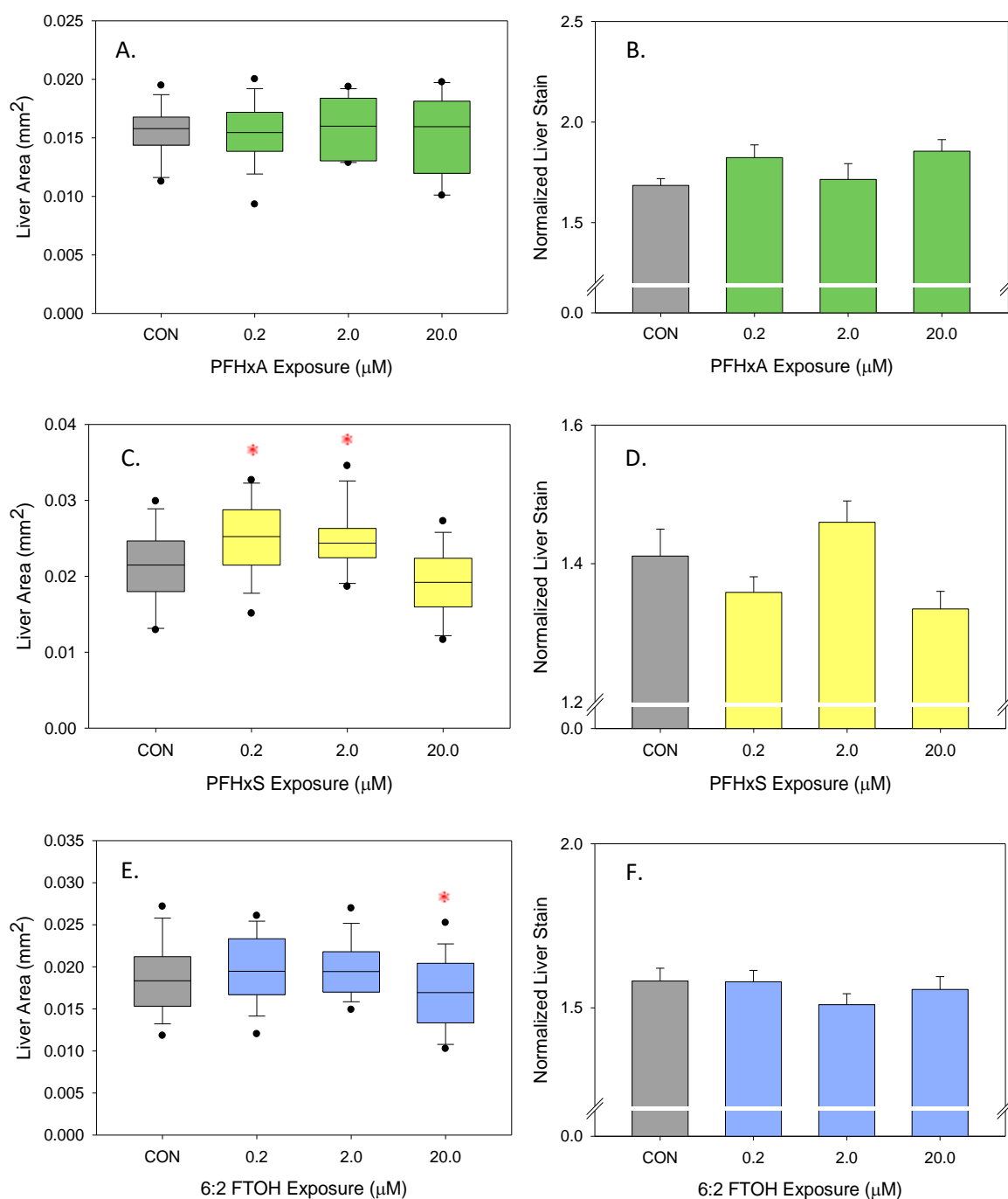
Figure 3.6 Liver area and Oil Red O (ORO) stain intensity of larvae at 14 dpf. Liver area is displayed as box plots representing 25-75% quartiles, whiskers as 10-90% , and dots as 5 and 95%., with exposure to (A) PFHxA (C) PFHxS (E) 6:2 FTOH. ORO staining in the liver, normalized to background stain intensity (mean + SEM), is displayed as bar graphs with exposure to (B) PFHxA (D) PFHxS (F) 6:2 FTOH. An asterisk (*) indicates p<0.05, one-way ANOVA, N=35-40.
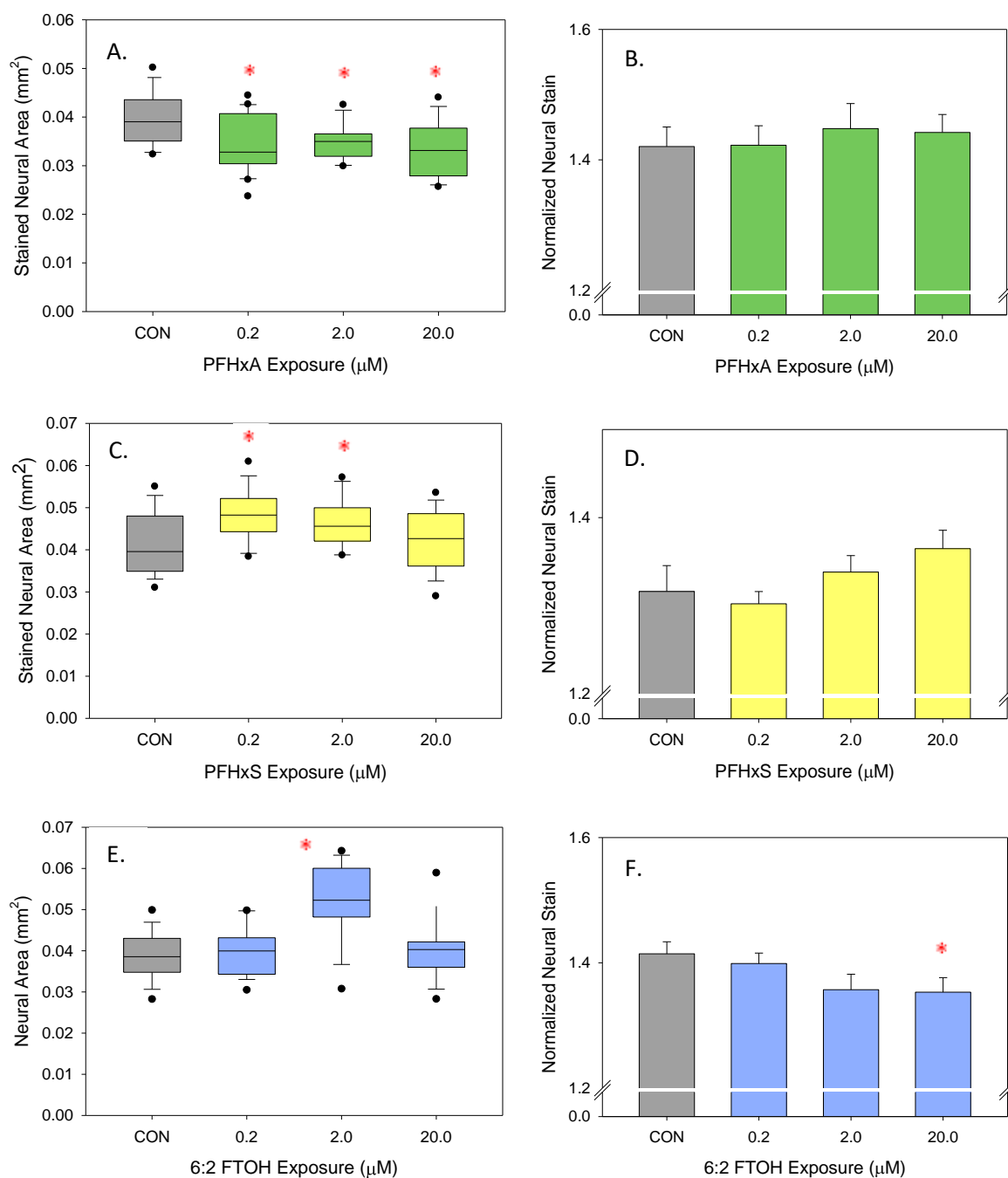
Figure 3.7. Stained neural area and Oil Red O (ORO) stain intensity of larvae at 14 dpf. Stained neural area is displayed as box plots representing 25-75% quartiles, whiskers as 10-90% , and dots as 5 and 95%., with exposure to (A) PFHxA (C) PFHxS (E) 6:2 FTOH. ORO staining in the neural area, normalized to background stain intensity (mean + SEM), is displayed as bar graphs with exposure to (B) PFHxA (D) PFHxS (F) 6:2 FTOH. An asterisk (*) indicates p<0.05, one-way ANOVA, N=35-40.
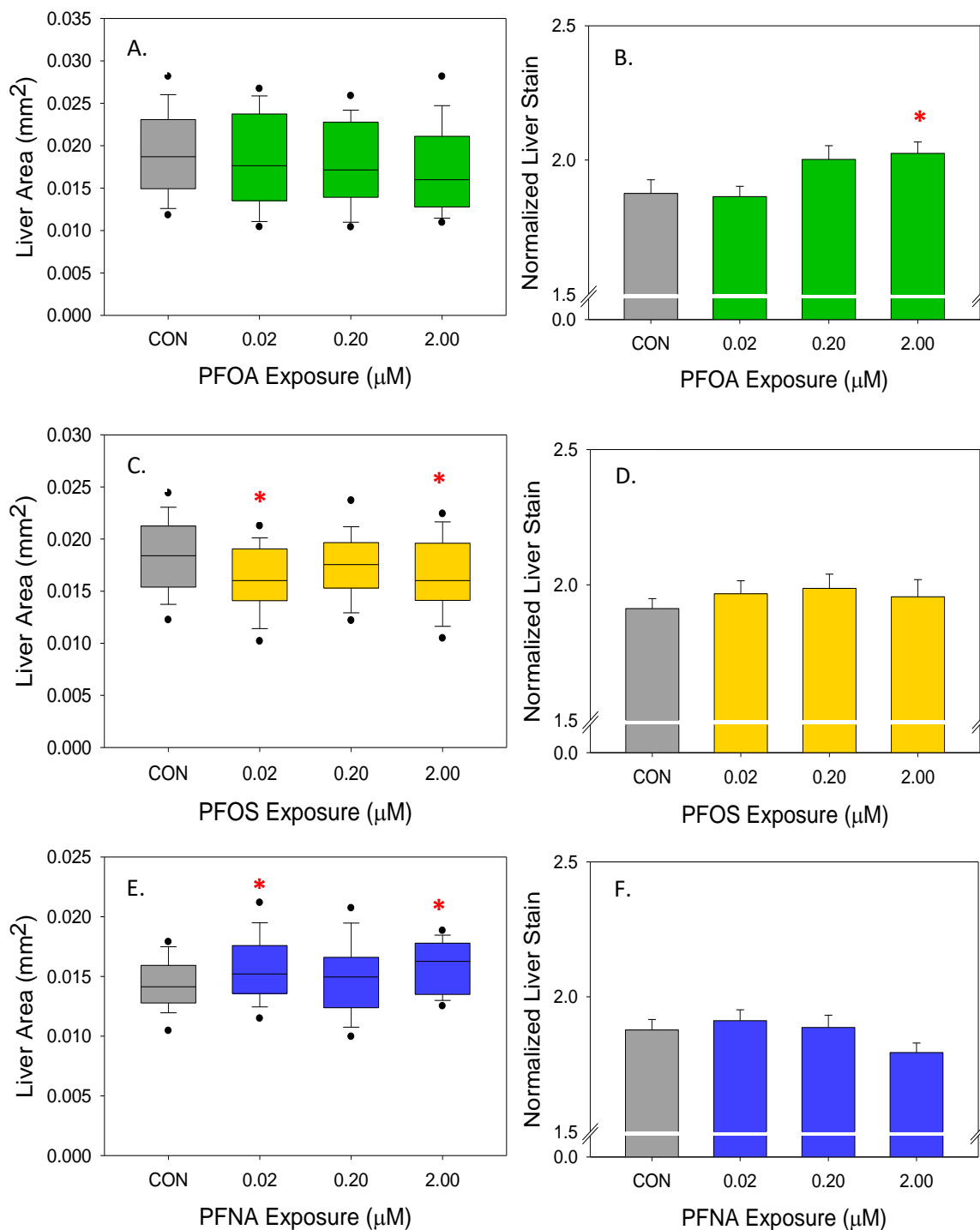
Figure 3.8. Liver area and Oil Red O (ORO) stain intensity of PFAS-exposed larvae at 14 dpf. Liver area is displayed as box plots representing 25-75% quartiles, whiskers as 10-90% , and dots as 5 and 95%., with exposure to (A) PFOA (C) PFOS (E) PFNA. ORO staining in the liver, normalized to background stain intensity (mean + SEM), is displayed as bar graphs with exposure to (B) PFOA (D) PFOS (F) PFNA. An asterisk (*) indicates p<0.05, one-way ANOVA, N=36-40.
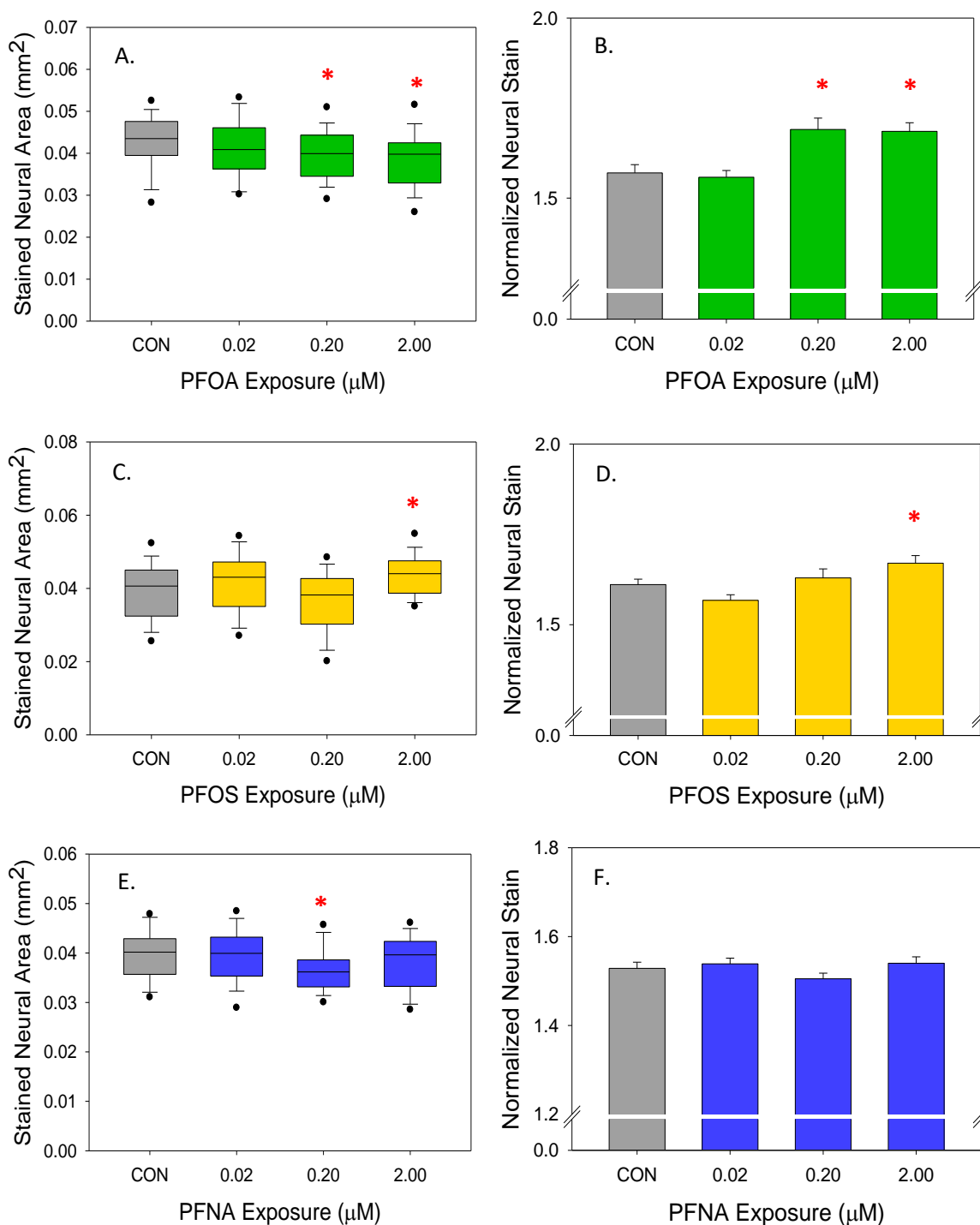
Figure 3.9. Stained neural area and Oil Red O (ORO) stain intensity of PFAS-exposed larvae at 14 dpf. Stained neural area is displayed as box plots representing 25-75% quartiles, whiskers as 10-90% , and dots as 5 and 95%., with exposure to (A) PFOA (C) PFOS (E) PFNA. ORO staining in the neural region, normalized to background stain intensity (mean + SEM), is displayed as bar graphs with exposure to (B) PFOA (D) PFOS (F) PFNA. An asterisk (*) indicates p<0.05, one-way ANOVA, N=36-40.

CHAPTER 4

Exposure to PFASs impacts lipid mobilization and distribution in larval zebrafish

4.1. Introduction

One of the hallmarks of PFOS, perfluorooctane sulfonate, PFNA, perfluorononanoic acid, and PFOA, perfluorooctanoic acid, is liver toxicity (Lau 2012; Lau et al. 2007). This includes hepatomegaly, histological change, increased β-oxidation of fatty acids, and accumulation of triglycerides and cholesterol. Additionally, mice exposed to PFOS and PFOA have lower serum triglycerides and cholesterol along with increased hepatic lipid accumulation (Wang et al. 2013a; Wang et al. 2014). Changes in lipid homeostasis have been observed through epidemiological studies as well. Long chain PFASs in serum has been associated with obesity, diabetes, and increased weight gain (Barry et al. 2014; He et al. 2017; Liu et al. 2018b). Together these data suggest lipid dysregulation AOPs are a critical component in PFAS toxicity.

Dysregulation of lipid homeostasis has been observed in the zebrafish model as well. PFOS exposure has been linked to the development of hepatic steatosis (Cui et al. 2017; Fai Tse et al. 2016). Exposure to 0.5 µM PFOS for 5 months led to increased cholesterol and triglycerides in male livers, as well as a decrease in serum triglycerides, similar to the mammalian studies (Cheng et al. 2016). Similarly, chronic 180 day exposure to 0.1 and 1 mg/L PFNA led to increased cholesterol and triglycerides in male livers (Zhang et al. 2012). In both experiments, there was a sexually dimorphic response, where more lipid accumulation was observed in males compared to females. In zebrafish, PFOA exposure has not been shown to increase liver lipid accumulation, but transcriptomics analysis have identified that some genes regulating lipid metabolism are altered with exposure (Hagenaars et al. 2013). Disruption of lipid homeostasis has also been noted in other fish species; fatty acids profiles were altered with 50 day 0.2 µM PFOS and PFOA exposures in salmon (Arukwe et al. 2013). Together, these studies identify the zebrafish as a potential model for studying effects on lipid metabolism following exposure to PFASs.

As a developmental model, the zebrafish model can be tested for compound effects on liver formation and function, as well as, the uptake and distribution of lipids early in development. The early developing zebrafish embryo must rely on a maternally deposited yolk cell for its nutrients, which differs from mammalian development (Kimmel et al. 1995). The yolk cell provides the triglycerides, proteins, cholesterol, and vitamins to sustain embryonic growth (Quinlivan and Farber 2017). Therefore, total lipids can be monitored. The yolk cell is a dynamic structure, containing enzymes that aid in the packaging and metabolism of maternal lipids, which is critical for proper distribution in the embryo (Carvalho and Heisenberg 2010). Along the yolk cell sits the yolk syncytial layer (YSL), which is a layer a few cells thick where many of these enzymes that package and metabolize lipids are located (Kondakova and Efremov 2014). Some of these enzymes include microsomal triglyceride transfer protein (mttp), lipoprotein lipase (lpl), fatty acid transporter (slc27a1), and apolipoproteins (apoa1, apoc2) (Quinlivan and Farber 2017; Sanchez Garcia et al. 2018). The positions of these factors along the YSL during early development are depicted in Figure 4.1. These factors are critical to development, and lack of proper function of these enzymes can be lethal or affect growth in zebrafish (Pickart et al. 2006; Schlegel and Stainier 2006). Additionally, there is homology to these enzymes as they function not only during the early stages of development, but also larval and adult stages where they are located in the liver, fat, intestines, and digestive organs. There is homology between zebrafish and humans with these organ systems (Wallace and Pack 2003).

Other regulating factors may also play a role in mediating the effects observed with PFASs. Pparα (peroxisome proliferator activating receptor), a nuclear receptor was originally reasoned to cause PFAS-mediated liver toxicity (Sohlenius et al. 1992). Pparα is endogenously activated by fatty acids, which share structural similarity to PFASs, and when activated will increase peroxisomes as well as activating a number of downstream genes related to lipid metabolism (Dreyer et al. 1993; Mandard et al. 2004). The hallmarks of pparα agonism, such as β-oxidation of fatty acids, lower serum cholesterol, and hepatomegaly, have been observed with PFAS exposures (Lau et al. 2007). It has also been reported that PFASs are able to activate *in vitro* models of pparα (Wolf et al. 2008a). However, studies utilizing pparα-null mice have

demonstrated that PFASs cause hepatotoxicity without this nuclear receptor present (Albrecht et al. 2013; Das et al. 2017; Rosen et al. 2010). This suggests that there are other molecular targets.

This study examined two other factors involved in regulating lipid homeostasis: pparγ and leptin. While pparγ regulates the expression of many of the same genes as pparα, this nuclear receptor is highly expressed in adipose tissue where it plays an important role in adipogenesis (Ahmadian et al. 2013; Frohnert et al. 1999; Salmeron 2018). In mammals, the hormone leptin regulates satiety and therefore is associated with food intake (Pan and Myers 2018). However, the zebrafish leptin does not impact food intake, but rather glucose homeostasis and metabolic rate (Dalman et al. 2013; Michel et al. 2016). It is possible that leptin still impacts lipid metabolism as it has been reported to impact lipoprotein lipase levels in trout (Salmeron et al. 2015).

This study is based on an early zebrafish yolk metabolism model utilizing microinjections of BODIPY-FL fatty acids and gene expression to determine possible mechanisms for alterations in lipid distribution and metabolism following PFAS exposure. Gene expression was completed on factors that regulate lipid metabolism pparα, pparγ, and *lepa* (leptin). Additionally, gene expression analysis was completed on *mttp*, *lpl*, *slc27a1*, *apoa1*, and *apoc2*, which function in lipid uptake and metabolism on the YSL and in larval fish. All endpoints were examined following exposure to PFOA, PFOS, and PFNA. Gene expression analysis was completed in low molecular weight alternatives, PFHxA, PFHxS, and 6:2 FTOH, to identify possible conserved pathways as fewer studies have examined the effects of these compounds on lipid metabolism.

4.2. Methods

4.2.1 Zebrafish Husbandry:

Zebrafish, strain AB (Zebrafish International Resource Center, Eugene, OR) were housed in Aquatic Habitat (Apopka, FL) recirculating systems. Municipal water supplies following sand and carbon filtration filled the systems. Water quality was monitored monthly to ensure water was

maintained at <0.05 ppm nitrite, <0.2 ppm ammonia, DO, and 7.2-7.7 pH. The temperature was monitored twice daily to ensure that tank water was held between 26 and 28 °C. Fish were maintained on a 14:10 hour light: dark cycle, and fed twice daily a diet of artemia in the mornings and aquatox/tetramin flake mix in the evenings. All experiments were conducted following Rutgers University Animal Care and Facilities Committee guidelines under the zebrafish husbandry and embryonic exposure protocol (08-025).

4.2.2 Exposure Setup

Stock solutions of PFOA (perfluorooctanoic acid, Sigma Aldrich, St. Louis MO), PFOS (perfluorooctane sulfonate, Sigma Aldrich), PFNA (perfluorononanoic acid, Sigma Aldrich), PFHxA (perfluorohexanoic acid, Oakwood Chemical, Estill, SC), PFHxS (trideafluorohexane-1-sulfonic acid potassium salt, Sigma Aldrich), and 6:2 FTOH (1H,1H,2H,2H-perfluorooctan-1-ol, Sigma Aldrich) were prepared at concentrations of 2000 μM in egg water. Table 4.1 outlines the chemical structure of these compounds. Embryos were exposed to static, non-renewed, nominal concentrations of each compound. Figure 4.3 outlines the exposure paradigm, modified from OECD 212 (OECD 1998). For gene expression studies, healthy embryos were selected at approximately 3 hpf (hours post fertilization) where staging ranged from the 1000 cell to high stage (Kimmel et al. 1995). Exposures were continued through hatching to 120 hpf, or 5 days post fertilization (dpf), when larvae were in the sac fry stage (Figure 4.3A). Microinjection studies varied in that injections were completed roughly 6 hpf, and immediately following PFAS exposures began and were continued until 120 hpf (Figure 4.3B). All experiments had >85% control survival.

4.2.3 Microinjections of Fluorescently-Tagged Fatty Acids

Injections took place at roughly 6 hpf, when the embryos had reached the 60-80% epiboly stage. This time frame was chosen to ensure a functional YSL was present (Carvalho and Heisenberg 2010). Healthy embryos were loaded into lanes of a 1.5% agarose gel mold with ample egg water to prevent desiccation. Solutions were prepared of 0.5 mg/mL BODIPY-FL C12 fatty acids, (4,4-

difluoro-5,7-dimethyl-4-bora-3a,4a-diaza-s-indacene-3-dodecanoic acid, ThermoFisher) in 1%

DMF, dimethylformamide, in canola oil or 1% DMF in canola oil control. Solutions were frozen in

aliquots and kept under foil when in use. Fatty acid solutions were loaded into micro-pulled

needles, which were then loaded into a Leica Micromanipulator attached to a General Valve

Corporation Picospritzer II. Volumes were calibrated adjusting nitrogen gas flow through the

needle, until the desired volume of 1.5 µL was achieved. Under a Wild Heerbrugg M3B dissecting

scope, the needle was carefully inserted through the chorion and into the yolk sac of the fish,

avoiding the developing cell mass. After the injection, the needle was pulled out from the same

angle as entry in order to maintain the structural integrity of the chorion.

After injections were complete, embryos were randomly assigned treatment groups and housed

in 96-well plates. Each well received 200 µL of control or treatment egg water. Exposures

examined include 0.2 and 2 µM concentrations of PFOA, PFOS, or PFNA. Photographs of each

sample were collected at 24 and 120 hpf using an Olympus IX51 microscope mounted with a

AmScope HD1080 camera and X-Cite 120 Fluorescence Illumination System. Two images were

taken for each sample, one using only the fluorescent light and a bright light background to better

visualize the orientation of the larva in the arena. Larvae at 120 hpf were oriented on their side to

allow for full visualization of the yolk sac. Measurements were completed using ImageJ software

for area and mean fluorescence intensity. Mean fluorescence intensity of the entire yolk sac was

normalized to background intensity. A single experiment included all concentrations of a single

PFAS, and each experiment was independently replicated for a total of 3 trials. Due to variation

between trials, all trials were normalized to mean values of the controls from the first trial.

4.2.4 Confocal Microscopy

Separate injections were completed for live imaging under confocal microscopy. Embryos were

reared individually in either 0 or 2 µM PFOS, PFOA, or PFNA. At 120 hpf, larvae were transferred

into clean egg water to rinse off solutions, and anesthetized in 50 mg/L tricaine solution. Once

anesthetized, larvae were embedded within 0.8% agarose in a 100mm plastic plate and positioned laterally coated. The plate was then covered in a 100 mg/L tricaine solution.

The yolk sac of each larvae was imaged using a Olympus FV1000MPE microscope (Olympus XLPlan N 25x objective NA 1.05; Olympus UMPlanFL N 10x objective NA 0.3). Z-stack images were collected through the yolk sac in 30 μm steps, and stack collapsed for a complete view of the yolk sac. Three to four larvae were imaged per treatment from 2 independent exposure replicates. Images were collected under both 10X and 25X magnification.

Vesicle measurements were completed using ImageJ software. Four images under 25X magnification were chosen for vesicle measurements. At least one image from each replicate was selected. Measurements of vesicle diameter were made of all vesicles along the YSL and along a transverse section through the center of the yolk, as outlined in Figure 4.7C. From each transverse section, 50-100 vesicles were measured.

4.2.5 Gene Expression Analysis

Twenty-five embryos were exposed to either treated control or treated egg water. Doses for long chain PFASs (0, 0.02, 0.2, and 2 μM) were based on previous studies from our lab (Jantzen et al. 2016a). Higher doses (0, 0.2, 2, and 20 μM) were examined with PFHxA, PFHxS, and 6:2 FTOH to mirror doses examined in Chapter 2. The protocol is outlined in Chapter 2 (Section 2.2.5). Genes examined in the present study are outlined in Table 4.2. All experiments were independently replicated three times, and the transcript numbers were combined to determine the mean and standard error (SEM) for each treatment.

4.2.6 Statistical Analyses

Statistical analysis was completed using SigmaPlot™ 11.0 software. For fluorescence, area, and gene expression measurements, one-way analysis of variance (ANOVA) were completed to compare across concentrations for each compound, followed by either a Bonferroni post hoc test

or Student T test, when data passed normality and variance tests. For confocal vesicle measurements, T tests were completed for each treatment group. Significance was set at $p < 0.05$.

4.3. Results

4.3.1 Microinjections of BODIPY-FL Fatty Acids

Larvae were monitored at 24 and 120 hpf following microinjections of BODIPY-FL C12 fatty acids and waterborne PFAS exposures. Representative images from each treatment are depicted in the appendices A5-7. At both time points, fluorescence was spread throughout the entire yolk sac of the embryo or larvae. In addition, the site of injection was clearly visualized (Figure A6A). The site of injection was present in all samples. There was also an observable increase in fluorescence intensity at the yolk syncytial layer (Figure A6B). This was seen in all samples, which was expected as this is the site of lipid uptake into the developing fish (Carvalho and Heisenberg 2010). Across the 3 experiments, there was variability between the fluorescence intensity, and for this reason, later trials were normalized to the first for each respective treatment.

From these images, measurements were taken to quantify the area and intensity of fluorescence in the yolk sac at 24 and 120 hpf. At 24 hpf, no changes in yolk sac area were observed with exposures to 0.2 or 2 μM PFOA or PFNA (Figure 4.4A). There was a significant increase in yolk sac area at 2 μM PFOS. None of the PFASs examined caused a significant change in normalized fluorescence intensity (Figure 4.4B). At 120 hpf, there was a significant dose-dependent increase in yolk sac area with PFOA and PFNA exposures (Figure 4.5A). This aligns with what has previously been reported following the same exposures to these compounds (Jantzen et al. 2016a). Exposure to 2 μM PFOS caused a significant decrease in yolk sac area in Jantzen et al. 2016a, and while not significant from controls in this study, the yolk sac areas with PFOS exposure trend in this direction. The only compound that impacted fluorescence intensity was 2 μM PFNA, which caused a significant decrease in intensity at 120 hpf (Figure 4.5B).

4.3.2 Confocal Imaging of Fluorescently Tagged Fatty Acids in Larval Zebrafish

To increase resolution and focus on the YSL where increased fluorescence was observed, confocal microscopy was utilized on live 5 dpf larvae exposed to 2 µM PFAS. Figure 4.6 depicts a representative larva reared in control solution under a green and red fluorescent filter. The green filter captured the emission of the BODIPY-FL fatty acids (Figure 4.6A). The confocal imaging improved resolution so that individual vesicles inside the yolk sac could be visualized, and fluorescence could be seen in other regions of the fish, such as in the head. This confirmed the presence of lipids as reported in the oil red o findings (Chapter 3). The red filter captured any areas of autofluorescence (Figure 4.6B). Two areas were consistently highlighted under the red filter, the original site of injection and the gastrointestinal system which is oriented above the YSL.

Representative images from control and 2 µM PFOS treatment groups are depicted in Figure 4.7, under 10X magnification to visualize the orientation of the larvae. In the control image, the individual vesicles were visible in the yolk sac of the larva (Figure 4.7A). In the 2 µM PFOS-exposed larva, the patterning of the fluorescence was more diffuse throughout the yolk sac, and the clear outline of vesicles were only visible in the posterior yolk sac (Figure 4.7B). Differences in vesicle appearance were less visually striking with exposures to 2 µM PFOA and PFNA (representative images not shown). However, vesicle measurements were completed for all treatment groups.

Vesicle diameters were recorded utilizing images captured under 25X magnification for all vesicles landed along the YSL and a transverse through the center of the yolk cell, as outlined in Figure 4.7C. Exposure to 2 µM PFOA and PFOS caused a significant decrease in the size of the vesicles in the center of the yolk sac (Figure 4.8A). All PFASs were found to cause a decrease in vesicle diameter along the YSL (Figure 4.8B). In general, the vesicles along the YSL were smaller than the center vesicles. Additionally, there were no significant differences in the number of vesicles between control and treated larvae (data not shown).

4.3.3 Gene Expression Results: PFOA, PFOS, and PFNA

PFOA, PFOS, and PFNA caused unique patterns of expression of lipid-related genes at 5 dpf. A significant reduction in *pparα* transcript expression occurred following 0.02 and 2 µM PFOA exposures, but no changes were observed with PFOS or PFNA exposure (Figure 4.9A). At 0.02 and 0.2 µM PFOS, there was a significant increase in *pparγ* gene expression, but no changes in expression followed exposure to PFOA or PFNA (Figure 4.9B). A significant reduction in *lepa* occurred at all doses of PFOA and PFOS examined (Figure 4.9C).

Genes involved in lipid distribution and metabolism were also affected differently creating unique expression patterns for each PFAS. Exposure to 0.2 and 2 µM PFOA caused a small, significant increase in *mttp* expression (Figure 4.10A). There was an induction at 2 µM PFNA as well, but this was not significantly different from controls, most likely due to the variability. A significant increase in *slc27a1* occurred with exposure to 0.2 and 2 µM PFOS and 2 µM PFNA (Figure 4.10B). Additionally, 0.2 and 2 µM PFNA caused a significant increase in *lpl* gene expression (Figure 4.10C). No changes were observed in the gene expression of *apoa1* (Figure 4.11A). There was a significant increase in *apoc2* expression only with exposure to 2 µM PFNA (Figure 4.11B).

4.3.4 Gene Expression Results: PFHxA, PFHxS, and 6:2 FTOH

Transcript levels of the same genes were analyzed at higher doses (0.2, 2, and 20 µM) of the C-6 compounds compared to the C-8/C-9 PFASs. No changes in expression of any of the genes involved in regulation of lipid homeostasis, *pparα, pparγ*, and *lepa,* were observed following PFHxA and PFHxS exposures (Figure 4.12). However, there was a significant dose-dependent increase in *pparα* gene expression at all doses of 6:2 FTOH and increased expression of *pparγ* at all doses (Figures 4.12A , B). There was a significant decrease in *lepa* expression following only exposure to 0.2 µM 6:2 FTOH (Figure 4.12C).

The genes related to lipid distribution and metabolism were affected with PFHxA, PFHxS, and 6:2 FTOH exposures. Significant induction of *mttp* gene expression were observed in the 0.2 and 2 µM PFHxA and 20 µM 6:2 FTOH treatment groups (Figure 4.13A). Additionally, both PFHxA and

6:2 FTOH caused a dose-dependent increase in *slc27a1* expression, significant at 2 and 20 µM

concentrations for both compounds (Figure 4.13B). All doses of PFHxA and 6:2 FTOH also

caused induction of *lpl* gene expression (Figure 4.13C). No changes in gene expression of *mttp*,

slc27a1, or *lpl* followed any dose PFHxS. Significant changes occurred in transcript levels of the

apolipoprotein genes following exposures to the C-6 compounds which were not observed with

the long chain PFASs. Both PFHxS and 6:2 FTOH at 20 µM caused a small, significant induction

in *apoa1* (Figure 4.14A). A larger induction of *apoc2* was observed at 2 µM PFHxS and all doses

of PFHxA (Figure 4.14B).

4.4 Discussion

To examine the effects of PFAS exposures on fatty acid homeostasis, this study examined the

utilization of yolk cell lipids during early embryonic development in the zebrafish. This study took

advantage of the overlapping mechanisms of early yolk sac uptake and larval GI systems. Along

the yolk syncytial layer, YSL, sits many of the same factors responsible for the processing and

uptake of yolk cell lipid as in the larval systems (Fraher et al. 2016; Quinlivan and Farber 2017). A

schematic of these genes is depicted in Figure 4.1. Lipid distribution was monitored at early (24

hpf) and sac fry (120 hpf) life stages following long chain PFAS exposures to examine possible

changes on lipid uptake and distribution through the larvae. This was coupled with gene

expression analysis at 120 hpf to determine possible expression variation with PFAS exposures.

4.4.1 Alterations in Fatty Acid Uptake and Distribution with Long Chain PFAS Exposures

The BODIPY-FL fatty acid study examined yolk sac area and fluorescent distribution at both 24

and 120 hpf. At 24 hpf, there were no changes to yolk sac area with exposure to 0.2 or 2 µM

PFOA and PFNA, and a significant increase at 2 µM PFOS (Figure 4.4A). This suggests that at

this early time point, the larval morphological phenotype has not yet manifested, as these effects

do not mirror the phenotype observed at 120 hpf (Figure 4.5A), or that of previous studies

(Jantzen et al. 2016a). Exposure to 2 µM PFOS caused a significant increase in yolk sac area at

24 hpf. This might indicate a delay in the effects of PFOS, which cause a decrease at 120 hpf.

Additionally, no significant changes in fluorescence intensity in the yolk sac were reported at 24 hpf (Figure 4.4B).

At 120 hpf (Figure 4.5A), the yolk sac area findings mirrored what had been reported following the same developmental exposures of PFOS, PFOA and PFNA (Jantzen et al. 2016a). There were no changes in fluorescence intensity by 120 hpf with PFOS and PFOA- exposed larvae (Figure 4.5B). This indicated that the control and exposed larvae had similar concentrations of fluorescent labels in the yolk cell, and this suggests that the increase in yolk sac area does not correlate with an increase in yolk sac lipids with PFOA and PFNA exposures. However, the yolk is a dynamic region for lipid metabolism where BODIPY-FL fatty acids are metabolized into new lipids (Fraher et al. 2016), and lipid metabolism has been shown to be altered with exposure to PFOS and PFOA in salmon (Arukwe et al. 2013). Therefore, it is possible that the lipid profile has been altered. BODIPY-FL fatty acids can be incorporated into lipids, such as triglycerides, where the tag remains present; it is only after extensive metabolism, such as complete β-oxidation of the fatty acid, that the fluorescent tag is lost (Fraher et al. 2016; Miyares et al. 2014). However, lipid profiles were not assessed in the present study. By 120 hpf, larvae exposed to 2 µM PFNA had decreased fluorescent signal in their yolk sacs (Figure 4.5B), suggesting that overall lipid levels in these larvae were reduced. This could reflect increased lipid uptake or fatty acid metabolism.

Confocal microscopy enabled examination of lipid vesicle movement and allowed for increased resolution in living larvae in comparison to the traditional fluorescence microscope. With confocal imaging, fluorescence was visible in the body of the larvae, and resolution was increased in the yolk sac of the larvae. These studies reproduced the uptake of these fatty acids in a similar manner to other studies utilizing the BODIPY-FL C2 fatty acid methods (Carten et al. 2011; Fraher et al. 2016). The confocal imaging also allowed for observation of the distribution of lipids throughout the yolk sac, specifically the formation of subcellular vesicles. The vesicle formation was clear in the control larvae (Figure 4.6A); however, the pattern of fluorescence was more diffuse in the PFOS-exposed larvae (Figure 4.6B). Measurement of vesicle diameter along the YSL was decreased with all PFASs, and vesicle diameter was reduced in the yolk sac center with

PFOS and PFOA exposures (Figure 4.7). This may be a reflection of the surfactant properties of these compounds (Lau et al. 2007). It is also possible that these vesicles correspond to lipoproteins that are packaged and awaiting uptake across the YSL (Fraher et al. 2016). However, only a portion of the vesicles are small enough to fall within the standard diameter measurements of the largest class of lipoproteins, chylomicrons, which are 200-600 nm (German et al. 2006). Additional analysis must be completed to understand the lipid composition of these vesicles.

4.4.2 Potential Pathway Targets of Long Chain PFASs Identified Through Gene Expression

Long chain PFASs were originally thought to elicit their toxic effects through activation of pparα (Sohlenius et al. 1992), and all the PFASs in this study have been shown to activate pparα in *in vitro* models (Wolf et al. 2008a). However, studies have shown that this is not the only mechanism by which liver toxicity occurs (Albrecht et al. 2013; Das et al. 2017; Rosen et al. 2010). Expression analysis of *pparα* was completed first, and in this study, there was a significant decrease in *pparα* gene expression with PFOA exposure in 5 dpf larvae (Figure 4.9A). Downstream targets of *pparα* include *slc27a1*, *apoa1*, *lpl, mttp*, and *slco* transporters, as shown in Figure 4.2 (Klaassen and Aleksunes 2010; Mandard et al. 2004). However, decreased expression of these downstream genes did not occur with PFOA exposure (Figure 4.10, 4.11). Although, the same doses of PFOA caused a significant increase in *slco2b1* expression (Jantzen et al. 2016a). Inconsistencies were also observed with this pathway with exposures to PFOS and PFNA. In the PFOS and PFNA treatment groups, *pparα* expression was not changed, but changes in expression of the downstream genes were observed (Figure 4.9A). These findings align with the literature, as only slight alterations in gene expression has been demonstrated with PFAS exposures in rodent models at doses higher than in this study (Bijland et al. 2011; Rosen et al. 2010).

Pparγ is a nuclear receptor which regulates the expression of many genes associated with lipid breakdown (Ahmadian et al. 2013). However, there is overlap in genetic regulation with pparα, as

outlined in Figure 4.2 (Ahmadian et al. 2013; Mandard et al. 2004). Due to its role in lipid homeostasis, this factor has also been studied as a potential target of PFASs. In the present study, there was a significant increase in *pparγ* gene expression with PFOS exposure (Figure 4.9B). Increased *pparγ* expression has been observed with PFOS exposure in zebrafish and other models (Sant et al. 2018; Watkins et al. 2015). Additionally, downstream of pparγ are *lpl* and *slc27a1* (Ahmadian et al. 2013; Frohnert et al. 1999). While no changes were observed in *lpl* expression, there was a similar increase in *slc27a1* gene expression with PFOS exposure (Figure 4.10).

Leptin is another hormone involved in energy metabolism in zebrafish, specifically by regulating glucose homeostasis and metabolic rate (Dalman et al. 2013; Michel et al. 2016). This differs from the function in rodents and humans, where leptin regulates hunger and lipogenesis (Pan and Myers 2018). However, there may be some overlap as leptin activation causes a decrease in *lpl* activity in fish (Salmeron et al. 2015). In the present study both PFOS and PFOA caused significant decreased *lepa* gene expression at all doses examined (Figure 4.9C). Additionally, there was no increase in *lpl* expression at any dose of PFOS or PFOA (Figure 4.10C). It is possible that *lpl* expression is not altered as expected due to the competing regulators of its expression, *pparα, pparγ* and *lepa.*

While traditional activation of receptor and consistent effects on downstream targets was not observed in this study, it is still possible that activation of the receptors has occurred. Expression of these genes varies over the course of development (Salmeron et al. 2018), and it could be that certain time points are more sensitive than the 5 dpf selected in this study.

4.4.3 Regulation of Genes Responsible for Lipid Distribution and Metabolism Altered with Long Chain PFAS Exposure

The following genes, *mttp*, *slc27a1*, *lpl*, *apoa1*, and *apoc2*, are related to lipid distribution and metabolism in the developing zebrafish, reviewed in (Quinlivan and Farber 2017; Salmeron 2018). Microsomal triglyceride transfer protein, mttp, functions in the packages of neutral lipids in

lipoproteins containing apolipoprotein b (Marza et al. 2005). There was a small, significant increase in *mttp* gene expression with exposure to 0.2 and 2 μM PFOA, and a greater increase, albeit not significant, in *mttp* expression at 2 μM PFNA (Figure 4.10A). In the YSL, mttp is necessary for the uptake of yolk lipids (Schlegel and Stainier 2006). This increase in *mttp* expression with PFNA may be one reason for the observed significant decrease in yolk sac fluorescence at the same time point (Figure 4.5). However, it has been noted that *mttp* transcript expression increases with dietary lipids in zebrafish, but this did not translate to an increase in mttp protein (Schlegel and Stainier 2006), and similarly, a protein increase in mttp might not have occurred in this study.

The fatty acid transporter, slc27a1, is involved in the uptake of long chain fatty acids in skeletal muscle, adipose tissue, and the heart (Anderson and Stahl 2013; Salmeron et al. 2015). It is often associated with long chain fatty acyl-coenzyme A synthetase which activates the newly transported fatty acids (Anderson and Stahl 2013). While slc27a1 has not been confirmed in the YSL, its synthetase partner is reported in the YSL, suggesting slc27a1 plays a role there as well (Quinlivan and Farber 2017). Gene expression of *slc27a1* was significantly increased following exposure to 0.2 and 2 μM PFOS and 2 μM PFNA (Figure 4.10B). The increased expression with PFOS exposure corresponds with the rodent literature (Bijland et al. 2011; Rosen et al. 2010). Increased *slc27a1* expression has also been reported with PFNA exposure; although in this study, PFOA also induced *slc27a1* expression, which was not observed in the present study (Das et al. 2017). Similar to *mttp*, the increase in *slc27a1* expression with PFNA exposure might contribute to the decreased yolk fluorescence observed at the same dose (Figure 4.5).

Lipoprotein lipase, lpl, catalyzes the hydrolysis of triglycerides into fatty acids, reviewed in (Kersten 2014). In zebrafish, it is ubiquitously expressed throughout the developing embryo, including the YSL, and in adult fish, it is highly expressed in the liver (Feng et al. 2014). In this study, neither PFOS nor PFOA caused significant changes in *lpl* gene expression (Figure 4.10C). In rodent studies, PFOA exposure led to an increase in lpl expression, presumably due to pparα stimulation (Das et al. 2017; Guruge et al. 2006). Studies have been less consistent with lpl

expression following PFOS exposures (Bijland et al. 2011; Cheng et al. 2016; Fai Tse et al. 2016). There was a dose-dependent increase in *lpl* expression with PFNA exposure (Figure 4.9C), which aligns with what has been reported in the rodent literature (Das et al. 2017).

Apolipoproteins are critical elements in the lipoproteins which allow for lipid packaging and movement throughout the body. Both *apoa1* and *apoc2* genes were examined in this study. These proteins function in the YSL, as well as liver and digestive systems of larval fish (Otis et al. 2015; Pickart et al. 2006). Apoa1 is the major protein component of HDL (Schonfeld and Pfleger 1974), and in this study *apoa1* gene expression did not alter with PFAS exposure (Figure 4.11A). Effects on *apoa1* transcript level may be dose or time dependent, as in the literature both transcript induction (Fai Tse et al. 2016; Sant et al. 2018) and reduction (Bijland et al. 2011; Cui et al. 2017) have been observed with PFOS exposures. Apoc2 plays a role not only in the uptake of yolk lipids, but also in the activation of lipoprotein lipase, lpl (Kersten 2014; Pickart et al. 2006). In this study, 2 μM PFNA exposure resulted in a significant increase in *apoc2* expression (Figure 4.11B), and this most likely relates to the increased *lpl* expression at the same PFNA concentration (Figure 4.10C).

Many of the factors discussed are necessary for lipoprotein development and movement of the yolk lipids across the YSL (Quinlivan and Farber 2017). With the measurement of fluorescence at 5 dpf, there was a decrease in yolk sac fluorescence only following 2 μM PFNA (Figure 4.5B). Similarly, there was an increase in expression of *slc27a1*, *lpl*, and *apoc2*, all of which contribute to lipid processing and uptake, which may explain this observed effect following PFNA exposure (Figures 4.10, 4.11).

Expression changes in the genes in this study cannot fully explain all effects observed with the BODIPY-FL fatty acids, as a decrease in vesicle diameter was observed with all PFASs (Figure 4.8). As this study has only assessed gene expression, it is possible that these factors are impacted on a functional level. These genes were also only a selection of those present in the developing embryo, for instance, there are 7 paralogues to the slc27 family and 11

apolipoproteins (Quinlivan and Farber 2017). Other factors may better explain the effects on vesicle formation in the yolk sac. It might also be that the changes in yolk vesicles are due to compositional changes to the yolk sac lipids. In adult salmon, PFOS and PFOA exposures changed the tissue lipid profiles, leading to a decrease in most fatty acids (Arukwe et al. 2013). In the Arukwe et al.(2013) study, transcription of fatty acid elongases was altered with exposure. This study also did not examine the possible endocytosis of lipids across the YSL. The vesicle differences may also not result from gene and/or protein changes, but rather be an effect of the surfactant properties of these compounds (Lau et al. 2007).

4.4.4 Pathway Comparison PFASs Chain Length on Gene Expression

Gene expression analysis in these same genes was also completed at higher doses (0.2, 2, and 20 µM) for PFHxA, PFHxS, and 6:2 FTOH to see if these compounds may target the same pathways as the long chain PFASs they were intended to replace. These compounds do have different effects on the genes regulating lipid homeostasis compared to C-8/C-9 PFASs. Both PFHxA and PFHxS have been shown to activate PPARα *in vitro* (Wolf et al. 2008a). However, neither of these compounds impacted expression of *pparα*, as well as, *pparγ* or *lepa* gene expression levels (Figure 4.12). This suggests that the terminal group does not drive this effect as PFHxA, PFOA, and PFNA, all of which contain a terminal carboxylic acid group, displayed different regulation patterns for these genes (Figure 4.9). Similarly, PFOS impacted expression of *pparγ* and *lepa* (Figure 4.9), which PFHxS, which also contains a terminal sulfonate group, did not. This reinforces the need to assess the toxicity of these compounds on an individual basis using an adverse outcome pathways (AOPs) approach.

PFHxA and PFHxS exposures did lead to some changes in the expression of genes related to fatty acid uptake and distribution. PFHxA exposure caused an increase in *mttp*, *slc27a1*, *lpl*, and *apoc2* expression, which suggests increased lipid uptake and metabolism (Figures 4.13, 4.14). PFNA exposure caused a similar gene expression profile and an increase in fatty acid uptake (Figures 4.5, 4.10, 4.11). It is therefore possible that PFHxA would cause a phenotype more

similar to PFNA than PFOA in term of lipid distribution, but this has not yet been examined. PFHxS was similar to PFOS in that only a few changes in transcript levels were elicited (Figures 4.9-4.14). However, *apoa1* and *apoc2* increased with PFHxS exposure, yet these genes were unaltered with PFOS. It is possible that based on these observed changes in gene expression with PFHxA and PFHxS that these compounds would also elicit effects on lipid distribution, and therefore, warrants further study with BODIPY-FL fatty acids and lipid composition.

The incorporation of the 6:2 FTOH compound was to serve as a control for the end groups, and additionally it has been incorporated in manufacturing processes (Martin et al. 2005; Rice 2015; Yuan et al. 2016). However, compared to the other C-6 compounds, 6:2 FTOH had a greater impact on gene expression. Exposure to all doses 6:2 FTOH caused a significant increase in *pparα* and *pparγ* expression (Figure 4.12). PPARα activation can create increased expression of downstream targets, such as *mttp*, *slc27a1*, *lpl*, and *apoa1* (Ameen et al. 2005; Mandard et al. 2004). PPARγ overlaps in regulating expression of *mttp*, *slc27a1*, and *lpl* (Frohnert et al. 1999; Salmeron 2018). This is outlined in Figure 4.2 and demonstrated with 6:2 FTOH, which caused increased transcript levels of these genes (Figure 4.13 and 4.14). This suggests that 6:2 FTOH may trigger these pathways more than PFHxA and PFHxS. This occurs despite the lack of morphological effects observed following exposure (Table 2.4).Therefore, it is important to incorporate this compound in future lipid distribution and metabolism studies.

4.4.5 Conclusions

This study is the first that utilized the model of early yolk uptake and lipid distribution in larval zebrafish with PFAS exposures. The examination of early lipid distribution has added to the established phenotypes of 5 dpf zebrafish larvae (Hagenaars et al. 2011; Jantzen et al. 2016a; Zheng et al. 2011). These studies established that the endpoint of yolk sac area is altered with PFAS exposure, which was not only confirmed in this study, but changes in lipid distribution patterns were also observed in the larval yolk sac (Figures 4.5-4.8). These changes were visualized through confocal microscopy which provided the resolution necessary to make these

assessments. Measure of total fluorescence was not as sensitive, and did not provide much information on distribution of yolk sac lipids.

The relationship between PFASs and PPAR activation is complex. While PFASs activate PPAR and are involved in some of the observed toxicity (Wolf et al. 2008a), activation of these nuclear receptors is not the sole mechanism by which toxicity can occur (Das et al. 2017; Rosen et al. 2010; Yang et al. 2002). Our understanding of other mechanisms is made difficult by species differences in response to ppar activation (Albrecht et al. 2013). Zebrafish do respond to PPAR agonists, but it is unknown how much PPAR activation contributes to the observed effects (Flynn et al. 2009; Salmeron 2018). Following a similar exposure paradigm as the present study, exposure to clofibrate and gemfibrozil, pparα agonists, impacted similar endpoints as were observed in this study. Larvae exposed to these compounds had decreased length, yolk sac area, lipid staining in the body, and little effect on *apoa1* and *mttp* expression (Raldua et al. 2008). This phenotype is similar to that of PFOS. Therefore, there is potential for this model to be used to screen ppar agonism; however, this model will need further characterization with either known agonists or genetic alteration.

Gene expression analysis at 5 dpf also identified potential molecular targets, which was the most sensitive endpoint examined. Unique patterns of expression were observed with each PFAS examined (Figures 4.9-4.14). These changes may begin to explain the different phenotypes observed. Additionally, many of the gene targets examined are related to ppar activation (Mandard et al. 2004; Salmeron 2018), and therefore the exact mechanism of activation of these genes would need to be further explored. Additionally, endpoints were only examined at 5 dpf, and time course analysis during development may demonstrate unique patterns of expression not observed in the present study. It could be that these genes change in regulation at different points in development that account for the phenotypic effects. Also, changes in gene expression may not reflect changes in concentration or functionality at the protein level. However, these studies identify different effects at the gene level with PFAS exposure identifying possible impacted pathways. These data highlight that unique targets may be more impacted depending of the

PFAS, but these modifications in expression may still fall under the general lipid dysregulation AOP.

Comparison of the effects throughout this study has revealed different profiles for each of the PFASs. Despite that PFOS and PFOA are both C-8 PFASs, they caused different effects at 5 dpf on yolk sac morphology (Jantzen et al. 2016a), yolk sac vesicle appearance (Figure 4.8), and gene expression of lipid homeostasis regulators (Figure 4.9) and their downstream genetic targets (Figure 4.10, 4.11). Similarly, PFHxA, PFHxS, and 6:2 FTOH, all C-6 compounds, have different effects at 5 dpf on morphological endpoints (Table 2.4) and expression patterns of genes related to lipid distribution and metabolism (Figures 4.12 - 4.14). PFOA, PFNA, and PFHxA all contain a terminal carboxylic acid group, but as discussed differ in morphologic effects, fatty acid uptake, and gene expression. PFOS and PFHxS, both of which contain a terminal sulfonate group, also caused varied responses in the zebrafish. Therefore, both fluorinated chain length and terminal groups appear to drive the PFAS toxicity phenotype in early zebrafish development.
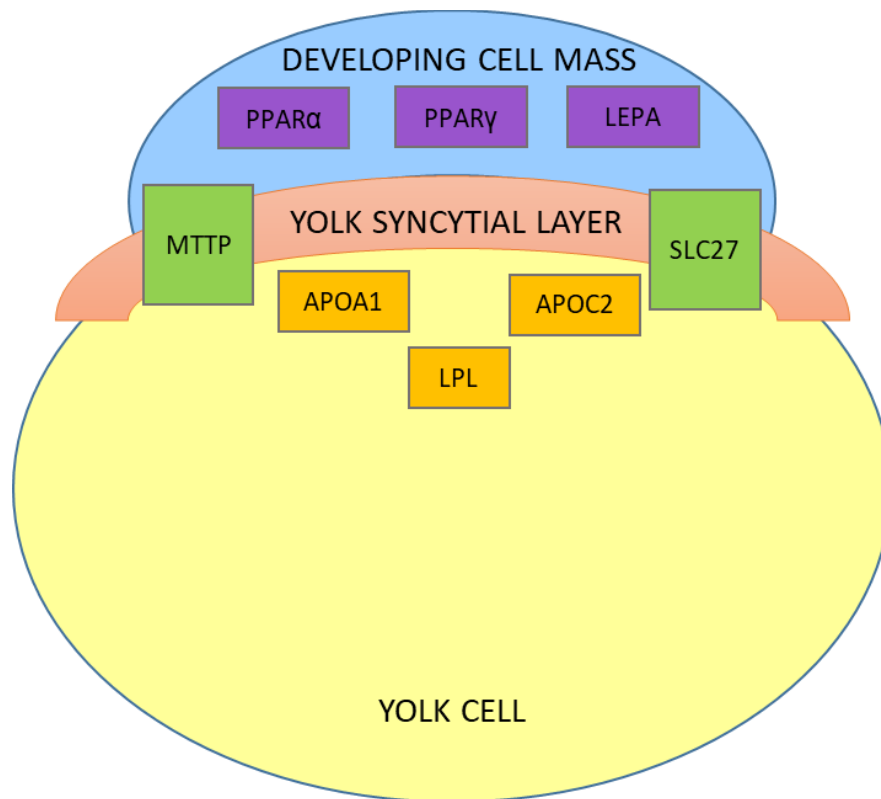
Figure 4.1. Expression pattern and localization of lipid-related genes during early development in the zebrafish embryo. These factors include mttp, microsomal triglyceride transfer protein, lpl, lipoprotein lipase, slc27a1, fatty acid transporter, and apoa1/apoc2, apolipoproteins.
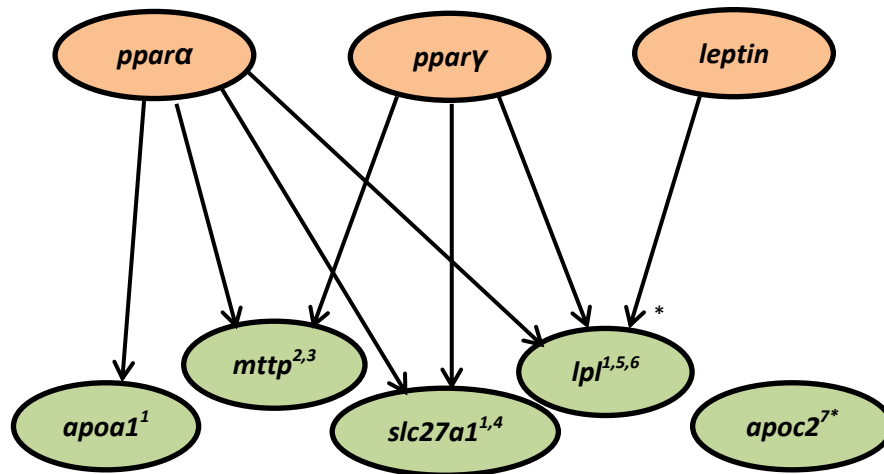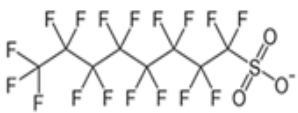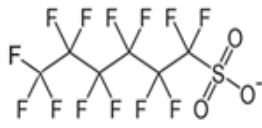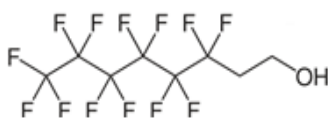
Figure 4.2. Regulation of genes in this study by pparα, pparγ, and leptin. Arrows indicate the nuclear receptor increases expression of the gene. Asterisk (*) indicates inverse relationship in activation. [1]reviewed in (Mandard et al. 2004), [2](Ameen et al. 2005), [3](Moran-Salvador et al. 2011), [4](Frohnert et al. 1999), [5]reviewed in (Salmeron 2018), [6](Salmeron et al. 2015), [7]*regulated by pparδ (Peters et al. 2003).

Table 4.1. Chemical structure of perfluorooctanoic acid (PFOA), perfluorooctane sulfonate (PFOS), perfluorononanoic acid (PFNA), perfluorohexanoic acid (PFHxA), perfluorohexane sulfonate (PFHxS), and 6:2 fluorotelomer alcohol (6:2 FTOH).

Figure 4.3. Exposure paradigms in the present study. (A) Waterborne PFAS exposures began at 3 hpf and continued through hatching until 120 hpf. Sac fry larvae were examined for gene expression endpoints. (B) Microinjections of fluorescently-tagged fatty acids were completed at roughly 7 hpf, when embryos had reached the 60-80% epiboly stage. Waterborne exposures began following injections and were carried out until 120 hpf. Fluorescence was monitored at 24 and 120 hpf via fluorescent microscopy and confocal microscopy.

Table 4.2. Gene name, ID, function, and primer sequences (5'-3') for the gene examined in this study.

GENE		GENE ID	FORWARD PRIMER	REVERSE PRIMER	FUNCTION
actb	β-actin	NM_131031	CGAGCAGG AGATGGGA ACC	CAACGGAA ACGCTCATT GC	Housekeeping gene
pparα	Peroxisome-proliferator activating receptor α	NM_001161333	CATCTTGC CTTGCAGA CATT	CACGCTCA CTTTTCATT TCAC	Nuclear receptor
pparγ	Peroxisome-proliferator activating receptor γ	NM_131467	GGCATGTC ACACAACG CG	CCTTCTCA GCCTGCGG C	Nuclear receptor
apoa1	Apolipoprotei n A1	NM_131128	AGCAGCCT TGGTGTAC CTGA	AAAGCCTG GGAGGTGG TC	Lipid carrier protein
apoc2	Apolipoprotei n C2	NM_001326448	TGGCTATC ACGGTTTTT GTTGC	GGTTCCCT TCTCATCCT CAGC	Lipid carrier protein
slc27a1	Solute carrier family 27, member a1	NM_001013537	TTCGGACG GCTAAAAG GGAC	GGTATGGT GTTTCGGTT GCG	Fatty acid transporter
mttp	Microsomal triglyceride transfer protein	NM_212970	GAGGCCAC GCTGGATT TCAT	TTGGACAC CGTCTCTCT GAAG	Triglyceride transporter
lepa	Leptin A	NM_001128576	AGATTCCC GCTGACAA ACCC	TCGGCGTA TCTGGTCA ACAT	Hormone
lpl	Lipoprotein lipase	NM_131127	ACATTTCCT CGGGATTG GAAACT	TCCATCATC CATTCTGTG GCAT	Lipid breakdown
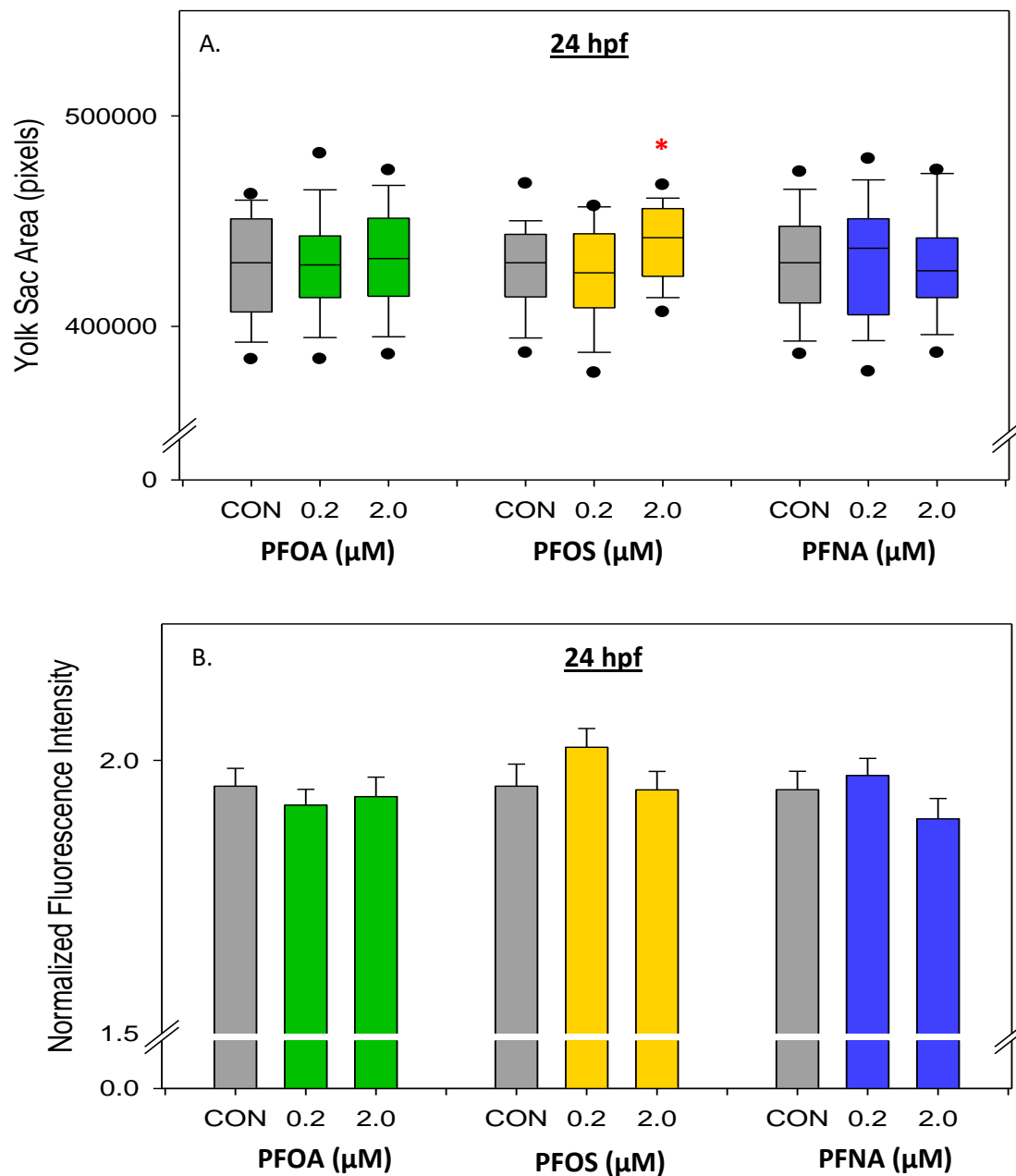
Figure 4.4. Yolk sac area and fluorescence intensity measurements at 24 hpf following microinjection of BODIPY-FL fatty acids and waterborne PFAS exposures. (A) Yolk sac area in pixels in each treatment group. Box plots encompass 25-75%, whiskers 10-90% and dots 5 and 95%. (B) Fluorescence pixel intensity normalized to background intensity (mean ± SEM) in larval yolk sacs. An asterisk (*) indicates $p < 0.05$, one-way ANOVA, N=30-45.
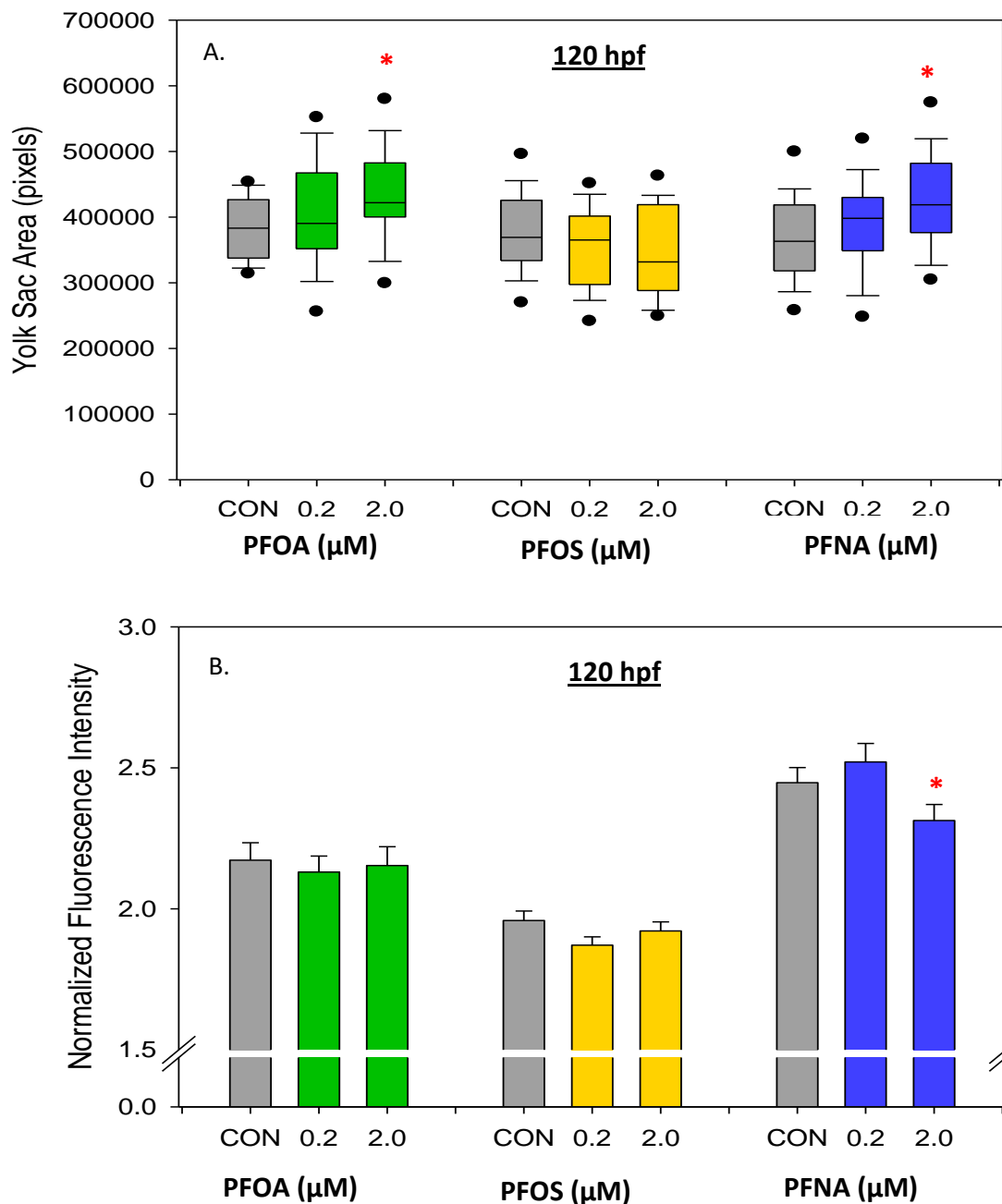
Figure 4.5. Yolk sac area and fluorescence intensity measurements at 120 hpf following microinjection of BODIPY-FL fatty acids and waterborne PFAS exposures. (A) Yolk sac area in pixels in each treatment group. Box plots encompass 25-75%, whiskers 10-90% and dots 5 and 95%. (B) Fluorescence pixel intensity normalized to background intensity (mean ± SEM) in larval yolk sacs. An asterisk (*) indicates $p < 0.05$, one-way ANOVA, N=30-45.

A.

B.
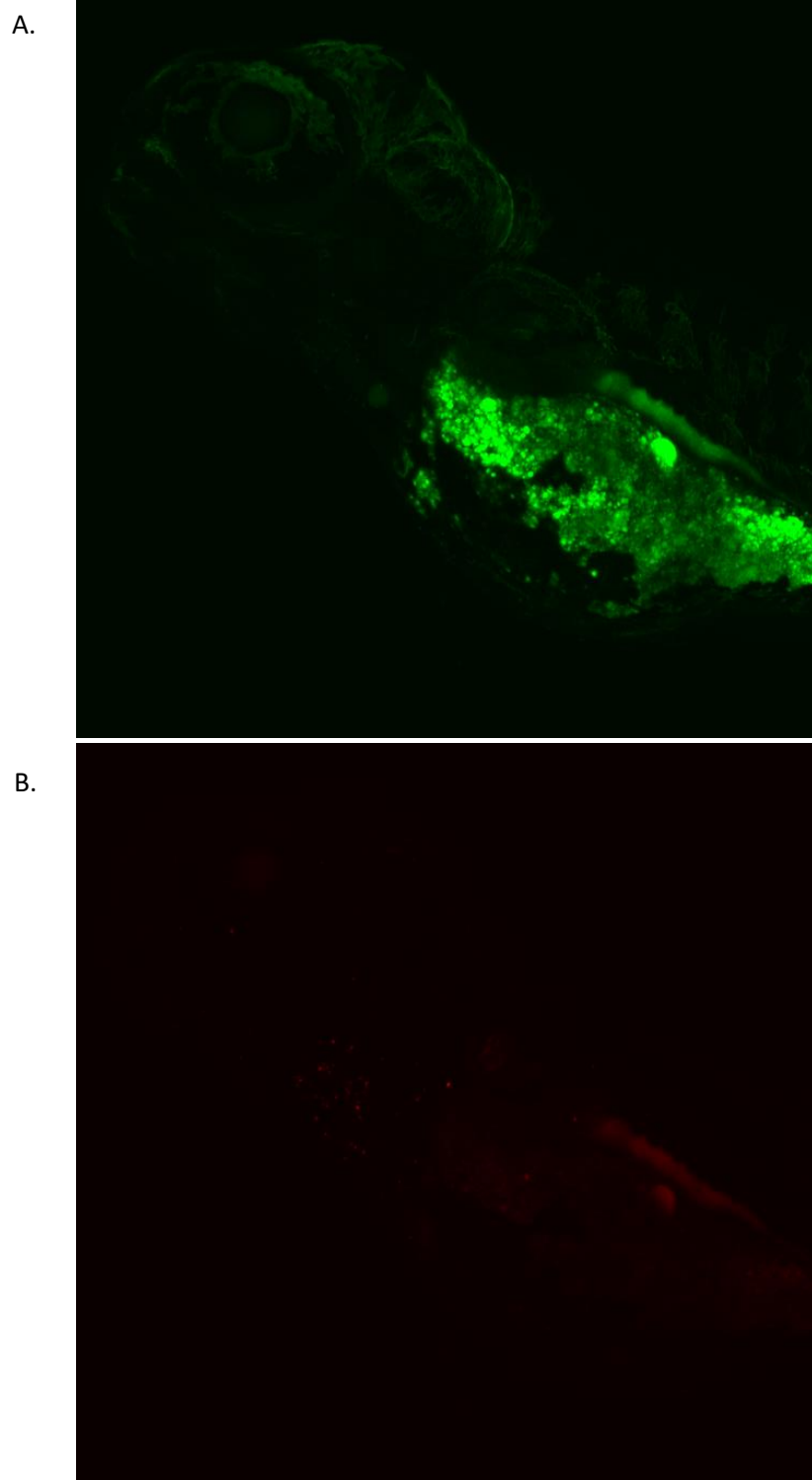
Figure 4.6. Representative images of a larval zebrafish microinjected with BODIPY-FL fatty acids and reared in control solution. Images were captured using confocal microscopy under 10x magnification and (A) green fluorescent filter and (B) red fluorescent filter.
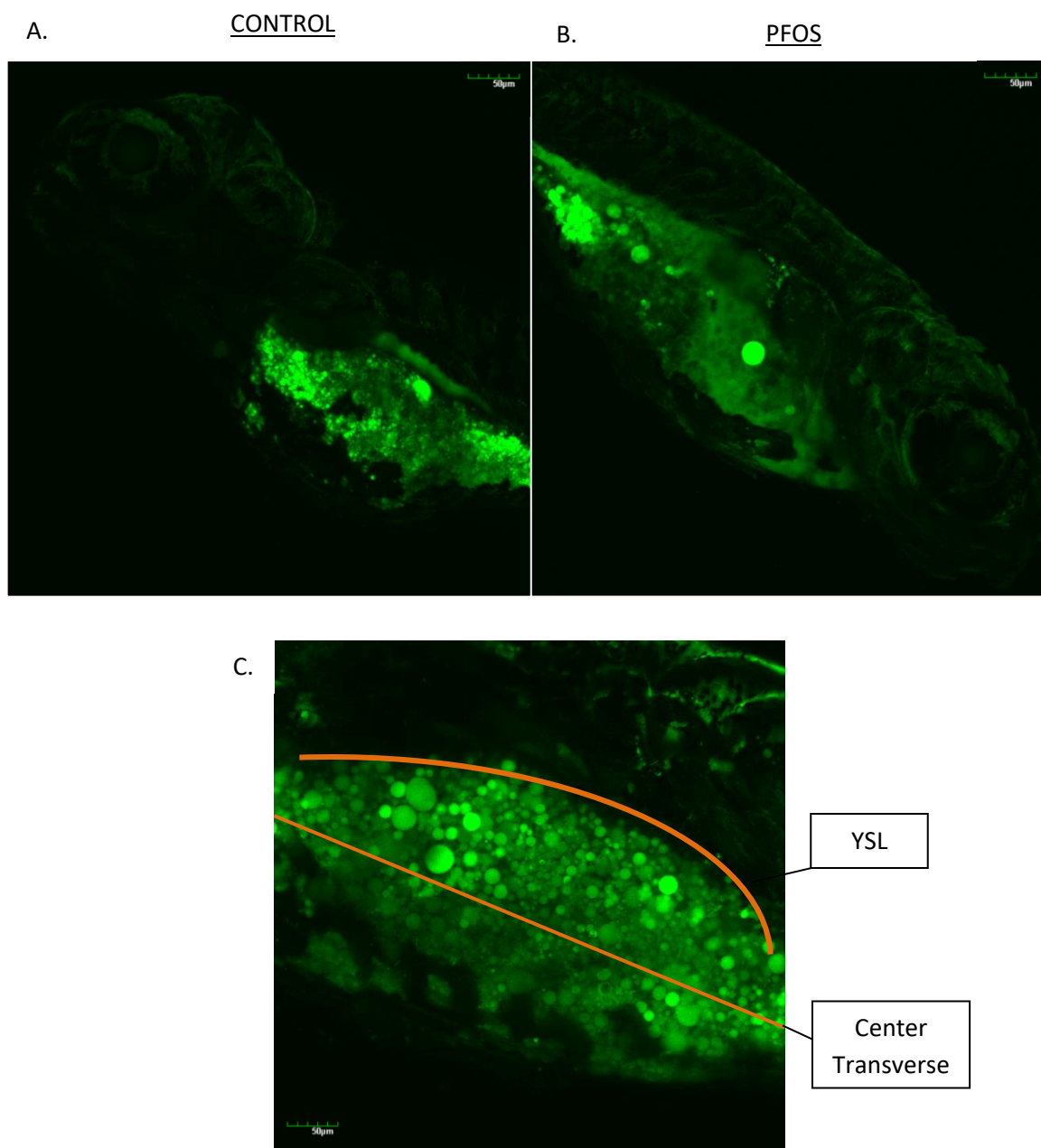
Figure 4.7. Representative confocal images of larval zebrafish microinjected with fluorescently tagged fatty acids reared in (A) control (B) 2 µM PFOS captured under 10X magnification. (C) Representative of site of vesicle measurements along YSL and center yolk cell transverse captured under 25X magnification.
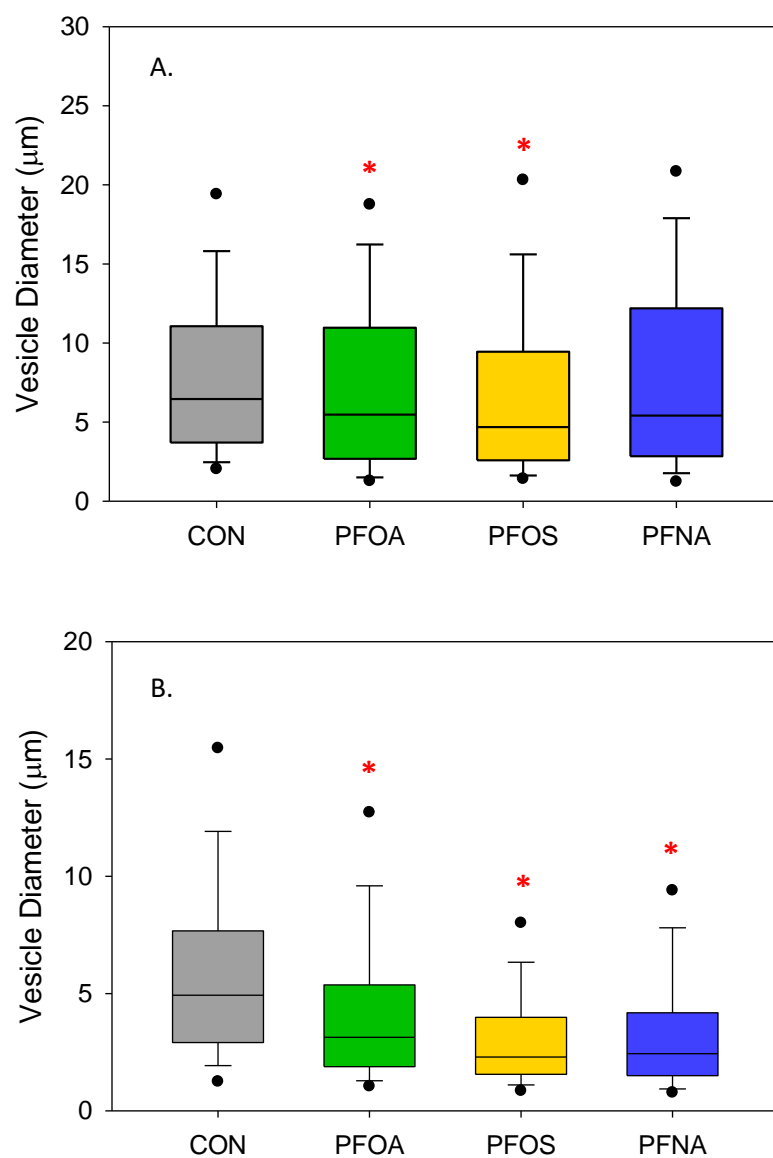
Figure 4.8. Vesicles diameter in 5 dpf yolk sac of PFAS-exposed larvae through (A) transverse through the yolk sac center and (B) transverse along the yolk syncytial layer. Box plots encompass 25-75%, whiskers 10-90% and dots 5 and 95%. An asterisk (*) indicates $p<0.05$, rank sum T Test, N=180-293.
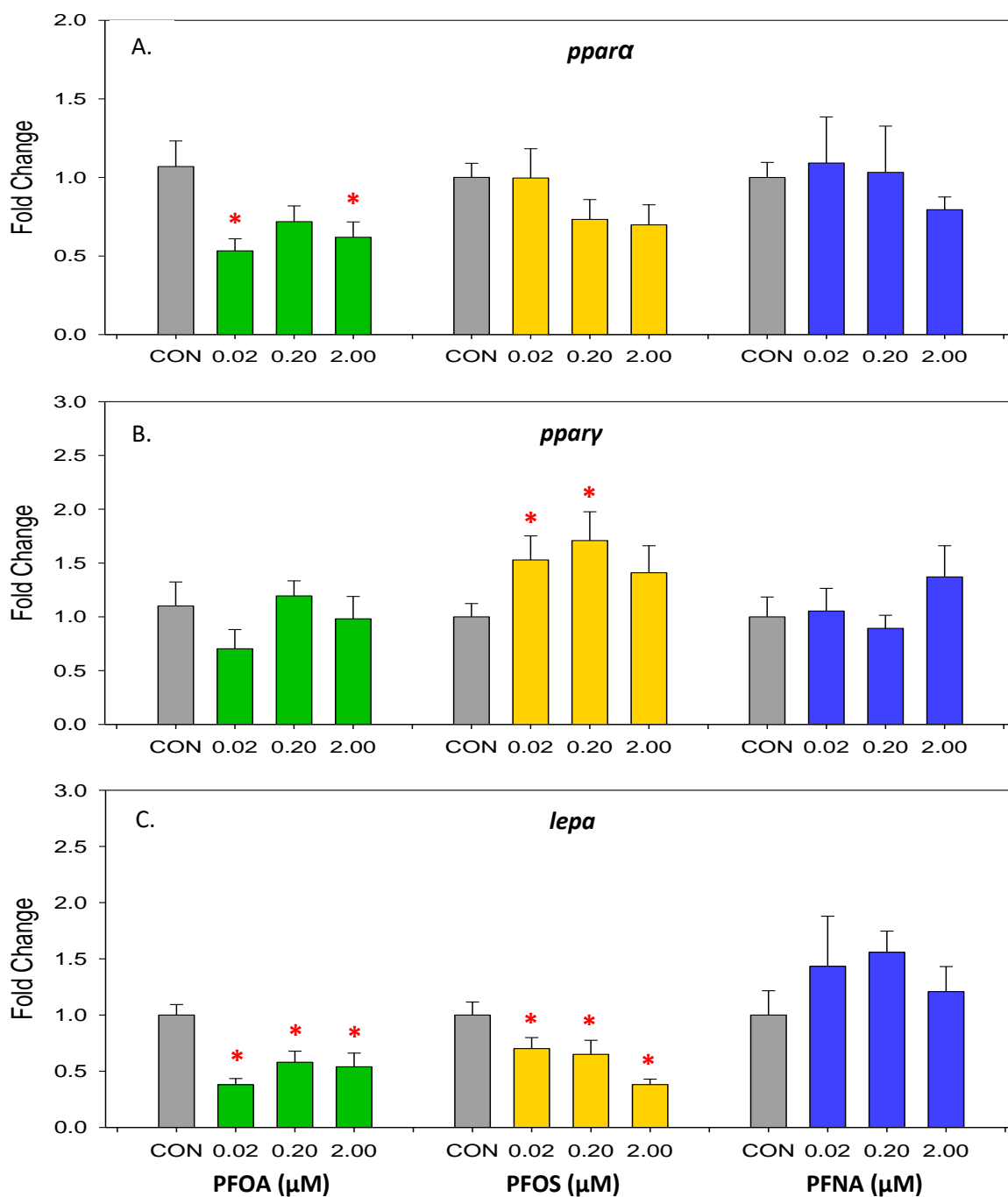
Figure 4.9. Gene expression at 5 dpf following 0, 0.02, 0.2, and 2 µM PFOA, PFOS, or PFNA. Gene expression represented as mean and standard error (SEM) fold change of (A) *pparα*, peroxisome proliferator activating receptor α (B) *pparγ,* peroxisome proliferator activating receptor γ (C) *lepa*, leptin A hormone. An asterisk (*) indicates $p < 0.05$, one-way ANOVA, N=8-14.
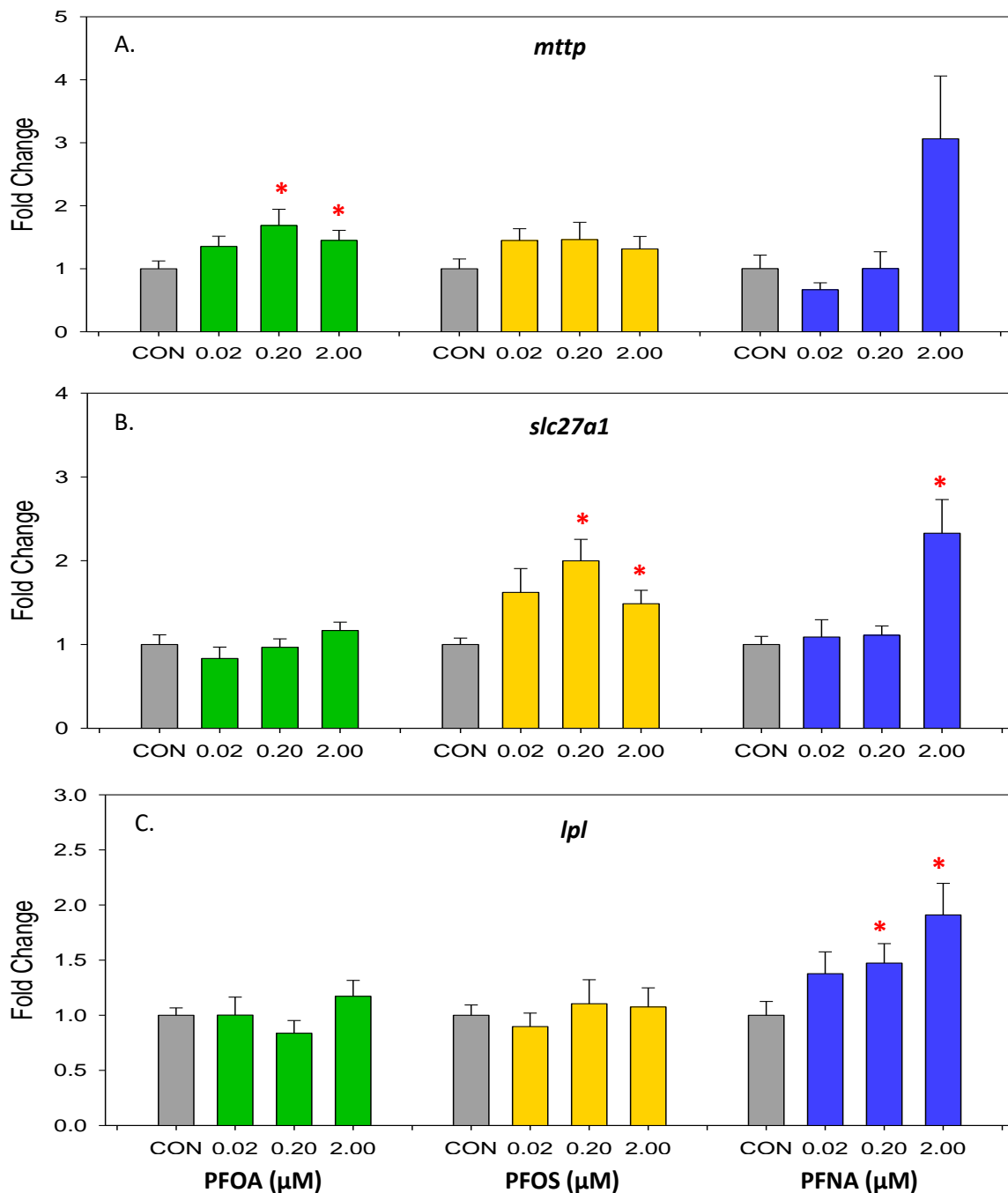
Figure 4.10. Gene expression at 5 dpf following 0, 0.02, 0.2, and 2 µM PFOA, PFOS, or PFNA. Gene expression represented as mean and standard error (SEM) fold change of (A) *mttp,* microsomal triglyceride transfer protein (B) *slc27a1,* solute carrier family 27, member a1 (C) *lpl,* lipoprotein lipase. An asterisk (*) indicates $p<0.05$, one-way ANOVA, N=8-14.
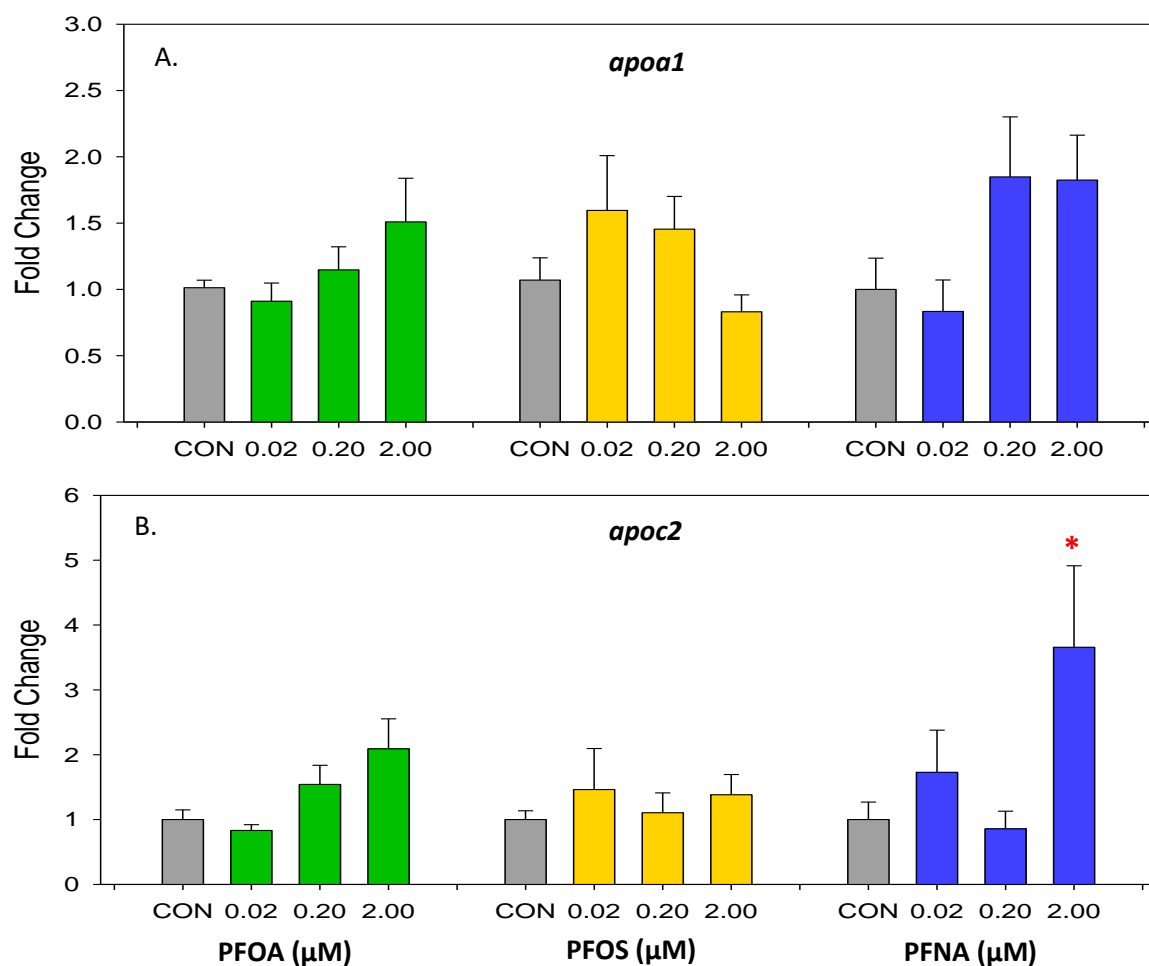
Figure 4.11. Gene expression at 5 dpf following 0, 0.02, 0.2, and 2 µM PFOA, PFOS, or PFNA. Gene expression represented as mean and standard error (SEM) fold change of (A) *apoa1*, apolipoprotein A1 (B) *apoc2*, apolipoprotein C2. An asterisk (*) indicates $p < 0.05$, one-way ANOVA, N=8-14.
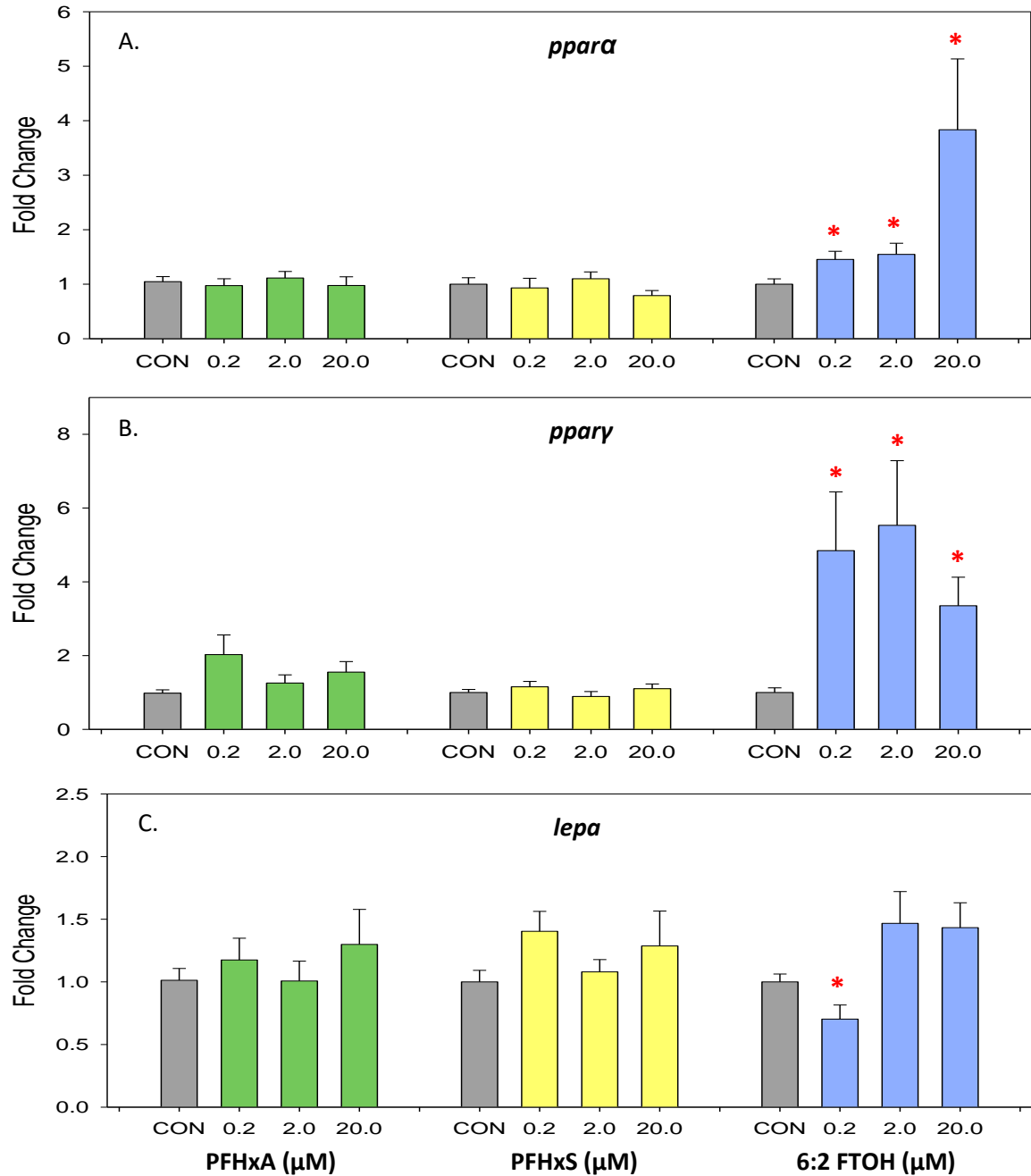
Figure 4.12. Gene expression at 5 dpf following 0, 0.2, 2, and 20 µM PFHxA, PFHxS, or 6:2 FTOH. Gene expression represented as mean and standard error (SEM) fold change of (A) *pparα*, peroxisome proliferator activating receptor α (B) *pparγ,* peroxisome proliferator activating receptor γ (C) *lepa*, leptin A hormone. An asterisk (*) indicates $p < 0.05$, one-way ANOVA, N=8-14.
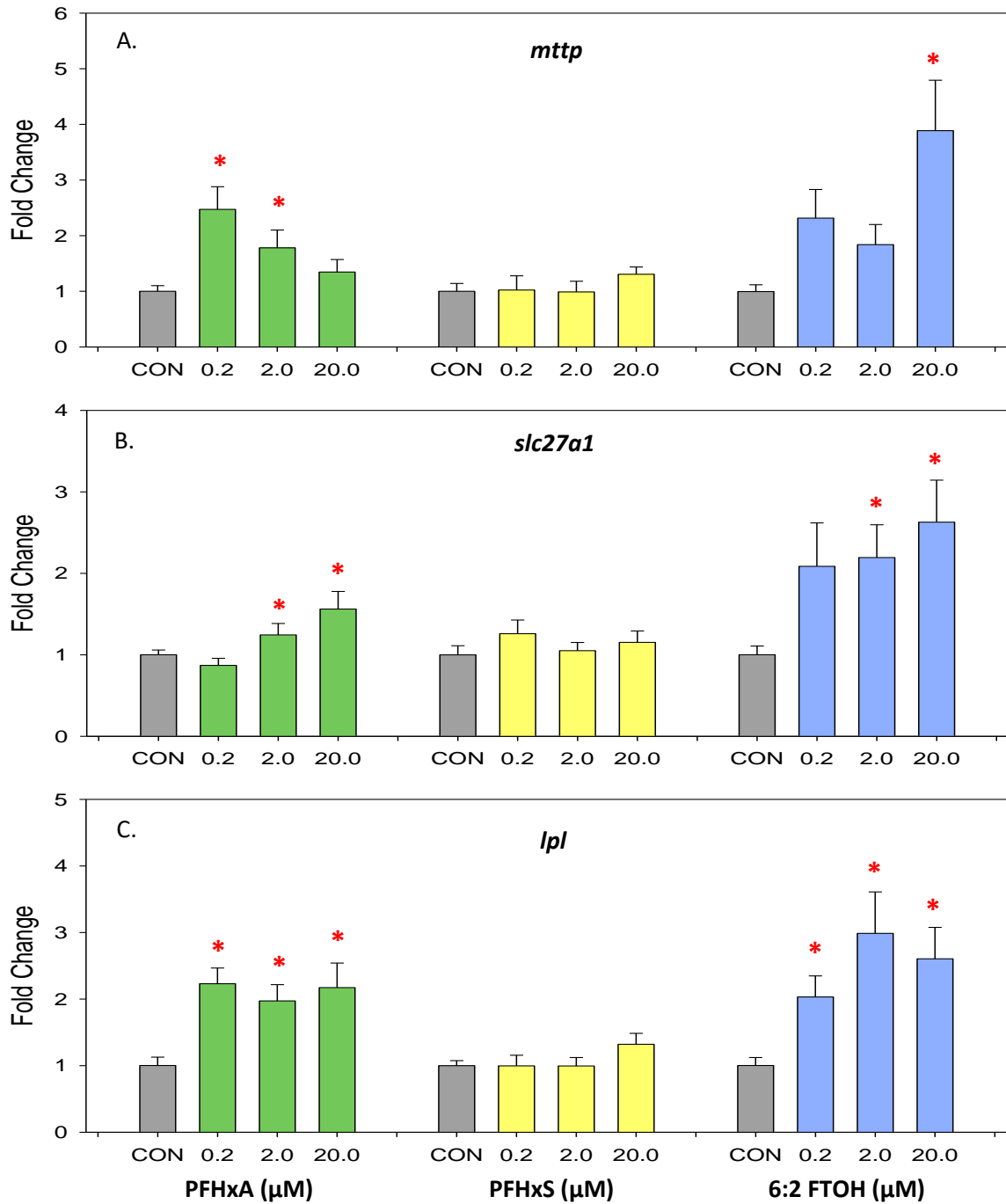
Figure 4.13. Gene expression at 5 dpf following 0, 0.2, 2, and 20 µM PFHxA, PFHxS, or 6:2 FTOH. Gene expression represented as mean and standard error (SEM) fold change of (A) *mttp,* microsomal triglyceride transfer protein (B) *slc27a1,* solute carrier family 27, member a1 (C) *lpl,* lipoprotein lipase. An asterisk (*) indicates $p<0.05$, one-way ANOVA, N=8-14.
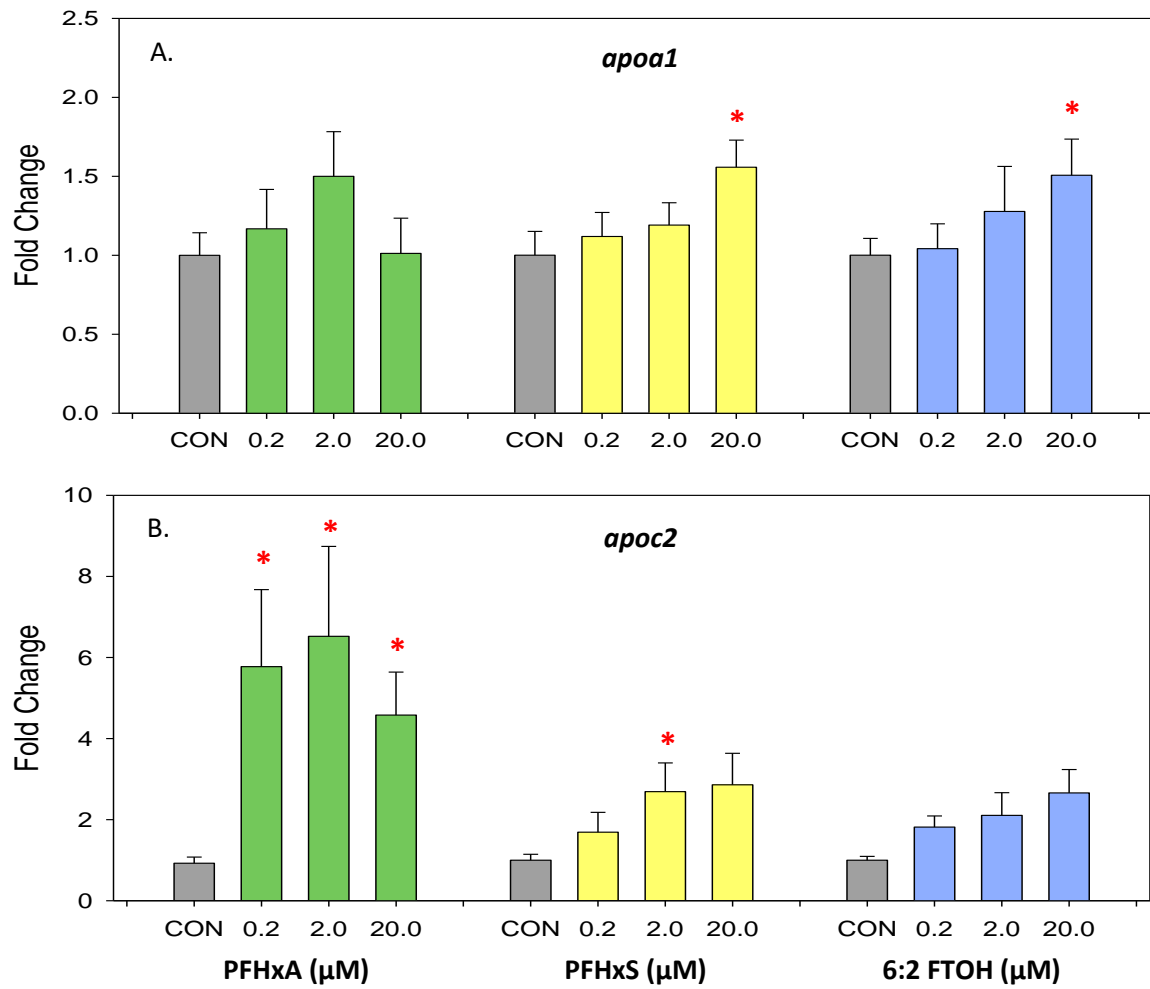
Figure 4.14. Gene expression at 5 dpf following 0, 0.2, 2, and 20 µM PFHxA, PFHxS, or 6:2 FTOH. Gene expression represented as mean and standard error (SEM) fold change of (A) *apoa1*, apolipoprotein A1 (B) *apoc2*, apolipoprotein C2. An asterisk (*) indicates p<0.05, one-way ANOVA, N=8-14.

Table 4.3. Summary of gene expression results related to lipid homeostasis at highest doses of long chain PFASs (20 µM) and low molecular weight alternatives (20 µM) in 5 dpf larvae.

	2 µM PFOA	2 µM PFOS	2 µM PFNA	20 µM PFHxA	20 µM PFHxS	20 µM 6:2 FTOH
pparα	⬇	N.S.	N.S.	N.S.	N.S.	⬆
pparγ	N.S.	⬆	N.S.	N.S.	N.S.	⬆
lepa	⬇	⬇	N.S.	N.S.	N.S.	N.S.
mttp	⬆	N.S.	N.S.	N.S.	N.S.	⬆
slc27a1	N.S.	⬆	⬆	⬆	N.S.	⬆
lpl	N.S.	N.S.	⬆	⬆	N.S.	⬆
apoa1	N.S.	N.S.	N.S.	N.S.	⬆	⬆
apoc2	N.S.	N.S.	⬆	⬆	N.S.	N.S.

Chapter 5

General Conclusions, Discussion, and Future Directions

5.1 Summary of Key Findings

This dissertation examined the toxicity profiles of 3 low molecular weight PFAS alternatives: PFHxA, PFHxS, and 6:2 FTOH. Morphometric, behavioral, gene expression, and lipid distribution profiles were examined in larval zebrafish following exposures to these C-6 compounds. Different profiles were observed for all 3 compounds, suggesting that chain length of PFAS does not determine toxicity. While changes were observed on physical and behavioral outcomes, the endpoint most consistently altered was gene expression. In some cases, gene expression was altered without manifestation of morphological outcomes, suggesting potential pathways activated by exposure, but that the doses selected may have been too low to elicit effects, indicating that the doses selected were below the LOEL. Outcomes following 2 and 20 µM exposures in 5 dpf and 14 dpf larvae are summarized in Tables 5.1 and 5.2, respectively.

Behavioral patterns reflect the incorporation of multiple biological systems, and examination of behavioral patterns allows for an assessment of sensitive outcomes. This was supported in the present studies, where effects were observed following exposure to low molecular weight PFAS alternatives that did not manifest into morphological effects. This demonstrates the sensitivity of this type of assessment. However, the complexity of behavioral pathways makes it difficult to tease out targeted pathways from these results. In this study, gene expression was completed for a small selection of possible targets, which provides a starting point for future studies.

The long chain C-8/C-9 PFASs were utilized to validate the lipid uptake methods in these studies. The lipid dysregulation following PFOS and PFOA exposure is well-documented (Albrecht et al. 2013; Das et al. 2017; Lau 2012), so these compounds were tested in early embryonic uptake and larval zebrafish distribution. BODIPY-FL fatty acids were injected into the yolk sac during early stages of development, which allowed for visualization of vesicle formation in the yolk sac

and uptake into the embryos. Through this model, alterations in the formation of lipid vesicles in the yolk were demonstrated following PFAS exposures. There were minimal changes in uptake from the yolk sac, which suggests that this model is best suited for drastic changes on yolk uptake and the method of measuring total fluorescence may not be sensitive enough to detect subtle changes. However, the ability to monitor the movement of fluorescent yolk fatty acids uptake to different tissues and incorporation into different complex lipid molecules makes this model advantageous in zebrafish.

5.2 Adverse Outcome Pathways (AOPs)

The use of AOPs, adverse outcome pathways, provides an understanding of the related pathways and effects observed with PFAS toxicity. Generally, AOPs follow a molecular initiating event (MIE) that leads to key events (KE) through increasingly higher levels of biological organization. This cascade is ultimately associated with an adverse outcome (AO), which is observed at the organism and population levels. The outline of this type of analysis, as described by the OECD, is summarized in Figure 5.1 (OECD 2016). While the identification and elucidation of AOPs is still underway, hundreds of potential pathways and AOs have been identified (AOPWiki.org).

This discussion will be limited to 3 general AOPs impacted with exposure to the low molecular weight PFAS alternatives as demonstrated in this dissertation. These general AOPs include growth, lipid dysregulation, and neural adverse outcomes. The AOPs for these effects related to PFHxA, PFHxS, and 6:2 FTOH exposures are depicted in Figures 5.2-5.4. These diagrams provide a synthesis of this work and relevant information from the literature. Before discussion can begin, there are a few caveats that must be acknowledged. As a synthesis of information from this dissertation and the literature, these findings represent a variety of exposure doses, durations of exposure, and model organisms. These factors can all contribute to variability in response, especially considering the noted differences in half-lives across species and sexes with the PFASs (Lau et al. 2007; Wang et al. 2015; Wang et al. 2013b).

These AOPs serve a greater purpose than identifying adverse outcomes and potential impacted pathways. When applied to an aquatic model, such as the zebrafish, these AOPs can indicate potential population and therefore environmental concerns with PFAS exposures. The effects on larval growth can have implications on larval survivability in the wild. The decreased size observed with exposure to the long chain PFASs could mean that the smaller larvae would more readily be eaten as prey. Similarly, behavioral effects could impact populations. Increased activity, as was observed with PFOS and 6:2 FTOH exposures, also increases the opportunity of a larva to become prey. Increased predation could negatively impact wild population. While zebrafish are not native to US waterways, similar effects could occur in aquatic species that are critical to US ecosystems.

5.3 PFHxA Toxicity Profile

Despite the lowest LC_{50} (290 μM) of the low molecular weight PFAS alternatives at 5 dpf (Table 2.3), PFHxA elicited no morphological effects in the endpoints assessed, which were total length, yolk sac area, and pericardial sac area (Table 2.4). Gene expression was the most sensitive target of PFHxA exposures, where alterations in genes related to nervous tissue development, muscle formation, lipid uptake, and lipid distribution were observed (Figures 2.2, 2.3, 4.12-4.14). The same developmental PFHxA exposures followed by a 9 day depuration in clean water in 14 dpf larvae produced no effects on any of the behavioral endpoints examined (Figures 3.2-3.4). The only observed morphologic or lipid stain effect was a significant decrease in the area of stained lipids in the neural region (Figure 3.6, 3.7). Based on the lack of growth effects observed at 5 and 14 dpf, it appears that PFHxA does not impact the growth AOP (Tables 2.4, 3.2). Reductions in growth were not observed in rodent models as well (Chengelis et al. 2009b; Klaunig et al. 2014). Similarly, behavioral outcomes in the neural AOP were not impacted with PFHxA exposure, as observed in this study and others (Klaunig et al. 2014). Figure 5.2 provides a complete summary of these findings as they related to growth, neural, and lipid dysregulation AOPs.

Despite, the lack of physical and behavioral effects assessed in the present study, gene expression changes were observed, and these genes relate to the growth and neural AOPs (Figure 2.3). There was an increase in *tgfb1a*, which is involved in striated muscle development (Kim and Ingham 2009), which means this gene could relate to overall growth as well as behavior. This gene, along with *bdnf* are also involved in lateral line formation (Germana et al. 2010a; Xing et al. 2015), which is necessary for proper orientation of the fish in the water column (Froehlicher et al. 2009). Additionally, *bdnf* is necessary for neuronal development, and *ap1s1* is involved in vesicle trafficking between organelles, including neurotransmitters (Hashimoto and Heinrich 1997; McAllister 2001; Montpetit et al. 2008; Nakatsu et al. 2014). The dysregulation of these genes lead to the hypothesis that these larvae would have altered behavior; however, this was not observed. This suggests that these doses were able to elicit molecular changes on the gene level, and not manifested at higher levels of organization resulting in physical outcomes or key events in these AOPs.

The lipid dysregulation AOP is most impacted with PFHxA exposure, and a potential molecular initiating event (MIE) of this pathway is PPARα activation. It has been reported in the literature that PFHxA activates PPARα (Wolf et al. 2008a), which is supported by the current studies which found increased gene expression of downstream markers including *mttp*, *slc27a1*, and *lpl* (Figure 4.13). Key events that support this AOP have been reported in the literature at the cellular level, such as increased β-oxidation of fatty acids (Chengelis et al. 2009b) and decreased serum cholesterol (Klaunig et al. 2014), and organ level, such as hypertrophy (Chengelis et al. 2009b) and hepatomegaly (Klaunig et al. 2014). In addition, there was a decrease in the lipid stain in the neural region of the PFHxA-exposed larvae, which may be related to this AOP. While there is evidence to support the pathway of dysregulation of lipid homeostasis, it is unknown what impact this will have at the organism or population level.

Interactions of PFHxA with potential molecular targets, MIEs, were not addressed in the present studies. The potential MIEs in the literature that may relate to the discussed AOPs include the partitioning of PFASs to lipids, interaction of PFASs with subcellular transporters, and agonism of

PPARα. These, in part or in total, may contribute to the few effects observed with PFHxA exposure. It is possible that other MIEs, such as estrogen receptor interaction (Benninghoff et al. 2011), may contribute to the toxicity profiles and perhaps provide a more sensitive effect than those assessed in the present study. Similarly, *ap1s1* function was discussed in its potential neuromodulator role, but it can also function in other tissues (Gariano et al. 2014; Zizioli et al. 2010). With a 14-fold induction of *ap1s1* expression (Figure 2.3), it would be beneficial to examine other endpoints to assess if this change in regulation can be translated to other physical outcomes. Based on an assessment of the present data, PFHxA does not appear to be toxic to larval zebrafish. In comparison to the long chain PFASs, PFHxA is less toxic to the developing zebrafish and could be considered a safe alternative. However, based on the limited literature base on this compound, it still warrants further study.

5.4 PFHxS Toxicity Profile

PFHxS had a similar LC$_{50}$ value (340 µM) to PFHxA (Table 2.3); however this compound created a very different profile in terms of the growth, lipid, and neural AOPs, summarized in Figure 5.3. Exposures of PFHxS led to a consistent increase in total length observed at both 5 dpf and 14 dpf time points (Tables 2.4, 3.2). This was accompanied by an increase in yolk sac area in the 5 dpf larvae. Similarly, increased weight has been observed with PFHxS exposure in rats (Butenhoff et al. 2009a). The increase in growth with exposure to PFHxS could result from a stimulation of growth factors with exposure; however, the growth factor examined in this study, *tgfb1a*, was not altered in expression (Figure 2.3). Potential MIEs and cellular and tissue-specific responses that lead to this increased growth have not yet been identified.

Impacts to the neural AOP, specifically alterations in behavioral endpoints, were observed in the current studies. PFHxS exposure led to a decrease in larval activity and a decrease in response to photo-stimulation compared to controls (Figures 3.2-3.4). Decreased activity with PFHxS exposure has also been reported in rodent models (Viberg et al. 2013). While the MIE is not yet determined in this AOP, there are a number of cellular responses noted in the literature that may

be critical to manifestation of these outcomes. For example, one area of PFHxS accumulation is within neurons (Berntsen et al. 2017), which may explain why nervous system tissue is a target. It also has been demonstrated that PFHxS can lead to apoptosis in neurons (Lee et al. 2014a; Lee et al. 2014b), and alteration to the neurochemistry of the brain (Lee and Viberg 2013). Finally, on a tissue level, there was an observed increase in ORO-stained area in the neural region of the larvae (Figure 3.7), indicating a disruption of lipid distribution, which is also possibly related to the neural AOP. Despite these effects, very few of the genes examined in the gene expression analysis were altered following PFHxS exposure. There was a slight, non-dose-dependent increase in *bdnf* expression (Figure 2.3), which is related to neuronal development (McAllister 2001). An increase in expression may be related to the behavioral effects observed in the later larval stages; however the lack of response at higher doses does not make bdnf a promising candidate.

There were a number of effects observed at the tissue level in the lipid homeostasis AOP. At 5 dpf, there was an increase in yolk sac area, which can signify either edema or a reduction in uptake of the early nutrient source (Table 2.4). At 14 dpf, there was an increase in the liver area of the larvae (Figure 3.6), and similarly, increased liver weight has been reported with PFHxS exposure in rodent models (Bijland et al. 2011; Butenhoff et al. 2009a; Chang et al. 2018). These studies also confirmed that the increased liver weight was associated with an increase in hepatic cholesterol levels (Bijland et al. 2011; Butenhoff et al. 2009a), and a decrease in serum triglycerides (Bijland et al. 2011). The macromolecular targets of PFHxS have not yet been identified in this AOP. PPAR activation via PFHxS has been demonstrated (Wolf et al. 2008a), however, in the present study, only one gene downstream of PPARα (*apoa1*) was shown to increase with PFHxS exposure (Figure 4.14). Evidence in the literature of *in vivo* PPARα activation is inconclusive, as both induction of pparα (Bijland et al. 2011) and no changes in downstream genes (Chang et al. 2018) have been observed. It is possible that alterations in apolipoproteins, apoa1 and apoc2, can relate to the observed changes in lipid distribution, which is one of their main function (Dominiczak and Caslake 2011). Another possible contributing factor is the high partitioning coefficient of PFHxS into hepatic tissue (Kim et al. 2010).

Without a clear definition of steps in these 3 AOPs established, it is difficult to speculate the overall outcomes of PFHxS exposure. It is possible that ppar activation, transporter interaction and accumulation in lipids contribute to these pathways. Although with the overlap of biological processes, it is not difficult to imagine that there is overlap of the AOP pathways, especially considering the organismal level effects observed in the present studies. For example, is possible that the increase in larval size impacts the behavioral endpoints, that the larger size makes movements more cumbersome and difficult, which would explain the observed decrease in activity. It is also possible that alteration in lipid distribution, specifically the increase in lipid accumulation in the neural region and yolk sac, disrupts energy storage that can be utilized for movement. Additionally, the delayed mortality could be attributed to any of the AOPs discussed.

5.5 6:2 FTOH Toxicity Profile

The original hypothesis was that 6:2 FTOH would serve as a negative control to the C-6 PFASs in this study. This compound differs from the others in that it can undergo metabolism, which provides a means of rapid excretion (Rand and Mabury 2014). Similar to the PFASs, early studies of the fluorotelomers focused on the 8 fluorinated carbon compound, 8:2 FTOH. In hepatocytes, 78% of 8:2 FTOH was biotransformed within 4 hours, and the main products were conjugates with glucuronide, sulfate, and glutathione (Martin et al. 2005). The first few studies in this dissertation 6:2 FTOH elicited few toxic effects. In 5 dpf larvae, 6:2 FTOH had the highest LC_{50} (830 µM) of all low molecular weight alternatives tested (Table 2.3), and no morphological changes were observed at 2 or 20 µM exposures (Table 2.4). In addition, no effects on growth were observed at 14 dpf (Table 3.2). This aligned with the literature as early toxicity testing demonstrated limited and reversible effects up to 25 mg/kg 8:2 FTOH with a recovery period (Ladics et al. 2008). It was not until a few years later that the first toxicity studies were published on 6:2 FTOH, and similarly only high chronic doses of 125 mg/kg 6:2 FTOH produced toxic outcomes (O'Connor et al. 2014; Serex et al. 2014).

In the present studies there were changes in both gene expression and behavior at low dose 6:2 FTOH exposures, and these findings can be related to the same 3 AOPs as PFHxA and PFHxS (Figure 5.4). This suggests that 6:2 FTOH is biologically active in gene expression and behavior and should not be dismissed as essentially non-toxic.

While adverse outcomes were not observed at the organism level in the growth AOP, there was a significant increase in gene expression of the growth factor, *tgfb1a* (Figure 2.3). This development of changes at the gene level without manifestation of physical outcomes could indicate that the doses examined in this study were below the growth AOP LOEL, or that this AOP is not impacted by 6:2 FTOH exposure.

In these studies, effects were observed at the cellular, organ, and organism level in the neural AOP. In the behavioral assessment, larvae demonstrated both an increase in activity and reduction in ability to acclimate in response to a photostimulus change (Figures 3.2-3.4). This was not expected from the supposed negative control and had not been reported in rodents (Serex et al. 2014). At the cellular level, there was increased expression of *bdnf*, *ap1s1*, and *tgfb1a* (Figure 2.3), all of which are related to central and lateral line nervous tissue development (Germana et al. 2010a; Montpetit et al. 2008). In addition, increased *bdnf* expression has been linked to anxiety-like behaviors (Chakravarty et al. 2013), and the increased activity observed in this study is indicative of anxiety (Champagne et al. 2010). The changes in transcript level in these genes may indicate that they are in related pathways to the molecular targets in the neural AOP. These changes in gene expression may also be related to the observed effects at the organ level. In 14 dpf larvae, there was an increase in the neural region stained with ORO and a decrease in lipid stain intensity in this region (Figure 3.8), suggesting the lipid distribution patterns are altered in larval central nervous tissue.

The lipid dysregulation AOP was also impacted following 6:2 FTOH exposure. The ability of this compound to activate pparα and pparγ has not yet been examined. However, in this study, there was an increase in expression of these nuclear receptors in 5 dpf larvae (Figure 4.12). In

addition, downstream genes of ppar activity, including *mttp*, *slc27a1*, *lpl* and *apoa1*, were increased in expression (Figure 4.13, 4.14). Together these changes in gene expression suggest ppar activity may be the macromolecular initiating event in this AOP. These observations at the cellular level may also explain the organ responses observed with 6:2 FTOH exposure. In this study, lipid distribution was altered in the neural region (Figure 3.9). There was also a significant decrease in liver area in the exposed larvae and no changes in lipid staining (Figure 3.8). As mentioned previously, this may be due to exposure timeframe or dose because liver hyperplasia and increased cholesterol have been reported at chronic high dose, 250 mg/kg/day 6:2 FTOH exposure (Serex et al. 2014). The observed disruption in lipid distribution may be related to the changes in gene expression. Mttp, slc27a1, and apoa1 are involved in the transport and packaging of lipids, and lpl and slc27a1 have the ability to break triglycerides into fatty acids (Carten et al. 2011; Quinlivan and Farber 2017; Salmeron 2018). These outcomes support lipid dysregulation as a potential AOP for 6:2 FTOH.

There is also evidence that other pathways are critical in the development of the 6:2 FTOH exposure phenotype in larval zebrafish. One possibility is interaction with oatp transporters. It has been confirmed that PFASs of different lengths and terminal groups have substrate binding and inhibitory potential with these transporters (Kudo et al. 2002; Popovic et al. 2014; Weaver et al. 2010; Zhao et al. 2017). This has not been examined with 6:2 FTOH; however, in sac fry larvae, there was increased expression of *slco2b1* and *slco1d1*, suggesting they might be macromolecular targets. It is also possible that the AOPs might be driven by interaction with estrogen receptors, ER. There is limited evidence, but *in vitro* breast cancer cell line models have demonstrated that 6:2 FTOH can stimulate estrogen pathways and proliferation in breast cancer cell lines (Jahnke 2007; Maras et al. 2006). Two studies in aquatic models have also shown that 6:2 FTOH exposure caused induction of ER and subsequently, increased vitellogenin levels (Ishibashi et al. 2008; Liu et al. 2009). Therefore, this may be an important pathway in aquatic species as well as mammals. It is possible that this is a unique AOP for 6:2 FTOH because binding studies have revealed PFASs to have weak affinity for ER in aquatic models (Benninghoff

et al. 2011; Du et al. 2013). These macromolecular targets also may be related to the other AOPs discussed.

5.6 Comparison of C-8/C-9 PFASs and the C-6 Alternatives

Overall, the C-6 compounds were less toxic than C-8/C-9 PFASs in the larval zebrafish model. Morphological and behavioral effects were observed following low dose 0.2 and 2 μM PFOS, PFOA, and PFNA (Jantzen et al. 2016a). This was not a direct comparison as these studies were not run concurrently. Doses of 2 and 20 μM PFHxS and 6:2 FTOH were necessary to elicit effects in these same endpoints. No effects on behavior or morphometric endpoints were observed at the PFHxA doses examined. There were gene expression changes observed at low doses of these low molecular weight alternatives that did not manifest into tissue or organism level outcomes. Many of these same genes were altered with exposure to the long chain PFASs; however the gene expression profiles differed with each compound. Therefore, while the C-6 compounds together are less toxic, their toxicity profiles are not the same.

The different patterns of outcomes for all 6 compounds in this study suggest that chain length or terminal group alone are not responsible for the toxic outcomes, and that a combination of these factors contributes to the phenotypes in larval zebrafish. Unique profiles in larval zebrafish became apparent for the carboxylates. Long chain carboxylates, PFOA and PFNA, caused a similar morphometric response in larval zebrafish, a decreased length and the presence of yolk sac edema. However, no morphometric effects were observed with PFHxA exposures at a concentration 10-fold higher than that tested in the long chain PFASs. The long chain carboxylates also had different morphological effects at 14 dpf, which suggests that these long chain PFASs also produce different phenotypes. In addition, different behavioral effects were observed following developmental PFOA and PFNA exposures, and no behavioral effects were observed following PFHxA exposure. Similarly, the sulfonates, PFOS and PFHxS, produced different toxic outcomes. There was a consistent increase in larval size observed at 5 and 14 dpf with PFHxS exposure; however, PFOS caused a decrease in larval size at 5 dpf and no

difference from controls at 14 dpf. In addition, PFOS exposure caused hyperactive behavioral outcomes, whereas PFHxS-exposed larvae were hypoactive. Each PFAS impacted the growth and neural AOPs, but the outcomes differed for each PFAS. Additionally, the gene expression profiles were different for each compound suggesting different molecular initiating events may exist within this class of compounds.

Both C-6 and C-8/C9 compounds also produce very different profiles on lipid homeostasis. There is ample evidence in the literature to suggest that lipid dysregulation and lipid accumulation in the liver are toxic outcomes with long chain PFAS exposures (Lau 2012; Tsuda 2016). This was examined in the present study in larval zebrafish, summarized in Figure 5.5. These data demonstrate that yolk uptake is impacted at 5 dpf, and distribution of lipids is impacted in larvae at 14 dpf. The yolk uptake model was able to demonstrate the effects of PFAS exposure on the yolk syncytial layer, YSL, early in development. There were observed alterations in yolk uptake as well as vesicle formation within the yolk. It is possible that effects observed at the YSL may explain the alterations in lipid uptake and morphological yolk sac endpoints. This mechanism was further explored through gene expression where potential molecular targets were identified. Taken together these targets and effects at the YSL may translate to the effects observed at 14 dpf. At these later larval stages, the effects of developmental PFAS exposure on lipid homeostasis persisted and were observed as alterations in the accumulation of lipids in the liver and neural regions. These effects provide additional information to the lipid homeostasis AOP for each compound, as well as possibly contributing to the growth and neural AOPs.

Additionally, preliminary studies were completed following exposure to the C-6 compounds which have identified possible molecular and tissue level effects in larval zebrafish. From the 14 dpf lipid staining results, neural and liver lipid distribution were altered with these compounds. While morphological effects were generally not present in the 5 dpf C-6-exposed larvae, many potentially targeted pathways were identified in the lipid-related gene expression studies. As adverse outcomes have been reported in the lipid dysregulation AOP, these effects warrant further studies with the low molecular weight PFAS alternatives.

Throughout the course of this discussion, the growth, neural, and lipid AOPs have been described as separate pathways, however, there is potential for overlap. Effects on lipid distribution can have major implications on energy homeostasis, which could impact growth through the morphometric endpoints examined. Morphometric effects are observed at the individual level and could represent a culmination of effects on pathways at the biochemical and cellular levels. It could be possible that growth and lipid homeostasis pathways lead to the decreased larval growth observed with the long chain PFASs and increased growth observed with PFHxS exposure.

Behavioral outcomes represent complex interactions, so it is possible that there is overlap with these AOPs as well. It was generally discussed that effects on lipid distribution and therefore energy homeostasis has the potential to impact larval zebrafish behavior. However, it is also possible that direct interaction of the PFASs with some of the genes examined explain these effects. It has been shown that PPARγ deletion increases anxiety in rodents (Domi et al. 2016). Exposure to both PFOS and 6:2 FTOH exposures caused increased larval activity, suggesting elevated anxiety. These two compounds were also the only ones to cause increased pparγ expression at 5 dpf. Therefore, it is possible that direct interactions of these compounds with the nuclear receptor leads to the anxiety phenotype. Further studies are necessary to confirm effects on pparγ at the protein level and to fully elucidate this pathway. This also raises the question whether direct impacts on the other genes examined in chapter 4 could be related to the behavioral effects through more direct mechanisms than more generally altering lipid distribution.

5.7 Future Directions

Based on the data presented in this dissertation future studies should continue to examine the role of AOPs to better understand the toxicological outcomes of this diverse class of compounds. My findings have expanded the understanding of the toxicity profiles of PFHxA, PFHxS, and 6:2 FTOH in the larval zebrafish model, specifically in terms of growth, lipid dysregulation, and neural-based AOPs. In addition, my research calls into question the assertion that these

environmentally persistent compounds should be considered as non-toxic. While less toxic than the long chain PFASs, the C-6 compounds appear to up or down regulate a number of critical pathways. One important question that remains is the molecular initiating events that lead to these 3 AOPs. Through gene expression analysis, some potential gene targets have been identified, and as discussed, ppar activation, transporter interaction, and partitioning to lipids most likely contribute to these pathways. However, there are data gaps across the low molecular weight alternatives and model organisms.

The current study was limited to larval zebrafish, but adults may also provide compelling data on targeted pathways. A chronic exposure paradigm may provide a more environmentally-relevant scenario. In addition, studies in adults would allow for the examination of endpoints not possible in the larvae, such as reproductive effects and sexually dimorphic responses as sex in zebrafish cannot be determined until sexual maturity is reached. It has been demonstrated that long chain PFASs have sex-specific effects on behavior and gene expression (Jantzen et al. 2016b), so similar examination would be beneficial with exposure to the C-6 compounds. Also, steatosis has been observed in adult zebrafish livers with PFOS exposure (Cheng et al. 2016; Cui et al. 2017; Fai Tse et al. 2016), and with the changes in lipid distribution in larval livers with C-6 compounds, it is possible that similar effects would be observed with PFHxS and 6:2 FTOH exposures.

These studies only began to tease out the mechanisms by which PFAS exposure alter lipid mobilization and distribution at the yolk syncytial layer, YSL. Gene expression alterations of factors critical in this region were demonstrated to be altered with long chain PFAS exposure. Protein quantification and functional assays could be completed to determine mechanisms occurring at the YSL. The BODIPY-FL fatty acids were beneficial for determining uptake of fatty acids into the developing embryo. From these studies, changes in vesicle formation in the yolk were visible. Future studies can be completed with the low molecular weight alternatives, particularly 6:2 FTOH and PFHxS, which resulted in multiple alterations in the lipid dysregulation AOP. However, higher doses than those examined for the long chain PFASs should be examined due to the difference in dose sensitivity of these compounds. Another aspect of lipid regulation

not addressed in the current dissertation is the potential change to the lipid composition of the yolk sac. BODIPY-FL fatty acids could be utilized to trace the incorporation of these fatty acids into more complex lipid molecules and their subsequent distribution in the larvae.

Future studies could also be completed on the behavioral responses with these compounds and allow for a more mechanistic approach to the neurobehavioral effects of PFASs. Considering the effects of the low molecular weight alternatives and PFASs on the bdnf/tgfb1a/ap1s1 pathways and possible interrelatedness of these pathways, it may be beneficial to look further into these findings. The zebrafish behavioral model is well-suited for targeted behavioral tests. Specific knockdown or knockout of targets could confirm molecular targets. The zebrafish model is advantageous for this type of analysis because of the availability of both morpholino and CRISPR technologies.

One of the major discoveries in this project was that 6:2 FTOH caused changes in many of the endpoints examined, suggesting it was not an appropriate negative control. Exposure to this compound also produced a toxicity profile very different from the other PFASs. With the unique anxiety-like behavioral phenotype and increase in transcript level of many genes in the expression analysis, there are many future studies to be completed to elucidate the mechanisms of these effects. It is also possible that these changes are due to interaction with the estrogen receptor and hormone levels. These types of interactions can have much larger impacts on fecundity and reproductive abilities of adult fish, so this warrants further study.

| Macromolecular Interactions | | Cellular Responses | | Organ Responses | | Organism Responses | | Population Responses |

*Molecular Initiating Event (MIE)　　　　　*Key Events (KE)　　　　　　　*Adverse Outcomes (AO)
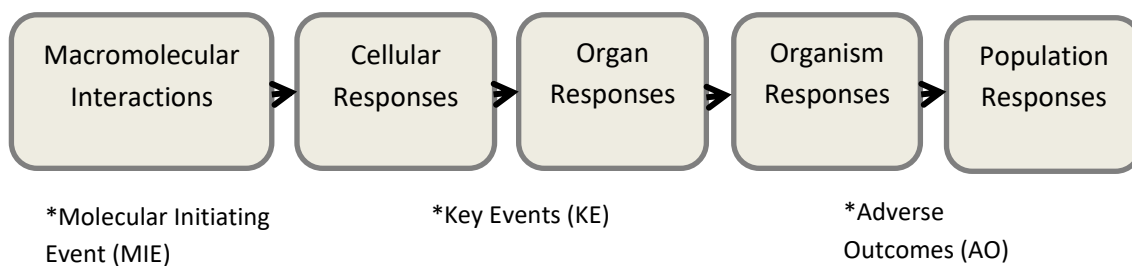
Figure 5.1. General outline of an adverse outcome pathway (AOP). Exposure of a compound results in a macromolecular interaction, referred to as a molecular initiating event, MIE, which triggers a cascade of outcomes. The outcomes include key events, KE, at the cellular and organ level. The ultimate adverse outcome (AO) of the pathway is observed at the organism or population level.

Table 5.1. Summary of endpoints in 5 dpf larvae with exposure to PFHxA, PFHxS, and 6:2 FTOH, described in Chapters 2 and 4.

	PFHxA		PFHxS		6:2 FTOH	
	2 µM	20 µM	2 µM	20 µM	2 µM	20 µM
MORPHOMETRICS						
Length	N.S.	N.S.	⬆	⬆	N.S.	N.S.
Yolk Sac Area	N.S.	N.S.	N.S.	⬆	N.S.	N.S.
GENE EXPRESSION CHAPTER 2						
slco2b1	⬇	N.S.	N.S.	N.S.	⬆	N.S.
slco1d1	N.S.	N.S.	N.S.	N.S.	N.S.	⬆⬆
tgfb1a	⬆	⬆⬆	N.S.	N.S.	⬆	⬆⬆
bdnf	N.S.	⬆⬆	⬆	N.S.	N.S.	⬆⬆
ap1s1	⬆⬆	⬆⬆	N.S.	N.S.	N.S.	⬆⬆
GENE EXPRESSION CHAPTER 4						
pparα	N.S.	N.S.	N.S.	N.S.	⬆	⬆⬆
pparγ	N.S.	N.S.	N.S.	N.S.	⬆	⬆⬆
lepa	N.S.	N.S.	N.S.	N.S.	N.S.	N.S.
mttp	⬆⬆	N.S.	N.S.	N.S.	N.S.	⬆⬆
slc27a1	⬆⬆	⬆⬆	N.S.	N.S.	⬆	⬆⬆
lpl	⬆⬆	⬆⬆	N.S.	N.S.	⬆	⬆⬆
apoa1	N.S.	N.S.	N.S.	⬆	N.S.	⬆⬆
apoc2	⬆⬆	⬆⬆	⬆	N.S.	N.S.	N.S.

Table 5.2. Summary of endpoints in 14 dpf larvae with exposure to PFHxA, PFHxS, and 6:2 FTOH, described in Chapter 3.

	PFHxA		PFHxS		6:2 FTOH	
	2 µM	20 µM	2 µM	20 µM	2 µM	20 µM
BEHAVIOR						
Total Distance	N.S.	N.S.	N.S.	↓	↑	N.S.
Cross Frequency	N.S.	N.S.	N.S.	↓	N.S.	N.S.
Velocity	N.S.	N.S.	N.S.	N.S.	N.S.	↑
MORPHOMETRICS AND LIPID STAINING						
Total Length	N.S.	N.S.	↑	N.S.	N.S.	N.S.
Liver Area	N.S.	N.S.	↑	N.S.	N.S.	↓
Liver Stain	N.S.	N.S.	N.S.	N.S.	N.S.	N.S.
Neural Area	↓	↓	↑	N.S.	↑	N.S.
Neural Stain	N.S.	N.S.	N.S.	N.S.	N.S.	↓

Table 5.3. Lipid dysregulation adverse outcomes following PFOA, PFOS, and PFNA in 5 and 14 dpf larvae. Data summarized from this dissertation and Janzten et al. 2016a.

	CELLULAR RESPONSE	ORGAN RESPONSE	ORGANISM RESPONSES
PFOA	↓ pparα pparγ ↓ lepa (Figure 4.9) ↑ mttp (Figure 4.10)	↑ 5 dpf yolk sac area (Figure 4.5, Jantzen et al. 2016a) 5 dpf yolk sac fatty acid uptake (Jantzen et al. 2016a) ↓ 5 dpf vesicles area in yolk sac (Figure 4.5) ↑ 14 dpf liver area (Figure 3.8) 14 dpf liver stain (Figure 3.8) ↓ 14 dpf stained neural area (Figure 3.9) ↑ 14 dpf neural stain (Figure 3.9)	↓ 5 dpf length ↓ 14 dpf length (Jantzen et al. 2016a)
PFOS	pparα ↑ pparγ ↓ lepa (Figure 4.9) ↑ slc27a1 (Figure 4.10)	↓ 5 dpf yolk sac area (Jantzen et al. 2016a) 5 dpf yolk sac fatty acid uptake (Jantzen et al. 2016a) ↓ 5 dpf vesicles area in yolk sac (Figure 4.5) ↓ 14 dpf liver area (Figure 3.8) 14 dpf liver stain (Figure 3.8) ↑ 14 dpf stained neural area (Figure 3.9) ↑ 14 dpf neural stain (Figure 3.9)	↓ 5 dpf length 14 dpf length (Jantzen et al. 2016a)
PFNA	pparα pparγ lepa (Figure 4.9) ↑ slc27a1 ↑ lpl ↑ apoc2 (Figure 4.10, 4.11)	↑ 5 dpf yolk sac area (Figure 4.5, Jantzen et al. 2016a) ↓ 5 dpf yolk sac fatty acid uptake (Jantzen et al. 2016a) ↓ 5 dpf vesicles area in yolk sac (Figure 4.5) ↑ 14 dpf liver area (Figure 3.8) 14 dpf liver stain (Figure 3.8) 14 dpf stained neural area (Figure 3.9) ↓ 14 dpf neural stain (Figure 3.9)	↓ 5 dpf length ↑ 14 dpf length (Jantzen et al. 2016a)
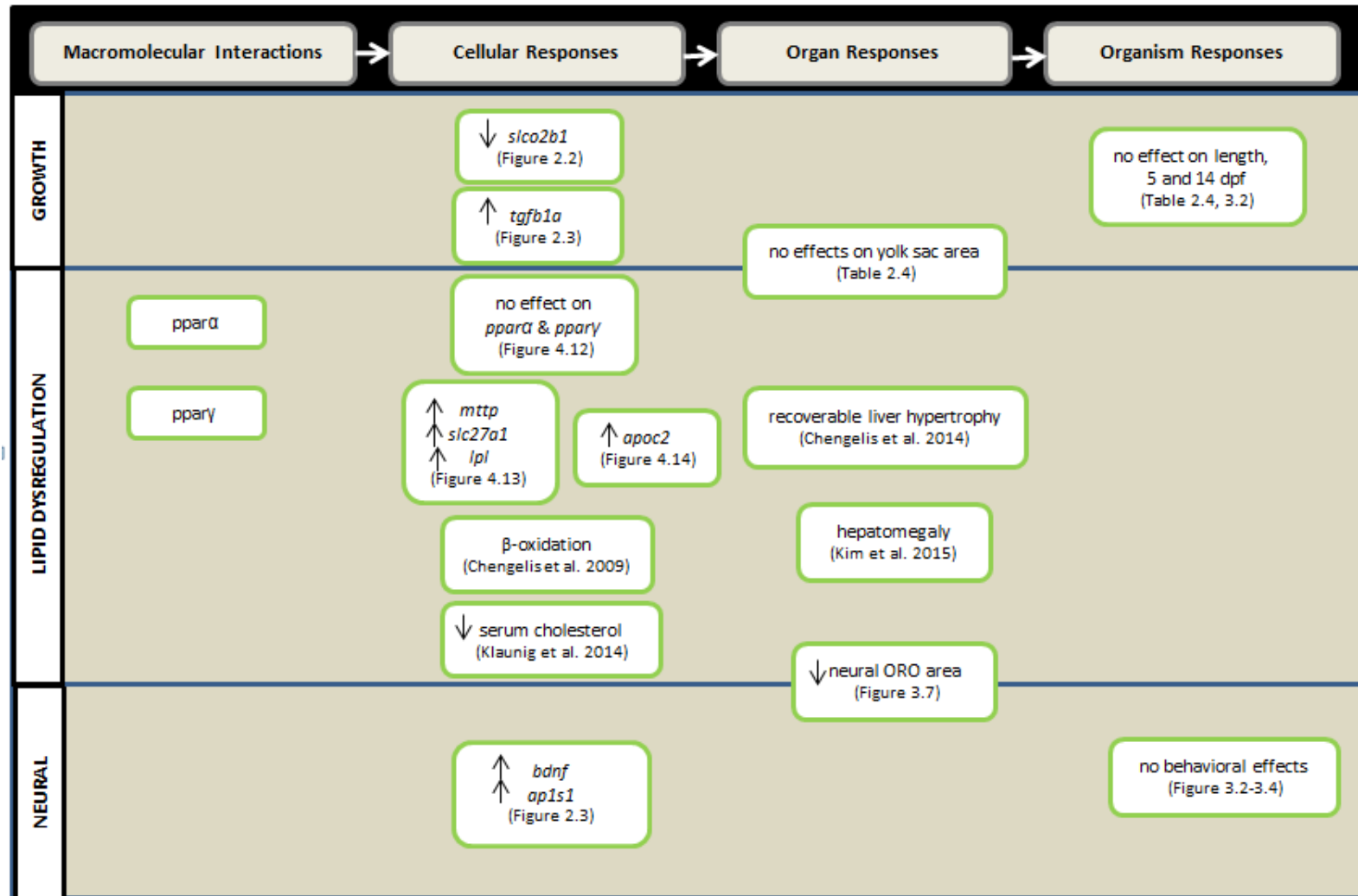
Figure 5.2. Endpoints altered in growth, neural, and lipid dysregulation AOPs following PFHxA exposures. Arrows indicate direction of response.
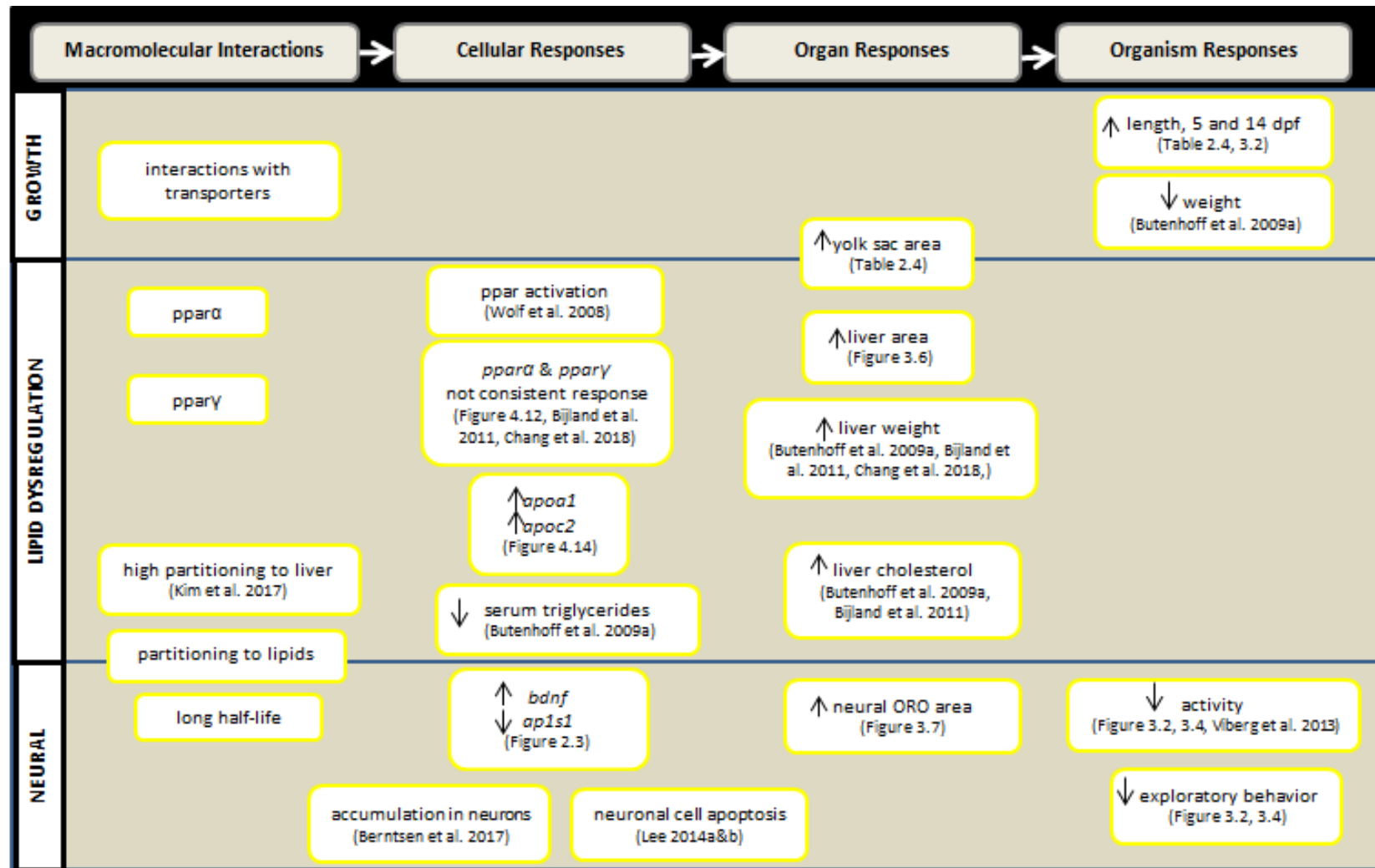
Figure 5.3. Endpoints altered in growth, neural, and lipid dysregulation AOPs following PFHxS exposures. Arrows indicate direction of response.
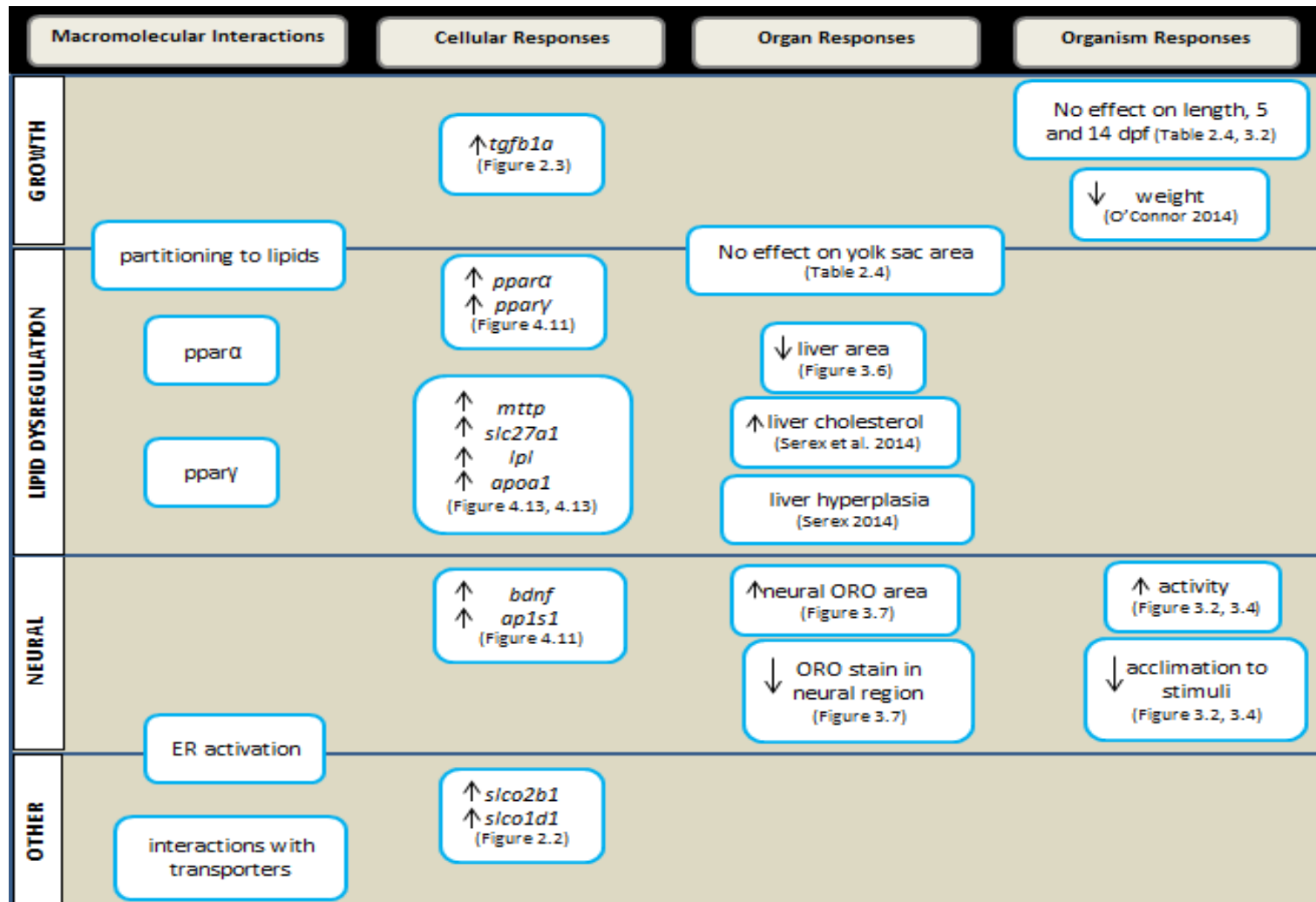
Figure 5.4. Endpoints altered in growth, neural, and lipid dysregulation AOPs following 6:2 FTOH exposures.

APPENDICES
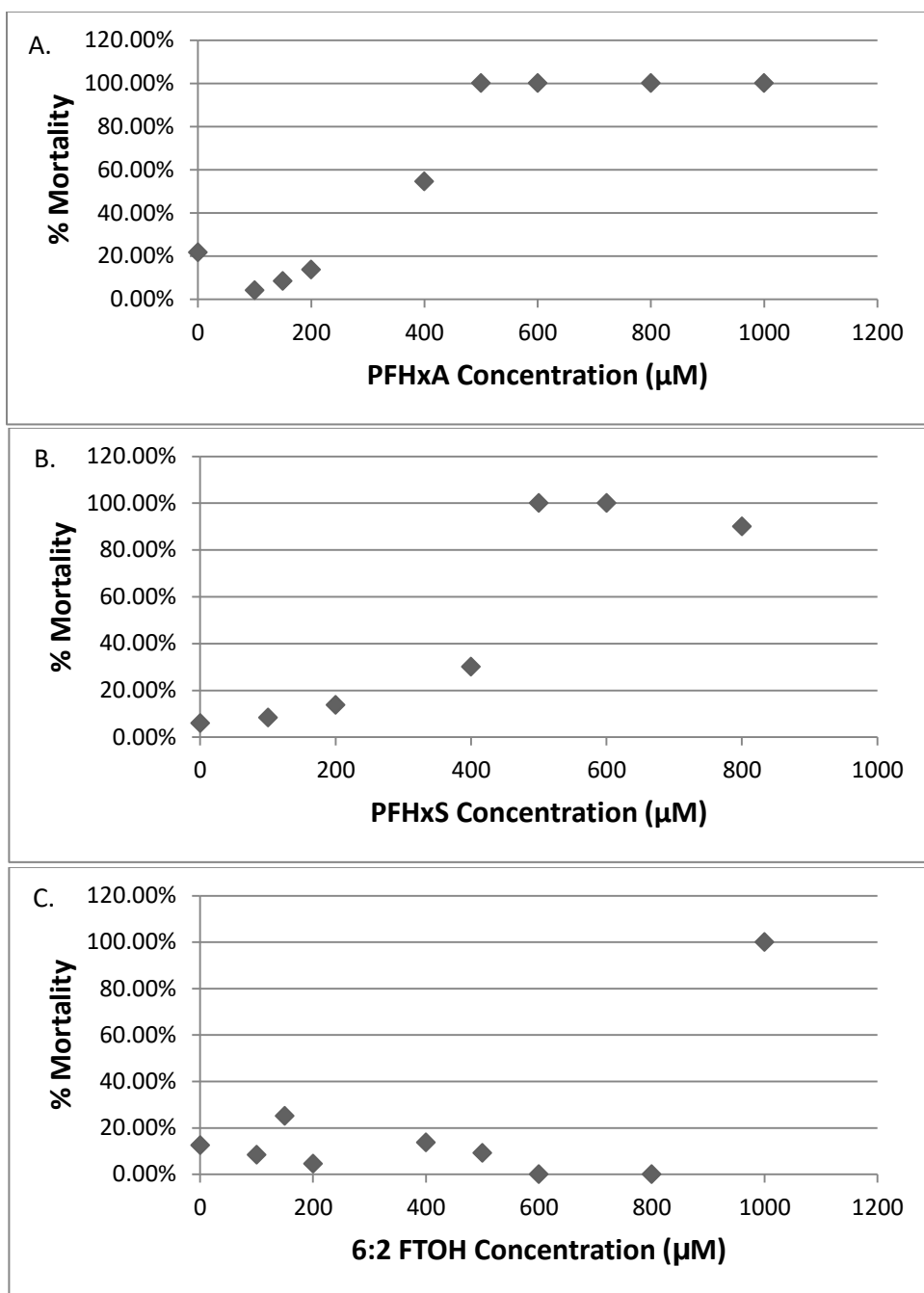
Figure A1. Dose response curves of percent mortality for 5 dpf larvae exposed to waterborne concentrations of (A) PFHxA, (B) PFHxS, and (C) 6:2 FTOH.
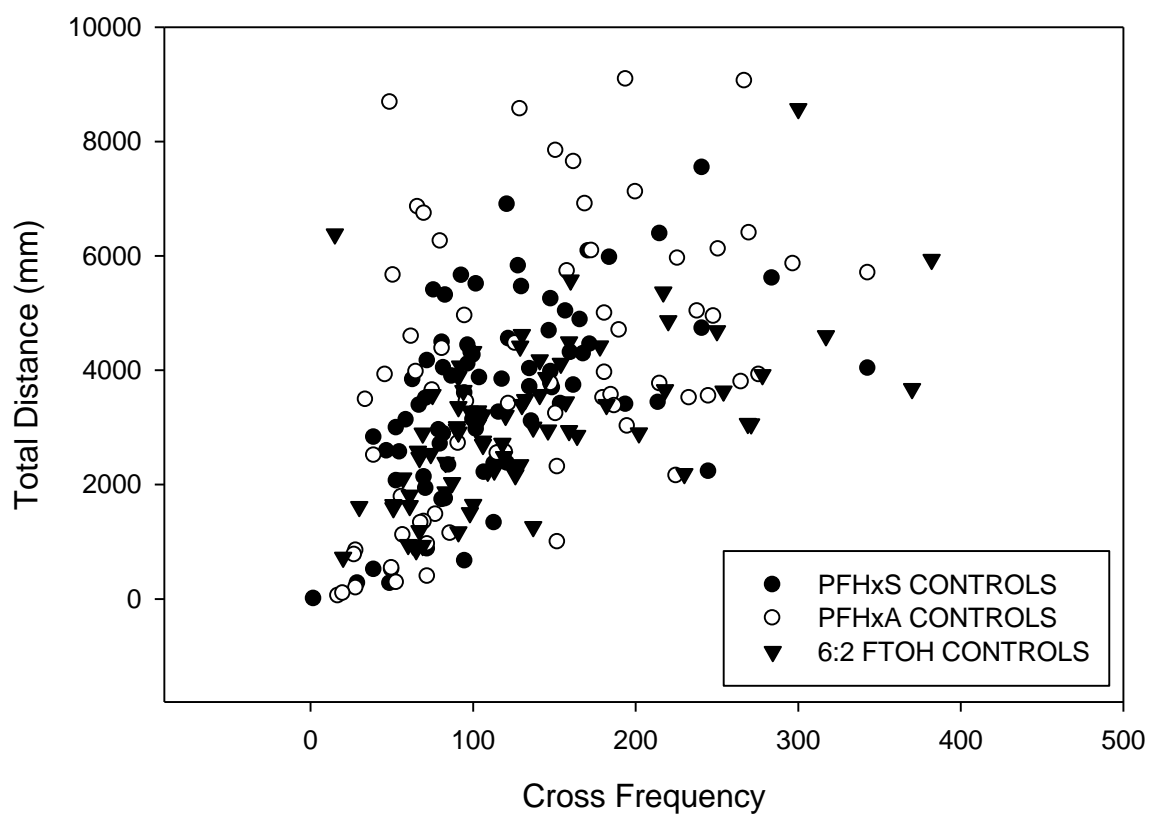
Figure A2. Cross frequency and total distance for individual larvae from the control groups. These endpoints correlated for the control larvae from each treatment group (Linear Regression, p<0.05).
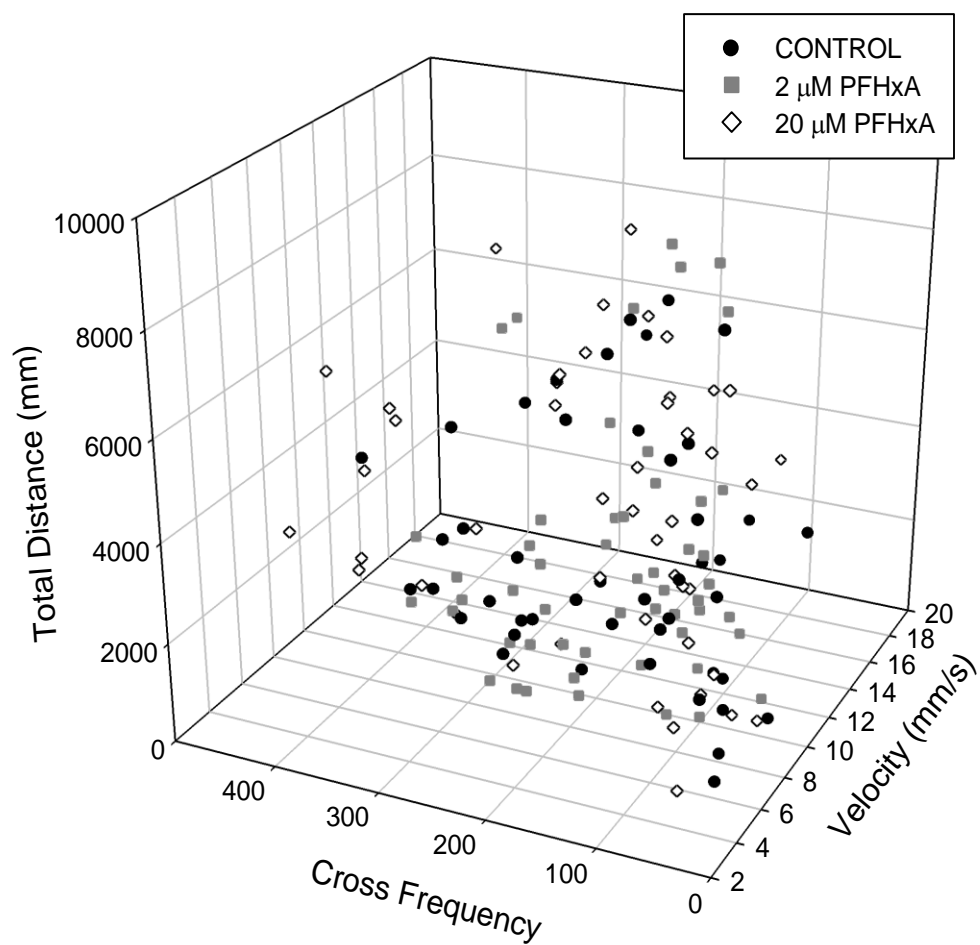
Figure A3. 3D scatterplot of behavioral results following 0, 2, and 20 µM PFHxA exposure. Velocity (mm/s), cross frequency, and total distance (mm) are plotted against each other. Data points represent individual larvae.
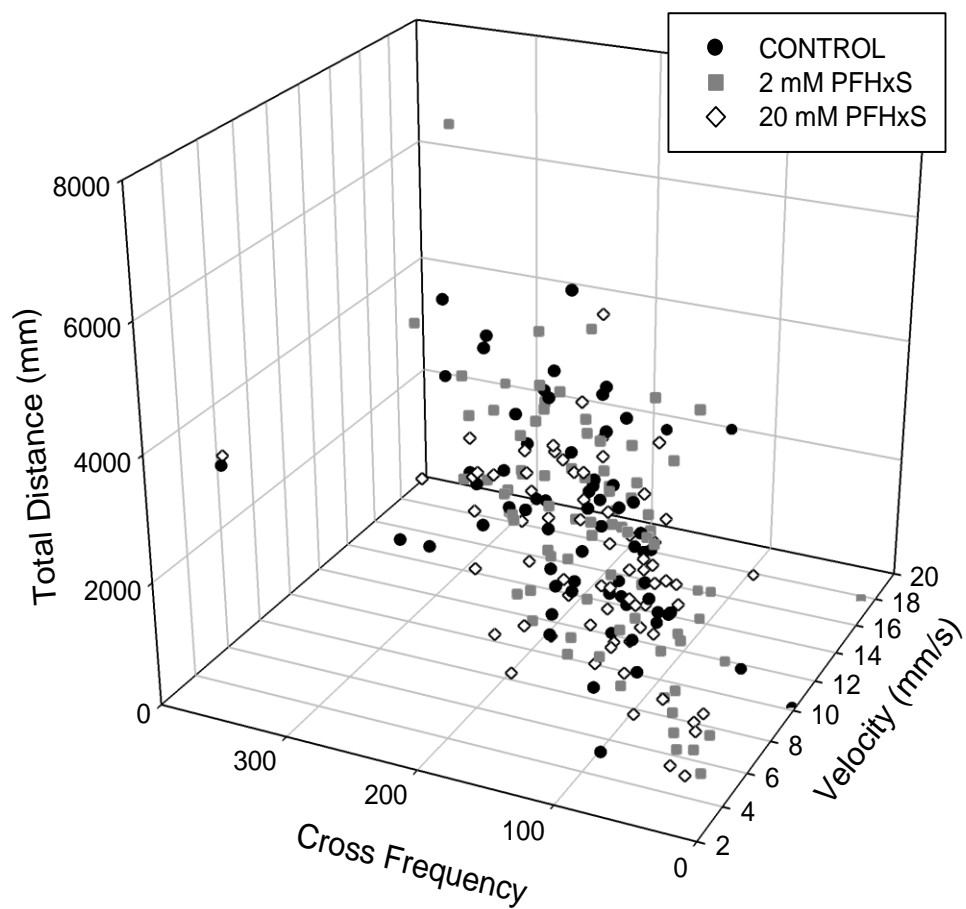
Figure A4. 3D scatterplot of behavioral results following 0, 2, and 20 µM PFHxS exposure. Velocity (mm/s), cross frequency, and total distance (mm) are plotted against each other. Data points represent individual larvae.
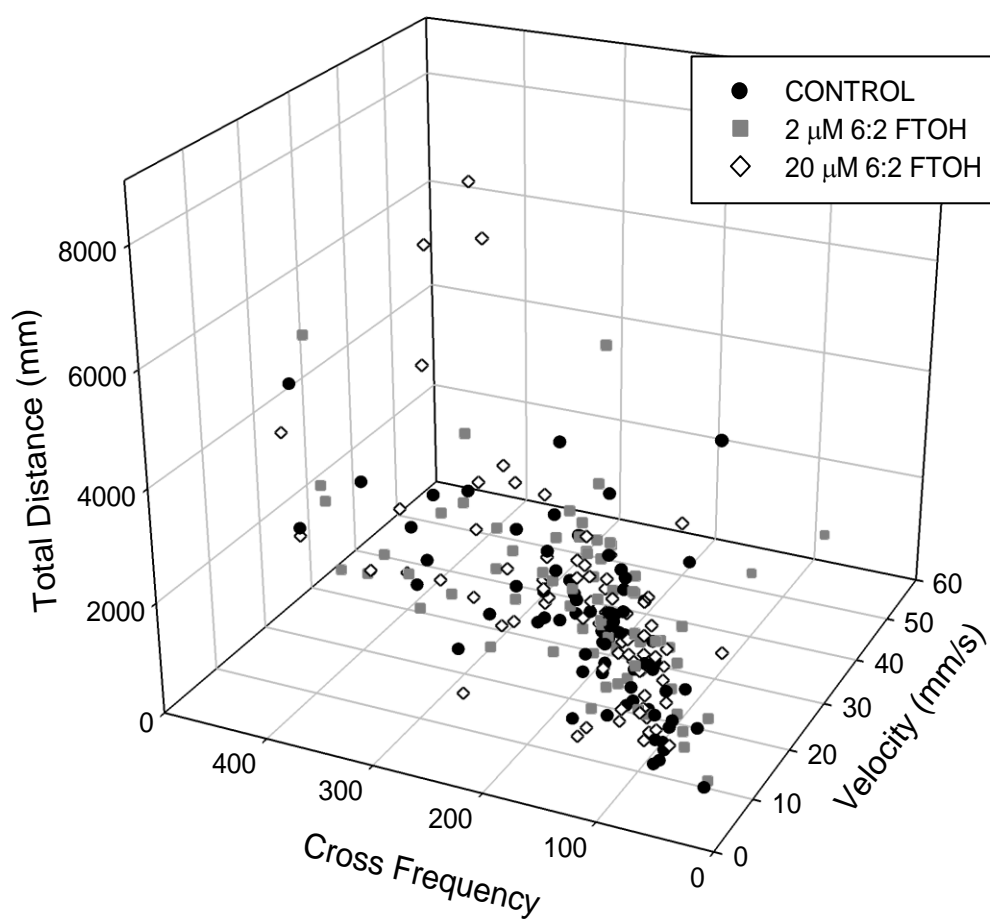
Figure A5. 3D scatterplot of behavioral results following 0, 2, and 20 µM 6:2 FTOH exposure. Velocity (mm/s), cross frequency, and total distance (mm) are plotted against each other. Data points represent individual larvae.
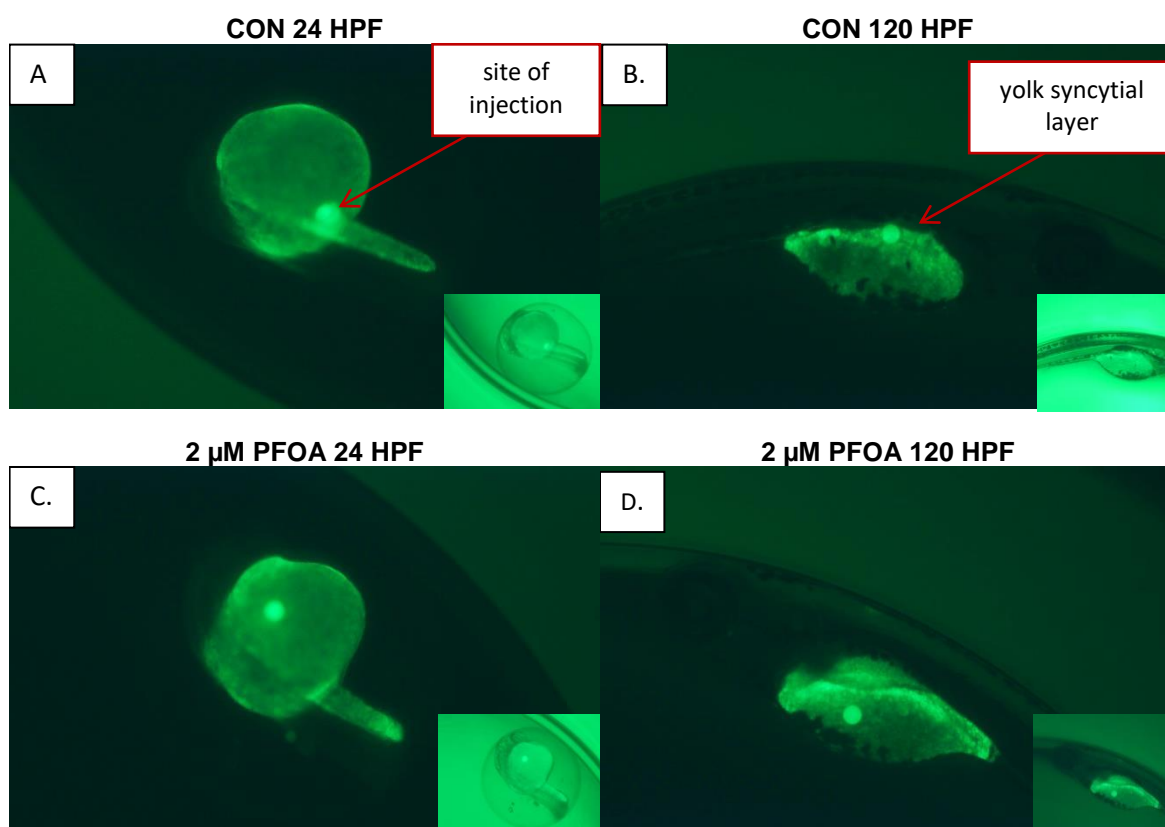
Figure A6. Representative images of two larvae microinjected with BODIPY-FL fatty acids followed by a waterborne PFOA exposure. Images were taken under fluorescent light and bright light (inlayed images) at 24 and 120 hpf. The top panel includes images of larvae reared in control solution at (A) 24 hpf and (B) 120 hpf. The bottom panel includes images of larvae reared in 2 μM PFOA solutions at (C) 24 hpf and (D) 120 hpf.

CON 24 HPF

CON 120 HPF

2 µM PFOS 24 HPF

2 µM PFOS 120 HPF
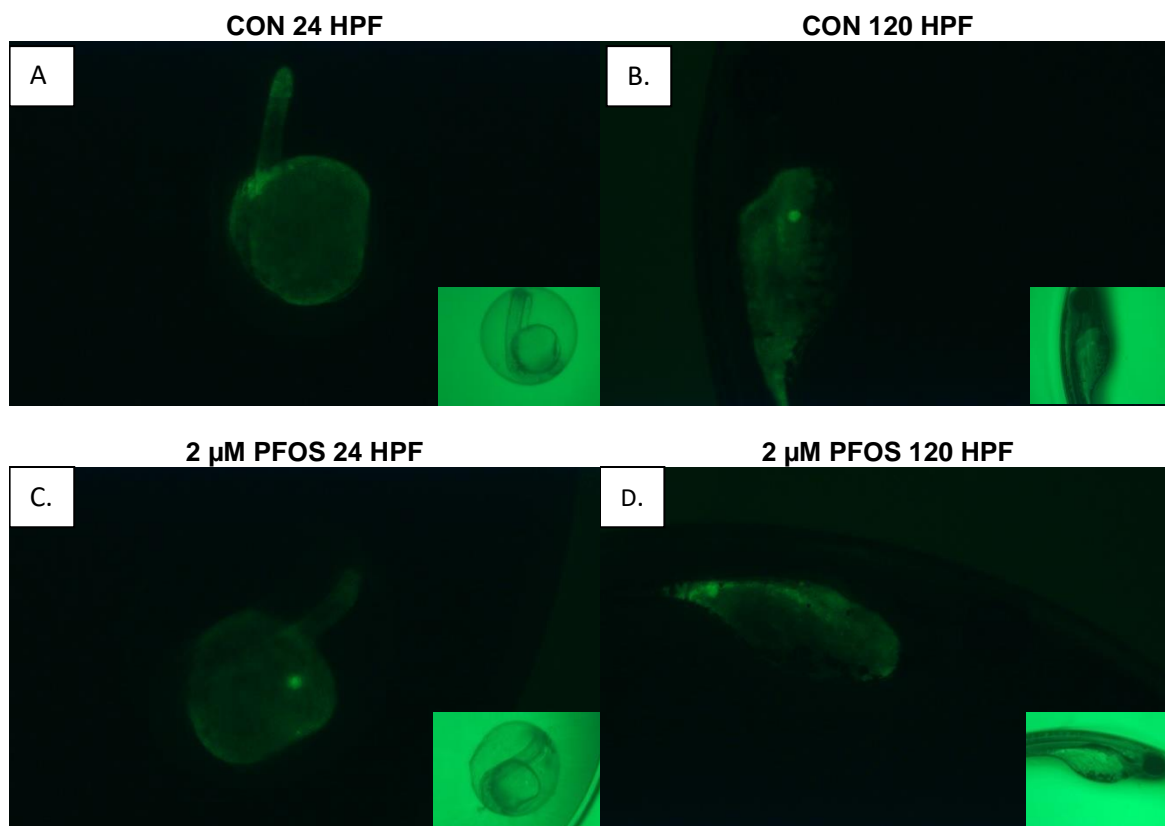
Figure A7. Representative images of two larvae microinjected with BODIPY-FL fatty acids followed by a waterborne PFOS exposure. Images were taken under fluorescent light and bright light (inlayed images) at 24 and 120 hpf. The top panel includes images of larvae reared in control solution at (A) 24 hpf and (B) 120 hpf. The bottom panel includes images of larvae reared in 2 µM PFOS solutions at (C) 24 hpf and (D) 120 hpf.

CON 24 HPF

CON 120 HPF

2 µM PFNA 24 HPF

2 µM PFNA 120 HPF
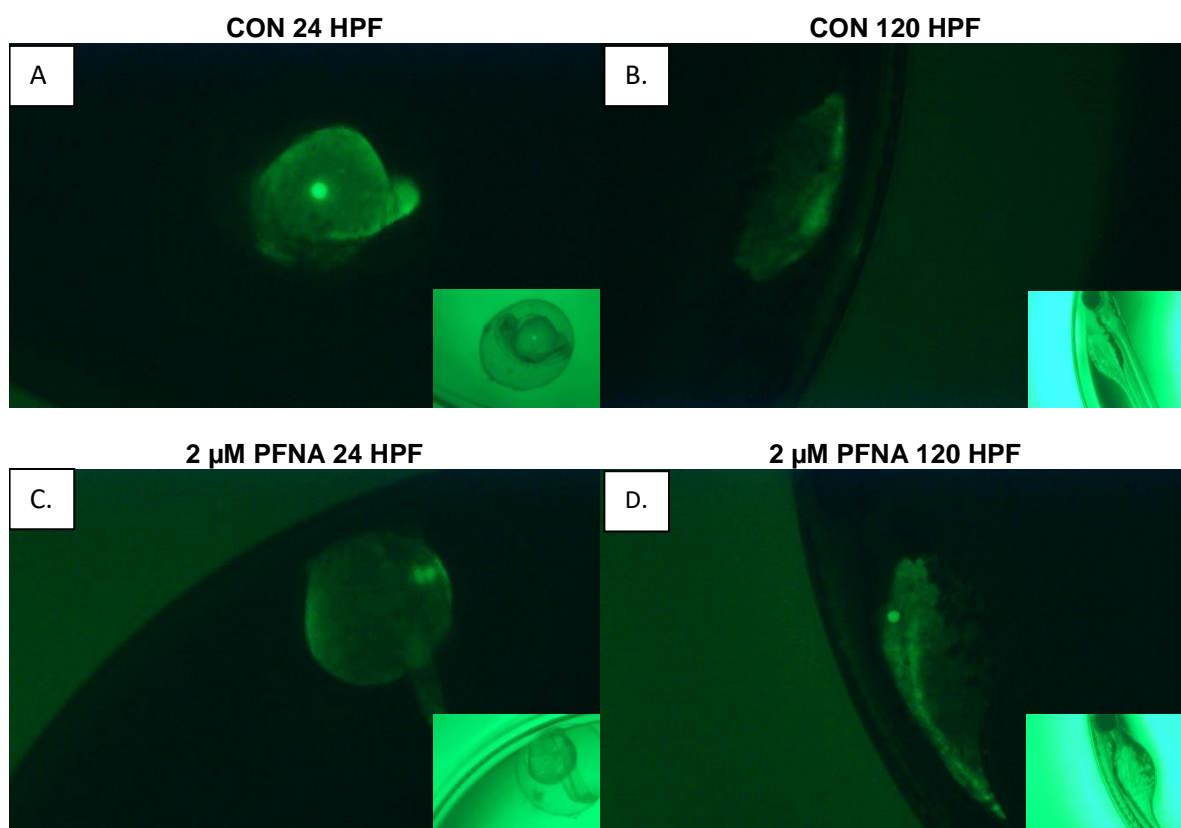
Figure A8. Representative images of two larvae microinjected with BODIPY-FL fatty acids followed by a waterborne PFNA exposure. Images were taken under fluorescent light and bright light (inlayed images) at 24 and 120 hpf. The top panel includes images of larvae reared in control solution at (A) 24 hpf and (B) 120 hpf. The bottom panel includes images of larvae reared in 2 µM PFNA solutions at (C) 24 hpf and (D) 120 hpf.

REFERENCES

Abbott BD, Wolf CJ, Das KP, Zehr RD, Schmid JE, Lindstrom AB, Strynar MJ, Lau C. (2009) Developmental toxicity of perfluorooctane sulfonate (PFOS) is not dependent on expression of peroxisome proliferator activated receptor-alpha (PPAR alpha) in the mouse. Reproductive Toxicology 27(3-4):258-65 doi:10.1016/j.reprotox.2008.05.061

Ahmadian M, Suh JM, Hah N, Liddle C, Atkins, AR, Downes M, Evans RM (2013) PPARgamma signaling and metabolism: the good, the bad and the future. Nature Medicine 19(5):557-66 doi:10.1038/nm.3159

Ahrens L (2011) Polyfluoroalkyl compounds in the aquatic environment: a review of their occurrence and fate. Journal of Environmental Monitoring 13(1):20-31 doi:10.1039/c0em00373e

Albrecht PP, Torsell NE, Krishnan P, Ehresman DJ, Frame SR, Change SC, Butenhoff JL, Kennedy GL, Gonzalez FJ, Peters JM. (2013) A species difference in the peroxisome proliferator-activated receptor alpha-dependent response to the developmental effects of perfluorooctanoic acid. Toxicological Sciences 131(2):568-82 doi:10.1093/toxsci/kfs318

Ameen C, Edvardsson U, Ljungberg A, Asp L, Akerblad P, Tuneld A, Olofsson SO, Linden D, Oscarsson J. (2005) Activation of peroxisome proliferator-activated receptor alpha increases the expression and activity of microsomal triglyceride transfer protein in the liver. The Journal of Biological Chemistry 280(2):1224-9 doi:10.1074/jbc.M412107200

Amsterdam A, Nissen RM, Sun Z, Swindell EC, Farrington S, Hopkins N (2004) Identification of 315 genes essential for early zebrafish development. Proceedings of the National Academy of Sciences of the United States of America 101(35):12792-7 doi:10.1073/pnas.0403929101

Anderson CM, Stahl A (2013) SLC27 fatty acid transport proteins. Molecular Aspects of Medicine 34(2-3):516-28 doi:10.1016/j.mam.2012.07.010

AOPWiki.org Collaborative Adverse Outcome Pathway Wiki (AOP-Wiki).

Apelberg BJ, Witter FR, Herbstman JB, Calafat AM, Halden RU, Needham LL, Goldman LR. (2007) Cord serum concentrations of perfluorooctane sulfonate (PFOS) and perfluorooctanoate (PFOA) in relation to weight and size at birth. Environmental Health Perspectives 115(11):1670-6 doi:10.1289/ehp.10334

Arnault F, Etienne J, Noe L, Raisonnier A, Brault D, Harney JW, Berry MJ, Tse C, Fromental-Ramain C, Hamelin J, Galibert F. (1996) Human lipoprotein lipase last exon is not translated, in contrast to lower vertebrates. Journal of Molecular Evolution 43(2):109-15

Arukwe A, Cangialosi MV, Letcher RJ, Rocha E, Mortensen AS (2013) Changes in morphometry and association between whole-body fatty acids and steroid hormone profiles in relation to bioaccumulation patterns in salmon larvae exposed to perfluorooctane sulfonic or perfluorooctane carboxylic acids. Aquatic Toxicology 130-131:219-30 doi:10.1016/j.aquatox.2012.12.026

Avraham-Davidi I, Ely Y, Pham VN, et al. (2012) ApoB-containing lipoproteins regulate angiogenesis by modulating expression of VEGF receptor 1. Nature Medicine 18(6):967-73 doi:10.1038/nm.2759

Barry V, Darrow LA, Klein M, Winquist A, Steenland K (2014) Early life perfluorooctanoic acid (PFOA) exposure and overweight and obesity risk in adulthood in a community with elevated exposure. Environmental Research 132:62-9 doi:10.1016/j.envres.2014.03.025

Benninghoff AD, Bisson WH, Koch DC, Ehresman DJ, Kolluri SK, Williams DE (2011) Estrogen-like activity of perfluoroalkyl acids in vivo and interaction with human and rainbow trout estrogen receptors in vitro. Toxicological Sciences 120(1):42-58 doi:10.1093/toxsci/kfq379

Berntsen HF, Bjorklund CG, Audinot JN, Hofer T, Verhaegen S, Lentzen E, Gutleb AC, Ropstad E. (2017) Time-dependent effects of perfluorinated compounds on viability in cerebellar granule neurons: Dependence on carbon chain length and functional group attached. Neurotoxicology 63:70-83 doi:10.1016/j.neuro.2017.09.005

Bijland S, Rensen PC, Pieterman EJ, Maas AC, van der Hoorn JW, van Erk MJ, Havekes LM, Willems van Dijik K, Chang SC, Ehresman DJ, Butenhoff JL. (2011) Perfluoroalkyl sulfonates cause alkyl chain length-dependent hepatic steatosis and hypolipidemia

mainly by impairing lipoprotein production in APOE*3-Leiden CETP mice. Toxicological Sciences 123(1):290-303 doi:10.1093/toxsci/kfr142

Bonefeld-Jorgensen EC, Long M, Bossi R, Ayotte P, Asmund G, Kruger T, Ghisari M, Mulvad G, Kern P, Nzulumiki P, Dewailly E. (2011) Perfluorinated compounds are related to breast cancer risk in Greenlandic Inuit: a case control study. Environmental Health 10:88 doi:10.1186/1476-069X-10-88

Boulanger B, Vargo J, Schnoor JL, Hornbuckle KC (2004) Detection of perfluorooctane surfactants in Great Lakes water. Environmental Science & Technology 38(15):4064-70

Brown C, Gardner C, Braithwaite VA (2005) Differential stress responses in fish from areas of high- and low-predation pressure. Journal of Comparative Physiology 175(5):305-12 doi:10.1007/s00360-005-0486-0

Bruce AE (2016) Zebrafish epiboly: Spreading thin over the yolk. Developmental Dynamics 245(3):244-58 doi:10.1002/dvdy.24353

Buck RC, Franklin J, Berger U, et al. (2011) Perfluoroalkyl and polyfluoroalkyl substances in the environment: terminology, classification, and origins. Integrated Environmental Assessment and Management 7(4):513-41 doi:10.1002/ieam.258

Butenhoff J, Costa G, Elcombe C, Farrar D, Hansen K, Iwai H, Jung R, Kennedy G Jr., Lieder P, Olsen G, Thomford P. (2002) Toxicity of ammonium perfluorooctanoate in male cynomolgus monkeys after oral dosing for 6 months. Toxicological Sciences 69(1):244-57

Butenhoff JL, Chang SC, Ehresman DJ, York RG (2009a) Evaluation of potential reproductive and developmental toxicity of potassium perfluorohexanesulfonate in Sprague Dawley rats. Reproductive Toxicology 27(3-4):331-41 doi:10.1016/j.reprotox.2009.01.004

Butenhoff JL, Ehresman DJ, Chang SC, Parker GA, Stump DG (2009b) Gestational and lactational exposure to potassium perfluorooctanesulfonate (K+PFOS) in rats: developmental neurotoxicity. Reproductive Toxicology 27(3-4):319-30 doi:10.1016/j.reprotox.2008.12.010

Cacialli P, D'Angelo L, de Girolamo P, Avallone L, Lucini C, Pellegrini E, Castaldo L. (2018) Morpho-functional features of the gonads of Danio rerio: the role of brain-derived neurotrophic factor. Anatomical Record (Hoboken) 301(1):140-147 doi:10.1002/ar.23702

Carten JD, Bradford MK, Farber SA (2011) Visualizing digestive organ morphology and function using differential fatty acid metabolism in live zebrafish. Developmental Biology 360(2):276-85 doi:10.1016/j.ydbio.2011.09.010

Carvalho L, Heisenberg CP (2010) The yolk syncytial layer in early zebrafish development. Trends Cell Biology 20(10):586-92 doi:10.1016/j.tcb.2010.06.009

CDPHE Colorado Department of Public Health and Environment (2017) Site-specific groundwater standard PFOA/PFOS. www.colorado.gov/cdphe/PFCs/water/gwstandard

Chakravarty S, Reddy BR, Sudhakar SR, Saxena S, Das T, Meghah V, Brahmendra Swamy CV, Kumar A, Idris MM. (2013) Chronic unpredictable stress (CUS)-induced anxiety and related mood disorders in a zebrafish model: altered brain proteome profile implicates mitochondrial dysfunction. PloS One 8(5):e63302 doi:10.1371/journal.pone.0063302

Champagne DL, Hoefnagels CC, de Kloet RE, Richardson MK (2010) Translating rodent behavioral repertoire to zebrafish (Danio rerio): relevance for stress research. Behavioral Brain Research 214(2):332-42 doi:10.1016/j.bbr.2010.06.001

Chang S, Butenhoff JL, Parker GA, Coder PS, Zitzow JD, Krisko RM, Bjork JA, Wallace KB, Seed JG. (2018) Reproductive and developmental toxicity of potassium perfluorohexanesulfonate in CD-1 mice. Reproductive Toxicology doi:10.1016/j.reprotox.2018.04.007

Chen F, Gong Z, Kelly BC (2016) Bioavailability and bioconcentration potential of perfluoroalkyl-phosphinic and -phosphonic acids in zebrafish (Danio rerio): Comparison to perfluorocarboxylates and perfluorosulfonates. The Science of the Total Environment 568:33-41 doi:10.1016/j.scitotenv.2016.05.215

Chen J, Tanguay RL, Tal TL, Gai Z, Ma X, Bai C, Tilton SC, Jin D, Yang D, Huang C, Dong Q. (2014) Early life perfluorooctanesulphonic acid (PFOS) exposure impairs zebrafish organogenesis. Aquatic Toxicology 150:124-32 doi:10.1016/j.aquatox.2014.03.005

Cheng J, Lv S, Nie S, Lie J, Tong S, Kang N, Xiao Y, Dong Q, Huang C, Yang D. (2016) Chronic perfluorooctane sulfonate (PFOS) exposure induces hepatic steatosis in zebrafish. Aquatic Toxicology 176:45-52 doi:10.1016/j.aquatox.2016.04.013

Cheng W, Guo L, Zhang Z, Soo HM, Wen C, Wu W, Peng J. (2006) HNF factors form a network to regulate liver-enriched genes in zebrafish. Developmental Biology 294(2):482-96 doi:10.1016/j.ydbio.2006.03.018

Cheng X, Klaassen CD (2008) Critical role of PPAR-alpha in perfluorooctanoic acid- and perfluorodecanoic acid-induced downregulation of Oatp uptake transporters in mouse livers. Toxicological Sciences 106(1):37-45 doi:10.1093/toxsci/kfn161

Chengelis CP, Kirkpatrick JB, Myers NR, Shinohara M, Stetson PL, Sved DW (2009a) Comparison of the toxicokinetic behavior of perfluorohexanoic acid (PFHxA) and nonafluorobutane-1-sulfonic acid (PFBS) in cynomolgus monkeys and rats. Reproductive Toxicology 27(3-4):400-6 doi:10.1016/j.reprotox.2009.01.013

Chengelis CP, Kirkpatrick JB, Radovsky A, Shinohara M (2009b) A 90-day repeated dose oral (gavage) toxicity study of perfluorohexanoic acid (PFHxA) in rats (with functional observational battery and motor activity determinations). Reproductive Toxicology 27(3-4):342-51 doi:10.1016/j.reprotox.2009.01.006

Choudhury AI, Chahal S, Bell AR, Tomlinson SR, Roberts RA, Salter AM, Bell DR. (2000) Species differences in peroxisome proliferation; mechanisms and relevance. Mutation Research 448(2):201-12

Coe NR, Smith AJ, Frohnert BI, Watkins PA, Bernlohr DA (1999) The fatty acid transport protein (FATP1) is a very long chain acyl-CoA synthetase. The Journal of Biological Chemistry 274(51):36300-4

Conder JM, Hoke RA, De Wolf W, Russell MH, Buck RC (2008) Are PFCAs bioaccumulative? A critical review and comparison with regulatory criteria and persistent lipophilic compounds. Environmental Science & Technology 42(4):995-1003

Cui Y, Lv S, Liu J, Nie S, Chen J, Dong Q, Huang C, Yang D. (2017) Chronic perfluorooctanesulfonic acid exposure disrupts lipid metabolism in zebrafish. Human and Experimental Toxicology 36(3):207-217 doi:10.1177/0960327116646615

Dalman MR, Liu Q, King MD, Bagatto B, Londraville RL (2013) Leptin expression affects metabolic rate in zebrafish embryos (D. rerio). Frontiers in Physiology 4:160 doi:10.3389/fphys.2013.00160

Das KP, Wood CR, Lin MT, Starkov AA, Lau C, Wallace KB, Corton JC, Abbott BD (2017) Perfluoroalkyl acids-induced liver steatosis: Effects on genes controlling lipid homeostasis. Toxicology 378:37-52 doi:10.1016/j.tox.2016.12.007

De Felice E, Porreca I, Alleva E, De Girolamo P, Ambrosino C, Ciriaco E, Germana A, Sordino P (2014) Localization of BDNF expression in the developing brain of zebrafish. Journal of Anatomy 224(5):564-74 doi:10.1111/joa.12168

Den Broeder MJ, Kopylova VA, Kamminga LM, Legler J (2015) Zebrafish as a model to study the role of peroxisome proliferating-activated receptors in adipogenesis and obesity. PPAR Research 2015:358029 doi:10.1155/2015/358029

Domi E, Uhrig S, Soverchia L, Spanagel R, Hansson AC, Barbier E, Hellig M, Ciccocioppo R, Ubaldi M (2016) genetic deletion of neuronal PPARγ enhances the emotional response to acute stress and exacerbates anxiety: an effect reversed by rescue of amygdala pparγ function. Journal of Neuroscience 36(50):12611-12623 doi:10.1523/jneurosci.4127-15.2016

Dominiczak MH, Caslake MJ (2011) Apolipoproteins: metabolic role and clinical biochemistry applications. Annals of Clinical Biochemistry 48(Pt 6):498-515 doi:10.1258/acb.2011.011111

Dreyer C, Keller H, Mahfoudi A, Laudet V, Krey G, Wahli W (1993) Positive regulation of the peroxisomal beta-oxidation pathway by fatty acids through activation of peroxisome proliferator-activated receptors (PPAR). Biology of the Cell 77(1):67-76

Du G, Hu J, Huang H, Qin Y, Han X, Wu D, Song L, Xia Y, Wang X. (2013) Perfluorooctane sulfonate (PFOS) affects hormone receptor activity, steroidogenesis, and expression of endocrine-related genes in vitro and in vivo. Environmental Toxicology and Chemistry / SETAC 32(2):353-60 doi:10.1002/etc.2034

Du Y, Shi X, Liu C, Yu K, Zhou B (2009) Chronic effects of water-borne PFOS exposure on growth, survival and hepatotoxicity in zebrafish: a partial life-cycle test. Chemosphere 74(5):723-9 doi:10.1016/j.chemosphere.2008.09.075

Emran F, Rihel J, Dowling JE (2008) A behavioral assay to measure responsiveness of zebrafish to changes in light intensities. Journal of Visualized Experiments (20) doi:10.3791/923

Eriksen KT, Raaschou-Nielsen O, Sorensen M, Roursgaard M, Loft S, Moller P (2010) Genotoxic potential of the perfluorinated chemicals PFOA, PFOS, PFBS, PFNA and PFHxA in human HepG2 cells. Mutation Research 700(1-2):39-43 doi:10.1016/j.mrgentox.2010.04.024

Fai Tse WK, Li JW, Kwan Tse AC, Chan TF, Hin Ho JC, Sun Wu RS, Chu Wong CK, Lai KP. (2016) Fatty liver disease induced by perfluorooctane sulfonate: Novel insight from transcriptome analysis. Chemosphere 159:166-177 doi:10.1016/j.chemosphere.2016.05.060

Feng D, Huang QY, Liu K, Zhang SC, Liu ZH (2014) Comparative studies of zebrafish Danio rerio lipoprotein lipase (lpl) and hepatic lipase (lipc) genes belonging to the lipase gene family: evolution and expression pattern. Journal of Fish Biology 85(2):329-42 doi:10.1111/jfb.12423

Flynn EJ, 3rd, Trent CM, Rawls JF (2009) Ontogeny and nutritional control of adipogenesis in zebrafish (Danio rerio). Journal of Lipid Research 50(8):1641-52 doi:10.1194/jlr.M800590-JLR200

Fraher D, Sanigorski A, Mellett NA, Meikle PJ, Sinclair AJ, Gibert Y (2016) Zebrafish embryonic lipidomic analysis reveals that the yolk cell is metabolically active in processing lipid. Cell Reports 14(6):1317-1329 doi:10.1016/j.celrep.2016.01.016

Fraser TWK, Khezri A, Lewandowska-Sabat AM, Henry T, Ropstad E (2017) Endocrine disruptors affect larval zebrafish behavior: Testing potential mechanisms and comparisons of behavioral sensitivity to alternative biomarkers. Aquatic Toxicology 193:128-135 doi:10.1016/j.aquatox.2017.10.002

Freyer C, Renfree MB (2009) The mammalian yolk sac placenta. Journal of Experimental Zoology: Molecular and Developmental Evolution 312(6):545-54 doi:10.1002/jez.b.21239

Froehlicher M, Liedtke A, Groh KJ, Neuhauss SC, Segner H, Eggen RI (2009) Zebrafish (Danio rerio) neuromast: promising biological endpoint linking developmental and toxicological studies. Aquatic Toxicology 95(4):307-19 doi:10.1016/j.aquatox.2009.04.007

Frohnert BI, Hui TY, Bernlohr DA (1999) Identification of a functional peroxisome proliferator-responsive element in the murine fatty acid transport protein gene. The Journal of Biological Chemistry 274(7):3970-7

Fuentes S, Vicens P, Colomina MT, Domingo JL (2007) Behavioral effects in adult mice exposed to perfluorooctane sulfonate (PFOS). Toxicology 242(1-3):123-9 doi:10.1016/j.tox.2007.09.012

Gaiddon C, Loeffler JP, Larmet Y (1996) Brain-derived neurotrophic factor stimulates AP-1 and cyclic AMP-responsive element dependent transcriptional activity in central nervous system neurons. Journal of Neurochemistry 66(6):2279-86

Gariano G, Guarienti M, Bresciani R, Borsani G, Carola G, Monti E, Giuliani R, Rezzani R, Bonomini F, Preti A, SchuP, Zizioli D.. (2014) Analysis of three mu1-AP1 subunits during zebrafish development. Developmental Dynamics 243(2):299-314 doi:10.1002/dvdy.24071

German JB, Smilowitz JT, Zivkovic AM (2006) Lipoproteins: When size really matters. Current Opinion Colloid and Interface Science 11(2-3):171-183 doi:10.1016/j.cocis.2005.11.006

Germana A, Laura R, Montalbano G, GuerreraMC, Amato V, Zichichi R, Campo S, Ciriaco E, Vega JA. (2010a) Expression of brain-derived neurotrophic factor and TrkB in the lateral line system of zebrafish during development. Cellular and Molecular Neurobiology 30(5):787-93 doi:10.1007/s10571-010-9506-z

Germana A, Sanchez-Ramos C, Guerrera MC, Calavia MG, Navarro M, Zichichi R, Garcia-Suarez O, Perez-Pinera P, Vega JA. (2010b) Expression and cell localization of brain-derived neurotrophic factor and TrkB during zebrafish retinal development. Journal of Anatomy 217(3):214-22 doi:10.1111/j.1469-7580.2010.01268.x

Gomis MI, Wang Z, Scheringer M, Cousins IT (2015) A modeling assessment of the physicochemical properties and environmental fate of emerging and novel per- and polyfluoroalkyl substances. The Science of the Total Environment 505:981-91 doi:10.1016/j.scitotenv.2014.10.062

Gorissen M, Bernier NJ, Nabuurs SB, Flik G, Huising MO (2009) Two divergent leptin paralogues in zebrafish (Danio rerio) that originate early in teleostean evolution. Journal of Endocrinology 201(3):329-39 doi:10.1677/JOE-09-0034

Gorrochategui E, Casas J, Porte C, Lacorte S, Tauler R (2015) Chemometric strategy for untargeted lipidomics: biomarker detection and identification in stressed human placental cells. Analytica Chimica Acta 854:20-33 doi:10.1016/j.aca.2014.11.010

Grandjean P, Andersen EW, Budtz-Jorgensen E, Nielsen F, Molbak K, Weihe P, Heilmann C. (2012) Serum vaccine antibody concentrations in children exposed to perfluorinated compounds. JAMA 307(4):391-7 doi:10.1001/jama.2011.2034

Guruge KS, Yeung LW, Yamanaka N, Miyazaki S, Lam PK, Giesy JP, Jones PD, Yamashita N. (2006) Gene expression profiles in rat liver treated with perfluorooctanoic acid (PFOA). Toxicological Sciences 89(1):93-107 doi:10.1093/toxsci/kfj011

Hagen DF, Belisle J, Johnson JD, Venkateswarlu P (1981) Characterization of fluorinated metabolites by a gas chromatographic-helium microwave plasma detector--the biotransformation of 1H, 1H, 2H, 2H-perfluorodecanol to perfluorooctanoate. Analytical Biochemistry 118(2):336-43

Hagenaars A, Stinckens E, Vergauwen L, Bervoets L, Knapen D (2014) PFOS affects posterior swim bladder chamber inflation and swimming performance of zebrafish larvae. Aquatic Toxicology 157:225-35 doi:10.1016/j.aquatox.2014.10.017

Hagenaars A, Vergauwen L, Benoot D, Laukens K, Knapen D (2013) Mechanistic toxicity study of perfluorooctanoic acid in zebrafish suggests mitochondrial dysfunction to play a key role in PFOA toxicity. Chemosphere 91(6):844-56 doi:10.1016/j.chemosphere.2013.01.056

Hagenaars A, Vergauwen L, De Coen W, Knapen D (2011) Structure-activity relationship assessment of four perfluorinated chemicals using a prolonged zebrafish early life stage test. Chemosphere 82(5):764-72 doi:10.1016/j.chemosphere.2010.10.076

Hagenbuch B, Gui C (2008) Xenobiotic transporters of the human organic anion transporting polypeptides (OATP) family. Xenobiotica 38(7-8):778-801 doi:10.1080/00498250801986951

Hansen KJ, Johnson HO, Eldridge JS, Butenhoff JL, Dick LA (2002) Quantitative characterization of trace levels of PFOS and PFOA in the Tennessee River. Environmental Science & Technology 36(8):1681-5

Hashimoto M, Heinrich G (1997) Brain-derived neurotrophic factor gene expression in the developing zebrafish. International Journal of Developmental Neuroscience 15(8):983-97

He X, Liu Y, Xu B, Gu L, Tang W (2017) PFOA is associated with diabetes and metabolic alteration in US men: National Health and Nutrition Examination Survey 2003-2012. The Science of the Total Environment 625:566-574 doi:10.1016/j.scitotenv.2017.12.186

Hoffman K, Webster TF, Weisskopf MG, Weinberg J, Vieira VM (2010) Exposure to polyfluoroalkyl chemicals and attention deficit/hyperactivity disorder in U.S. children 12-15 years of age. Environmental Health Perspectives 118(12):1762-7 doi:10.1289/ehp.1001898

Howe K, Clark MD, Torroja CF, et al. (2013) The zebrafish reference genome sequence and its relationship to the human genome. Nature 496(7446):498-503 doi:10.1038/nature12111

Hsu CW, Pan YJ, Wang YW, Tong SK, Chung BC (2018) Changes in the morphology and gene expression of developing zebrafish gonads. General and Comparative Endocrinology doi:10.1016/j.ygcen.2018.01.026

Hu XC, Andrews DQ, Lindstrom AB, et al. (2016) Detection of poly- and perfluoroalkyl substances (PFASs) in U.S. drinking water linked to industrial sites, military fire training areas, and wastewater treatment plants. Environmental Science & Technology Letters 3(10):344-350 doi:10.1021/acs.estlett.6b00260

Huang H, Huang C, Wang L, Ye X, Bai C, Simonich MT, Tanguay RL, Dong Q. (2010) Toxicity, uptake kinetics and behavior assessment in zebrafish embryos following exposure to

perfluorooctanesulphonicacid (PFOS). Aquatic Toxicology 98(2):139-47 doi:10.1016/j.aquatox.2010.02.003

Hundley SG, Sarrif AM, Kennedy GL (2006) Absorption, distribution, and excretion of ammonium perfluorooctanoate (APFO) after oral administration to various species. Drug and Chemical Toxicology 29(2):137-45 doi:10.1080/01480540600561361

Hurd MW, Cahill GM (2002) Entraining signals initiate behavioral circadian rhythmicity in larval zebrafish. Journal Biologial Rhythms 17(4):307-14 doi:10.1177/074873002129002618

Hussain MM, Iqbal J, Anwar K, Rava P, Dai K (2003) Microsomal triglyceride transfer protein: a multifunctional protein. Frontiers in Bioscience 8:s500-6

Huynh G, Heinrich G (2001) Brain-derived neurotrophic factor gene organization and transcription in the zebrafish embryo. International Journal of Developmental Neuroscience 19(7):663-73

Ibabe A, Bilbao E, Cajaraville MP (2005a) Expression of peroxisome proliferator-activated receptors in zebrafish (Danio rerio) depending on gender and developmental stage. Histochemistry and Cell Biology 123(1):75-87 doi:10.1007/s00418-004-0737-2

Ibabe A, Herrero A, Cajaraville MP (2005b) Modulation of peroxisome proliferator-activated receptors (PPARs) by PPAR(alpha)- and PPAR(gamma)-specific ligands and by 17beta-estradiol in isolated zebrafish hepatocytes. Toxicology In Vitro 19(6):725-35 doi:10.1016/j.tiv.2005.03.019

Ishibashi H, Yamauchi R, Matsuoka M, Kim JW, Hirano M, Yamaguchi A, Tominaga N, Arizono K. (2008) Fluorotelomer alcohols induce hepatic vitellogenin through activation of the estrogen receptor in male medaka (Oryzias latipes). Chemosphere 71(10):1853-9 doi:10.1016/j.chemosphere.2008.01.065

Iwai H, Hoberman AM (2014) Oral (Gavage) Combined developmental and perinatal/postnatal reproduction toxicity study of ammonium salt of perfluorinated hexanoic acid in mice. International Journal of Toxicology 33(3):219-237 doi:10.1177/1091581814529449

Jadrich JL, O'Connor MB, Coucouvanis E (2006) The TGF beta activated kinase TAK1 regulates vascular development in vivo. Development 133(8):1529-41 doi:10.1242/dev.02333

Jahnke A (2007) Polyfluorinated alkyl substances (PFAS) in the marine atmosphere-investigations on their occurence and districution in coastal regions. University of Luneberg

Jantzen CE, Annunziato KM, Bugel SM, Cooper KR (2016a) PFOS, PFNA, and PFOA sub-lethal exposure to embryonic zebrafish have different toxicity profiles in terms of morphometrics, behavior and gene expression. Aquatic Toxicology 175:160-70 doi:10.1016/j.aquatox.2016.03.026

Jantzen CE, Annunziato KM, Cooper KR (2016b) Behavioral, morphometric, and gene expression effects in adult zebrafish (Danio rerio) embryonically exposed to PFOA, PFOS, and PFNA. Aquatic Toxicology 180:123-130 doi:10.1016/j.aquatox.2016.09.011

Jantzen CE, Toor F, Annunziato KM, Cooper KR (2017) Effects of chronic perfluorooctanoic acid (PFOA) at low concentration on morphometrics, gene expression, and fecundity in zebrafish (Danio rerio). Reproductive Toxicology 69:34-42 doi:10.1016/j.reprotox.2017.01.009

Jensen AA, Leffers H (2008) Emerging endocrine disrupters: perfluoroalkylated substances. International Journal of Andrology 31(2):161-9 doi:10.1111/j.1365-2605.2008.00870.x

Johansson N, Fredriksson A, Eriksson P (2008) Neonatal exposure to perfluorooctane sulfonate (PFOS) and perfluorooctanoic acid (PFOA) causes neurobehavioural defects in adult mice. Neurotoxicology 29(1):160-9 doi:10.1016/j.neuro.2007.10.008

Kannan K, Tao L, Sinclair E, Pastva SD, Jude DJ, Giesy JP (2005) Perfluorinated compounds in aquatic organisms at various trophic levels in a Great Lakes food chain. Archives of Environmental Contamination and Toxicology 48(4):559-66 doi:10.1007/s00244-004-0133-x

Kersten S (2014) Physiological regulation of lipoprotein lipase. Biochimica et Biophysica Acta 1841(7):919-33 doi:10.1016/j.bbalip.2014.03.013

Khalil N, Chen A, Lee M, Czerwinski SA, Ebert JR, DeWitt, JC, Kannan K. (2016) Association of perfluoroalkyl substances, bone mineral density, and osteoporosis in the U.S. population

in NHANES 2009-2010. Environmental Health Perspectives 124(1):81-7 doi:10.1289/ehp.1307909

Kim HR, Ingham PW (2009) The extracellular matrix protein TGFBI promotes myofibril bundling and muscle fibre growth in the zebrafish embryo. Developmental Dynamics 238(1):56-65 doi:10.1002/dvdy.21812

Kim JK, Gimeno RE, Higashimori T, Kim HJ, Choi H, Punreddy S, Mozell RL, Tan G, Stricker-Krongrad A, Hirsch DJ, Fillmore JJ, Lui ZX, Dong J, Cline G, Stahl A, Lodish HF, Shulman GI. (2004) Inactivation of fatty acid transport protein 1 prevents fat-induced insulin resistance in skeletal muscle. Journal of Clinical Investigation 113(5):756-63 doi:10.1172/JCI18917

Kim M, Park MS, Son J, Park I, Lee HK, Kim C, Min BH, Ryoo J, Choi KS, Lee DS, Lee HS. (2015) Perfluoroheptanoic acid affects amphibian embryogenesis by inducing the phosphorylation of ERK and JNK. International Journal of Molecular Medicine 36(6):1693-700 doi:10.3892/ijmm.2015.2370

Kim SJ, Shin H, Lee YB, Cho HY (2017) Sex-specific risk assessment of PFHxS using a physiologically based pharmacokinetic model. Archives in Toxicology doi:10.1007/s00204-017-2116-5

Kim WK, Lee SK, Jung J (2010) Integrated assessment of biomarker responses in common carp (Cyprinus carpio) exposed to perfluorinated organic compounds. Journal of Hazardous Materials 180(1-3):395-400 doi:10.1016/j.jhazmat.2010.04.044

Kimmel CB, Ballard WW, Kimmel SR, Ullmann B, Schilling TF (1995) Stages of embryonic development of the zebrafish. Developmental Dynamics 203(3):253-310 doi:10.1002/aja.1002030302

Klaassen CD, Aleksunes LM (2010) Xenobiotic, bile acid, and cholesterol transporters: function and regulation. Pharmacological Reviews 62(1):1-96 doi:10.1124/pr.109.002014

Klaunig JE, Shinohara M, Iwai H, Chengelis CP, Kirkpatrick JB, Wang Z, Bruner RH. (2014) Evaluation of the chronic toxicity and carcinogenicity of perfluorohexanoic acid (PFHxA) in sprague-dawley rats. Toxicologic Pathology doi:10.1177/0192623314530532

Kondakova EA, Efremov VI (2014) Morphofunctional transformations of the yolk syncytial layer during zebrafish development. Journal of Morphology 275(2):206-16 doi:10.1002/jmor.20209

Koponen J, Airaksinen R, Hallikainen A, Vuorinen PJ, Mannio J, Kiviranta H (2014) Perfluoroalkyl acids in various edible Baltic, freshwater, and farmed fish in Finland. Chemosphere doi:10.1016/j.chemosphere.2014.08.077

Kristofco LA, Cruz LC, Haddad SP, Behra ML, Chambliss CK, Brooks BW (2016) Age matters: Developmental stage of Danio rerio larvae influences photomotor response thresholds to diazinion or diphenhydramine. Aquatic Toxicology 170:344-54 doi:10.1016/j.aquatox.2015.09.011

Krovel AV, Softeland L, Torstensen B, Olsvik PA (2008) Transcriptional effects of PFOS in isolated hepatocytes from Atlantic salmon Salmo salar L. Comparative Biochemistry and Physiology: Toxicology and Pharmacology 148(1):14-22 doi:10.1016/j.cbpc.2008.03.001

Kudo N, Katakura M, Sato Y, Kawashima Y (2002) Sex hormone-regulated renal transport of perfluorooctanoic acid. Chemico-Biological Interactions 139(3):301-16

Labadie P, Chevreuil M (2011) Partitioning behaviour of perfluorinated alkyl contaminants between water, sediment and fish in the Orge River (nearby Paris, France). Environmental Pollution 159(2):391-7 doi:10.1016/j.envpol.2010.10.039

Ladics GS, Kennedy GL, O'Connor J, Everd N, Malley LA, Fame SR, Gannon S, Jung R, Roth T, IwaiH, Shin-Ya S. (2008) 90-day oral gavage toxicity study of 8-2 fluorotelomer alcohol in rats. Drug and Chemical Toxicology 31(2):189-216 doi:10.1080/01480540701873103

Land M, De Wit CA, Bignert A, Cousins IT, Herzke D, Johansson J, Martin JW. (2018) What is the effect of phasing out long-chain per- and polyfluoroalkyl substances on the concentrations of perfluoroalkyl acids and their precursors in the environment? A systematic review. Environmental Evidence 7(4) doi:https://doi.org/10.1186/s13750-017-0114-y

Lau C (2012) Perfluorinated compounds. EXS 101:47-86 doi:10.1007/978-3-7643-8340-4_3

Lau C, Anitole K, Hodes C, Lai D, Pfahles-Hutchens A, Seed J (2007) Perfluoroalkyl acids: a review of monitoring and toxicological findings. Toxicological Sciences 99(2):366-94 doi:10.1093/toxsci/kfm128

Lau C, Butenhoff JL, Rogers JM (2004) The developmental toxicity of perfluoroalkyl acids and their derivatives. Toxicology and Applied Pharmacology 198(2):231-41 doi:10.1016/j.taap.2003.11.031

Lawrence DA (1996) Transforming growth factor-beta: a general review. European Cytokine Network 7(3):363-74

Lee I, Viberg H (2013) A single neonatal exposure to perfluorohexane sulfonate (PFHxS) affects the levels of important neuroproteins in the developing mouse brain. Neurotoxicology 37:190-6 doi:10.1016/j.neuro.2013.05.007

Lee JW, Lee JW, Kim K, Shin YJ, Kim J, Kim S, Kim H, Kim P, Park K. (2017) PFOA-induced metabolism disturbance and multi-generational reproductive toxicity in Oryzias latipes. Journal of Hazardous Materials 340:231-240 doi:10.1016/j.jhazmat.2017.06.058

Lee YJ, Choi SY, Yang JH (2014a) NMDA receptor-mediated ERK 1/2 pathway is involved in PFHxS-induced apoptosis of PC12 cells. The Science of the Total Environment 491-492:227-34 doi:10.1016/j.scitotenv.2014.01.114

Lee YJ, Choi SY, Yang JH (2014b) PFHxS induces apoptosis of neuronal cells via ERK1/2-mediated pathway. Chemosphere 94:121-7 doi:10.1016/j.chemosphere.2013.09.059

Lehmler HJ, Rama Rao VV, Nauduri D, Vargo JD, Parkin S (2007) Synthesis and structure of environmentally relevant perfluorinated sulfonamides. Journal of Fluorine Chemistry 128(6):595-607 doi:10.1016/j.jfluchem.2007.01.013

Letterio JJ, Roberts AB (1998) Regulation of immune responses by TGF-beta. Annual Review of Immunology 16:137-61 doi:10.1146/annurev.immunol.16.1.137

Lewis RC, Johns LE, Meeker JD (2015) Serum biomarkers of exposure to perfluoroalkyl substances in relation to serum testosterone and measures of thyroid function among adults and adolescents from NHANES 2011-2012. International Journal of Environmental Research and Public Health 12(6):6098-114 doi:10.3390/ijerph120606098

Li Y, Fletcher T, Mucs D, Scott K, Lindh CH, Talving P, Jakobsson K. (2018) Half-lives of PFOS, PFHxS and PFOA after end of exposure to contaminated drinking water. Occupational and Environmental Medicine 75(1):46-51 doi:10.1136/oemed-2017-104651

Liao C, Wang T, Cui L, Zhou Q, Duan S, Jiang G (2009) Changes in synaptic transmission, calcium current, and neurite growth by perfluorinated compounds are dependent on the chain length and functional group. Environmental Science & Technology 43(6):2099-104

Litchfield JT, Jr., Wilcoxon F (1948) A simplified method of evaluating dose-effect experiments. Federation Proceedings 7(1 Pt 1):240

Liu C, Deng J, Yu L, Ramesh M, Zhou B (2010a) Endocrine disruption and reproductive impairment in zebrafish by exposure to 8:2 fluorotelomer alcohol. Aquatic Toxicology 96(1):70-6 doi:10.1016/j.aquatox.2009.09.012

Liu C, Du Y, Zhou B (2007) Evaluation of estrogenic activities and mechanism of action of perfluorinated chemicals determined by vitellogenin induction in primary cultured tilapia hepatocytes. Aquatic Toxicology 85(4):267-77 doi:10.1016/j.aquatox.2007.09.009

Liu C, Yu L, Deng J, Lam PK, Wu RS, Zhou B (2009) Waterborne exposure to fluorotelomer alcohol 6:2 FTOH alters plasma sex hormone and gene transcription in the hypothalamic-pituitary-gonadal (HPG) axis of zebrafish. Aquatic Toxicology 93(2-3):131-7 doi:10.1016/j.aquatox.2009.04.005

Liu FY, Hsu TC, Choong P, Lin MH, Chuang YJ, Chen BS, Lin C. (2018a) Uncovering the regeneration strategies of zebrafish organs: a comprehensive systems biology study on heart, cerebellum, fin, and retina regeneration. BMC Systems Biology 12(Suppl 2):29 doi:10.1186/s12918-018-0544-3

Liu G, Dhana K, Furtado JD, Rood J, Zong G, Liang L, Qi L, Bray GA, DeJonge L, Coull B, Grandjean P, Sun Q. (2018b) Perfluoroalkyl substances and changes in body weight and resting metabolic rate in response to weight-loss diets: A prospective study. PLoS Medicine 15(2):e1002502 doi:10.1371/journal.pmed.1002502

Liu Q, Chen Y, Copeland D, et al. (2010b) Expression of leptin receptor gene in developing and adult zebrafish. General and Comparative Endocrinology 166(2):346-55 doi:10.1016/j.ygcen.2009.11.015

Liu XH, Zhang T, Rawson DM (1999) The effect of partial removal of yolk on the chilling sensitivity of zebrafish (Danio rerio) embryos. Cryobiology 39(3):236-42 doi:10.1006/cryo.1999.2206

Loccisano AE, Campbell JL, Jr., Andersen ME, Clewell HJ, 3rd (2011) Evaluation and prediction of pharmacokinetics of PFOA and PFOS in the monkey and human using a PBPK model. Regulatory Toxicology and Pharmacology 59(1):157-75 doi:10.1016/j.yrtph.2010.12.004

Long Y, Wang Y, Ji G, Yan L, Hu F, Gu A (2013) Neurotoxicity of perfluorooctane sulfonate to hippocampal cells in adult mice. PloS One 8(1):e54176 doi:10.1371/journal.pone.0054176

Luebker DJ, Case MT, York RG, Moore JA, Hansen KJ, Butenhoff JL (2005) Two-generation reproduction and cross-foster studies of perfluorooctanesulfonate (PFOS) in rats. Toxicology 215(1-2):126-48 doi:10.1016/j.tox.2005.07.018

MacPhail RC, Brooks J, Hunter DL, Padnos B, Irons TD, Padilla S (2009) Locomotion in larval zebrafish: Influence of time of day, lighting and ethanol. Neurotoxicology 30(1):52-8 doi:10.1016/j.neuro.2008.09.011

Mandard S, Muller M, Kersten S (2004) Peroxisome proliferator-activated receptor alpha target genes. Cellular and Molecular Life Science 61(4):393-416 doi:10.1007/s00018-003-3216-3

Maras M, Vanparys C, Muylle F, Robbens J, Berger U, Brber JL, Blust R, De Coen W. (2006) Estrogen-like properties of fluorotelomer alcohols as revealed by mcf-7 breast cancer cell proliferation. Environmental Health Perspectives 114(1):100-5

Mariussen E (2012) Neurotoxic effects of perfluoroalkylated compounds: mechanisms of action and environmental relevance. Archives in Toxicology 86(9):1349-67 doi:10.1007/s00204-012-0822-6

Martin JW, Mabury SA, O'Brien PJ (2005) Metabolic products and pathways of fluorotelomer alcohols in isolated rat hepatocytes. Chemico-Biological Interactions 155(3):165-80 doi:10.1016/j.cbi.2005.06.007

Marza E, Barthe C, Andre M, Villeneuve L, Helou C, Babin PJ (2005) Developmental expression and nutritional regulation of a zebrafish gene homologous to mammalian microsomal triglyceride transfer protein large subunit. Developmental Dynamics 232(2):506-18 doi:10.1002/dvdy.20251

McAllister AK (2001) Neurotrophins and neuronal differentiation in the central nervous system. Cellular and Molecular Life Sciences 58(8):1054-60 doi:10.1007/PL00000920

Mehlem A, Hagberg CE, Muhl L, Eriksson U, Falkevall A (2013) Imaging of neutral lipids by oil red O for analyzing the metabolic status in health and disease. Nature Protocols 8(6):1149-54 doi:10.1038/nprot.2013.055

Meier-Abt F, Hammann-Hanni A, Stieger B, Ballatori N, Boyer JL (2007) The organic anion transport polypeptide 1d1 (Oatp1d1) mediates hepatocellular uptake of phalloidin and microcystin into skate liver. Toxicology and Applied Pharmacology 218(3):274-9 doi:10.1016/j.taap.2006.11.015

Melzer D, Rice N, Depledge MH, Henley WE, Galloway TS (2010) Association between serum perfluorooctanoic acid (PFOA) and thyroid disease in the U.S. National Health and Nutrition Examination Survey. Environmental Health Perspectives 118(5):686-92 doi:10.1289/ehp.0901584

Metz JR, Huising MO, Leon K, Verburg-van Kemenade BM, Flik G (2006) Central and peripheral interleukin-1beta and interleukin-1 receptor I expression and their role in the acute stress response of common carp, Cyprinus carpio L. Journal of Endocrinology 191(1):25-35 doi:10.1677/joe.1.06640

Michel M, Page-McCaw PS, Chen W, Cone RD (2016) Leptin signaling regulates glucose homeostasis, but not adipostasis, in the zebrafish. Proceedings of the National Academy of Sciences of the United States of America 113(11):3084-9 doi:10.1073/pnas.1513212113

Miyares RL, de Rezende VB, Farber SA (2014) Zebrafish yolk lipid processing: a tractable tool for the study of vertebrate lipid transport and metabolism. Disease Models and Mechanisms 7(7):915-27 doi:10.1242/dmm.015800

Mogensen UB, Grandjean P, Nielsen F, Weihe P, Budtz-Jorgensen E (2015) Breastfeeding as an exposure pathway for perfluorinated alkylates. Environmental Science & Technology 49(17):10466-73 doi:10.1021/acs.est.5b02237

Montpetit A, Cote S, Brustein E, Drouin R, Lapointe A, Boudreau M, Meloche C, Drouin R, Hudson TJ, Drapeau P, Cossette P. (2008) Disruption of AP1S1, causing a novel neurocutaneous syndrome, perturbs development of the skin and spinal cord. PLoS Genetics 4(12):e1000296 doi:10.1371/journal.pgen.1000296

Moran-Salvador E, Lopez-Parra M, Garcia-Alonso V, Titos E, Martinez-Clemente M, Gonzalez-Periz A, Lopez-Vicario, C, Barak Y, Arroyo V, Claria J. (2011) Role for PPARgamma in obesity-induced hepatic steatosis as determined by hepatocyte- and macrophage-specific conditional knockouts. FASEB Journal: Official publication of the Federation of American Societies for Experimental Biology 25(8):2538-50 doi:10.1096/fj.10-173716

Mulkiewicz E, Jastorff B, Skladanowski AC, Kleszczynski K, Stepnowski P (2007) Evaluation of the acute toxicity of perfluorinated carboxylic acids using eukaryotic cell lines, bacteria and enzymatic assays. Environmental Toxicology and Pharmacology 23(3):279-85 doi:10.1016/j.etap.2006.11.002

Nakatsu F, Hase K, Ohno H (2014) The Role of the Clathrin Adaptor AP-1: Polarized Sorting and Beyond. Membranes (Basel) 4(4):747-63 doi:10.3390/membranes4040747

Nakayama S, Strynar MJ, Helfant L, Egeghy P, Ye X, Lindstrom AB (2007) Perfluorinated compounds in the Cape Fear drainage basin in North Carolina. Environmental Science & Technology 41(15):5271-6

Negri E, Metruccio F, Guercio V, Tosti L, Benfenati E, Bonzi R, La Vecchia C, Moretto A. (2017) Exposure to PFOA and PFOS and fetal growth: a critical merging of toxicological and epidemiological data. Critical Reviews in Toxicology 47(6):482-508 doi:10.1080/10408444.2016.1271972

NTP (2016) Monograph on Immunotoxicity Associated with Exposure to Perfluorooctanoic acid (PFOA) and perfluorooctane sulfonate (PFOS). Research Triangle Park, NC: National Toxicology Program

O'Connor JC, Munley SM, Serex TL, Buck RC (2014) Evaluation of the reproductive and developmental toxicity of 6:2 fluorotelomer alcohol in rats. Toxicology 317:6-16 doi:10.1016/j.tox.2014.01.002

OECD (1998) Test No. 212: Fish, Short-term Toxicity Test on Embryo and Sac-Fry Stages

OECD (2016) User's handbook supplement to the guidance document for developing and assessing AOPs. OECD Environment, Health and Safety Publications Series on Testing and Assessment No 233

Ohmori K, Kudo N, Katayama K, Kawashima Y (2003) Comparison of the toxicokinetics between perfluorocarboxylic acids with different carbon chain length. Toxicology 184(2-3):135-40

Olsen GW, Mair DC, Lange CC, Harrington LM, Church TR, Goldberg CL, Herron RM, Hanna H, Nobiletti JB, Rios JA, Reagen WK, Ley CA. (2017) Per- and polyfluoroalkyl substances (PFAS) in American Red Cross adult blood donors, 2000-2015. Environmental Research 157:87-95 doi:10.1016/j.envres.2017.05.013

Orger MB, de Polavieja GG (2017) Zebrafish behavior: opportunities and challenges. Annual Reviews in Neuroscience 40:125-147 doi:10.1146/annurev-neuro-071714-033857

Otis JP, Zeituni EM, Thierer JH, Anderson JL, Brown AC, Boehm ED, Cerchione DM, Ceasrine AM, Avraham-Davidi I, Tempelhof H, Yaniv K, Farber SA. (2015) Zebrafish as a model for apolipoprotein biology: comprehensive expression analysis and a role for ApoA-IV in regulating food intake. Disease Models and Mechanism 8(3):295-309 doi:10.1242/dmm.018754

Pan WW, Myers MG, Jr. (2018) Leptin and the maintenance of elevated body weight. Nature Reviews Neuroscience 19(2):95-105 doi:10.1038/nrn.2017.168

Pan Y, Zhang H, Cui Q, Sheng N, Yeung LWY, Sun Y, Guo Y, Dai J. (2018) Worldwide distribution of novel perfluoroether carboxylic and sulfonic acids in surface water. Environmental Science & Technology doi:10.1021/acs.est.8b00829

Parichy DM, Elizondo MR, Mills MG, Gordon TN, Engeszer RE (2009) Normal table of postembryonic zebrafish development: staging by externally visible anatomy of the living fish. Developmental Dynamics 238(12):2975-3015 doi:10.1002/dvdy.22113

Perez F, Nadal M, Navarro-Ortega A, Fabrega F, Domingo JL, Barcelo D, Farre M. (2013) Accumulation of perfluoroalkyl substances in human tissues. Environment International 59:354-62 doi:10.1016/j.envint.2013.06.004

Peters JM, Aoyama T, Burns AM, Gonzalez FJ (2003) Bezafibrate is a dual ligand for PPARalpha and PPARbeta: studies using null mice. Biochimica et Biophysica Acta 1632(1-3):80-9

Pickart MA, Klee EW, Nielsen AL, et al. (2006) Genome-wide reverse genetics framework to identify novel functions of the vertebrate secretome. PloS One 1:e104 doi:10.1371/journal.pone.0000104

Popovic M, Zaja R, Fent K, Smital T (2013) Molecular characterization of zebrafish Oatp1d1 (Slco1d1), a novel organic anion-transporting polypeptide. The Journal of Biological Chemistry 288(47):33894-911 doi:10.1074/jbc.M113.518506

Popovic M, Zaja R, Fent K, Smital T (2014) Interaction of environmental contaminants with zebrafish organic anion transporting polypeptide, Oatp1d1 (Slco1d1). Toxicology and Applied Pharmacology 280(1):149-58 doi:10.1016/j.taap.2014.07.015

Popovic M, Zaja R, Smital T (2010) Organic anion transporting polypeptides (OATP) in zebrafish (Danio rerio): Phylogenetic analysis and tissue distribution. Comparative Biochemistry and Physiology Part A, Molecular & Integrative Physiology 155(3):327-35 doi:10.1016/j.cbpa.2009.11.011

Post GB, Cohn PD, Cooper KR (2012) Perfluorooctanoic acid (PFOA), an emerging drinking water contaminant: a critical review of recent literature. Environmental Research 116:93-117 doi:10.1016/j.envres.2012.03.007

Post GB, Louis JB, Lippincott RL, Procopio NA (2013) Occurrence of perfluorinated compounds in raw water from New Jersey public drinking water systems. Environmental Science & Technology 47(23):13266-75 doi:10.1021/es402884x

Quinlivan VH, Farber SA (2017) Lipid uptake, metabolism, and transport in the larval zebrafish. Frontiers Endocrinololgy (Lausanne) 8:319 doi:10.3389/fendo.2017.00319

Raabe M, Flynn LM, Zlot CH, Wong JS, Veniant MM, Hamilton RL, Young SG. (1998) Knockout of the abetalipoproteinemia gene in mice: reduced lipoprotein secretion in heterozygotes and embryonic lethality in homozygotes. Proceedings of the National Academy of Sciences of the United States of America 95(15):8686-91

Raldua D, Andre M, Babin PJ (2008) Clofibrate and gemfibrozil induce an embryonic malabsorption syndrome in zebrafish. Toxicology and Applied Pharmacology 228(3):301-14 doi:10.1016/j.taap.2007.11.016

Rand AA, Mabury SA (2014) Protein binding associated with exposure to fluorotelomer alcohols (FTOHs) and polyfluoroalkyl phosphate esters (PAPs) in rats. Environmental Science &Technology 48(4):2421-9 doi:10.1021/es404390x

Reif DM, Truong L, Mandrell D, Marvel S, Zhang G, Tanguay RL (2016) High-throughput characterization of chemical-associated embryonic behavioral changes predicts teratogenic outcomes. Archives Toxicology 90(6):1459-70 doi:10.1007/s00204-015-1554-1

Ribes D, Fuentes S, Torrente M, Colomina MT, Domingo JL (2010) Combined effects of perfluorooctane sulfonate (PFOS) and maternal restraint stress on hypothalamus adrenal axis (HPA) function in the offspring of mice. Toxicology and Applied Pharmacology 243(1):13-8 doi:10.1016/j.taap.2009.11.001

Rice PA (2015) C6-Perfluorinated compounds: the new greaseproofing agents in food Ppackaging. Current Environmental Health Reports 2(1):33-40 doi:10.1007/s40572-014-0039-3

Rosen MB, Schmid JR, Corton JC, Zehr RD, Das KP, Abbott BD, Lau C. (2010) Gene expression profiling in wild-type and PPARalpha-null mice exposed to perfluorooctane sulfonate reveals PPARalpha-independent effects. PPAR Research 2010 doi:10.1155/2010/794739

Salmeron C (2018) Adipogenesis in fish. The Journal of Experimental Biology 221(Pt Suppl 1) doi:10.1242/jeb.161588

Salmeron C, Johansson M, Angotzi AR, Ronnestad I, Johnsson, E, Bjornsson BT, Gutierrez J, Navarro I, Capilla E. (2015) Effects of nutritional status on plasma leptin levels and in vitro regulation of adipocyte leptin expression and secretion in rainbow trout. General and Comparative Endocrinology 210:114-23 doi:10.1016/j.ygcen.2014.10.016

Sanchez Garcia D, Sjodin M, Hellstrandh M, Norinder U, Nikiforova V, Lindberg J, Wincent E, Bergman A, Cotgreave I, Munic Ks V. (2018) Cellular accumulation and lipid binding of perfluorinated alkylated substances (PFASs) - A comparison with lysosomotropic drugs. Chemico-Biological Interactions 281:1-10 doi:10.1016/j.cbi.2017.12.021

Sant KE, Jacobs HM, Borofski KA, Moss JB, Timme-Laragy AR (2017) Embryonic exposures to perfluorooctanesulfonic acid (PFOS) disrupt pancreatic organogenesis in the zebrafish, Danio rerio. Environmental Pollution 220(Pt B):807-817 doi:10.1016/j.envpol.2016.10.057

Sant KE, Sinno PP, Jacobs HM, Timme-Laragy AR (2018) Nrf2a modulates the embryonic antioxidant response to perfluorooctanesulfonic acid (PFOS) in the zebrafish, Danio rerio. Aquatic Toxicology 198:92-102 doi:10.1016/j.aquatox.2018.02.010

Schlegel A, Stainier DY (2006) Microsomal triglyceride transfer protein is required for yolk lipid utilization and absorption of dietary lipids in zebrafish larvae. Biochemistry 45(51):15179-87 doi:10.1021/bi0619268

Schonfeld G, Pfleger B (1974) The structure of human high density lipoprotein and the levels of apolipoprotein A-I in plasma as determined by radioimmunoassay. Journal of Clinical Investgation 54(2):236-46 doi:10.1172/JCI107758

Sedlak MD, Benskin JP, Wong A, Grace R, Greig DJ (2017) Per- and polyfluoroalkyl substances (PFASs) in San Francisco Bay wildlife: Temporal trends, exposure pathways, and notable presence of precursor compounds. Chemosphere 185:1217-1226 doi:10.1016/j.chemosphere.2017.04.096

Serex T, Anand S, Munley S, Donner EM, Frame SR, Buck RC, Loveless SE. (2014) Toxicological evaluation of 6:2 fluorotelomer alcohol. Toxicology 319:1-9 doi:10.1016/j.tox.2014.01.009

Siebenaler R, Cameron R, Butt CM, Hoffman K, Higgins CP, Stapleton HM (2017) Serum perfluoroalkyl acids (PFAAs) and associations with behavioral attributes. Chemosphere 184:687-693 doi:10.1016/j.chemosphere.2017.06.023

Sohlenius AK, Lundgren B, DePierre JW (1992) Perfluorooctanoic acid has persistent effects on peroxisome proliferation and related parameters in mouse liver. Journal Biochemical Toxicology 7(4):205-12

Stahl A, Hirsch DJ, Gimeno RE, et al. (1999) Identification of the major intestinal fatty acid transport protein. Molecular Cell 4(3):299-308

Stahl LL, Snyder BD, Olsen AR, Kincaid TM, Wathen JB, McCarty HB (2014) Perfluorinated compounds in fish from U.S. urban rivers and the Great Lakes. The Science of the Total Environment 499:185-95 doi:10.1016/j.scitotenv.2014.07.126

Stahl T, Mattern D., and Brunn H. (2011) Toxicology of perfluorinated compounds. Environmental Sciences Europe 23(38):1-52 doi:10.1186/2190-4715-23-38

Stein CR, McGovern KJ, Pajak AM, Maglione PJ, Wolff MS (2016) Perfluoroalkyl and polyfluoroalkyl substances and indicators of immune function in children aged 12-19 y: National Health and Nutrition Examination Survey. Pediatric Research 79(2):348-57 doi:10.1038/pr.2015.213

Sullivan M (2018) Addressing perfluorooctane sulfonate (PFOS) and perfluorooctanoic acid (PFOA) department of defense FY18 HASCbBrief on PFOS-PFOA

Sundstrom M, Chang SC, Noker PE, et al. (2012) Comparative pharmacokinetics of perfluorohexanesulfonate (PFHxS) in rats, mice, and monkeys. Reproductive Toxicology 33(4):441-51 doi:10.1016/j.reprotox.2011.07.004

Terasawa Y, Cases SJ, Wong JS, Jamil H, Jothi S, Traber MG, Packer L, Gordon DA, Hamilton RL, Farese RV Jr. (1999) Apolipoprotein B-related gene expression and ultrastructural characteristics of lipoprotein secretion in mouse yolk sac during embryonic development. Journal of Lipid Research 40(11):1967-77

Tsuda S (2016) Differential toxicity between perfluorooctane sulfonate (PFOS) and perfluorooctanoic acid (PFOA). Journal of Toxicological Sciences 41(Special):SP27-SP36 doi:10.2131/jts.41.SP27

Tucker DK, Macon MB, Strynar MJ, Dagnino S, Andersen E, Fenton SE (2015) The mammary gland is a sensitive pubertal target in CD-1 and C57Bl/6 mice following perinatal perfluorooctanoic acid (PFOA) exposure. Reproductive Toxicology 54:26-36 doi:10.1016/j.reprotox.2014.12.002

Tuvikene J, Pruunsild P, Orav E, Esvald EE, Timmusk T (2016) AP-1 Transcription factors mediate BDNF-positive feedback loop in cortical neurons. Journal of Neuroscience 36(4):1290-305 doi:10.1523/JNEUROSCI.3360-15.2016

Uhl SA, James-Todd T, Bell ML (2013) Association of osteoarthritis with perfluorooctanoate and perfluorooctane sulfonate in NHANES 2003-2008. Environmental Health Perspectives 121(4):447-52 doi:10.1289/ehp.1205673

Ulhaq M, Carlsson G, Orn S, Norrgren L (2013a) Comparison of developmental toxicity of seven perfluoroalkyl acids to zebrafish embryos. Environmental Toxicology and Pharmacology 36(2):423-6 doi:10.1016/j.etap.2013.05.004

Ulhaq M, Orn S, Carlsson G, Morrison DA, Norrgren L (2013b) Locomotor behavior in zebrafish (Danio rerio) larvae exposed to perfluoroalkyl acids. Aquatic Toxicology 144-145:332-40 doi:10.1016/j.aquatox.2013.10.021

USEPA (2014) 2010/2015 PFOA Stewardship Program. Docket ID: EPA-HQ-OPPT-2006-0621

USEPA (2017a) Drinking Water Health Advsories for PFOA and PFOS. Docket ID: EPA-HQ-OW-2014-0138

USEPA (2017b) PFOA stewardship program baseline year summary report. Docket ID: EPA-HQ-OPPT-2006-0621 EPA-HQ-OPPT-2006-0621-0022 and EPA-HQ-OPPT-2006-0621-0019

Vandenberg LN, Colborn T, Hayes TB, Heindel JJ, Jacobs DR Jr, Lee DH, Shioda T, Soto AM, vom Saal FS, Welshons WV, Zoeller RT, Myers JP. (2012) Hormones and endocrine-disrupting chemicals: low-dose effects and nonmonotonic dose responses. Endocrine Reviews 33(3):378-455 doi:10.1210/er.2011-1050

Vanparys C, Maras M, Lenjou M, Robbens J, Van Bockstaele D, Blust R, De Coen W. (2006) Flow cytometric cell cycle analysis allows for rapid screening of estrogenicity in MCF-7 breast cancer cells. Toxicology In Vitro 20(7):1238-48 doi:10.1016/j.tiv.2006.05.002

Viberg H, Lee I, Eriksson P (2013) Adult dose-dependent behavioral and cognitive disturbances after a single neonatal PFHxS dose. Toxicology 304:185-91 doi:10.1016/j.tox.2012.12.013

Vonica A, Rosa A, Arduini BL, Brivanlou AH (2011) APOBEC2, a selective inhibitor of TGFbeta signaling, regulates left-right axis specification during early embryogenesis. Developmental Biology 350(1):13-23 doi:10.1016/j.ydbio.2010.09.016

Vuong AM, Yolton K, Webster GM, Sjodin A, Calafat AM, Braun JM, Dietrich KN, Lanpear BP, Chen A. (2016) Prenatal polybrominated diphenyl ether and perfluoroalkyl substance exposures and executive function in school-age children. Environmental Research 147:556-64 doi:10.1016/j.envres.2016.01.008

Walker MB, Kimmel CB (2007) A two-color acid-free cartilage and bone stain for zebrafish larvae. Biotechnic and Histochemistry 82(1):23-8 doi:10.1080/10520290701333558

Wallace KN, Pack M (2003) Unique and conserved aspects of gut development in zebrafish. Developmental Biology 255(1):12-29

Wang L, Wang Y, Liang Y, Li J, Liu Y, Zhang J, Zhang A, Fu J, Jiang G. (2013a) Specific accumulation of lipid droplets in hepatocyte nuclei of PFOA-exposed BALB/c mice. Scientific Reports 3:2174 doi:10.1038/srep02174

Wang L, Wang Y, Liang Y, Li J, Liu Y, Zhang J, Zhang A, Fu J, Jiang G. (2014) PFOS induced lipid metabolism disturbances in BALB/c mice through inhibition of low density lipoproteins excretion. Scientfic Reports 4:4582 doi:10.1038/srep04582

Wang Z, Cousins IT, Scheringer M, Hungerbuehler K (2015) Hazard assessment of fluorinated alternatives to long-chain perfluoroalkyl acids (PFAAs) and their precursors: Status quo, ongoing challenges and possible solutions. Environment International 75:172-9 doi:10.1016/j.envint.2014.11.013

Wang Z, Cousins IT, Scheringer M, Hungerbuhler K (2013b) Fluorinated alternatives to long-chain perfluoroalkyl carboxylic acids (PFCAs), perfluoroalkane sulfonic acids (PFSAs) and their potential precursors. Environment International 60:242-8

Watkins AM, Wood CR, Lin MT, Abbott BD (2015) The effects of perfluorinated chemicals on adipocyte differentiation in vitro. Molecular and Cellular Endocrinology 400:90-101 doi:10.1016/j.mce.2014.10.020

Weaver YM, Ehresman DJ, Butenhoff JL, Hagenbuch B (2010) Roles of rat renal organic anion transporters in transporting perfluorinated carboxylates with different chain lengths. Toxicological Sciences 113(2):305-14 doi:10.1093/toxsci/kfp275

Webster GM, Rauch SA, Marie NS, Mattman A, Lanphear BP, Venners SA (2016) Cross-sectional associations of serum perfluoroalkyl acids and thyroid hormones in U.S. adults: variation according to TPOAb and iodine status (NHANES 2007-2008). Environmental Health Perspectives 124(7):935-42 doi:10.1289/ehp.1409589

Weiss JM, Andersson PL, Lamoree MH, Leonards PE, van Leeuwen SP, Hamers T (2009) Competitive binding of poly- and perfluorinated compounds to the thyroid hormone transport protein transthyretin. Toxicological Sciences 109(2):206-16 doi:10.1093/toxsci/kfp055

White SS, Calafat AM, Kuklenyik Z, Villanueva L, Zehr RD, Helfant L, Stryner MJ, Lindstrom AB,Thibodeaux JR, Wood C, Fenton SE. (2007) Gestational PFOA exposure of mice is associated with altered mammary gland development in dams and female offspring. Toxicological Sciences 96(1):133-44 doi:10.1093/toxsci/kfl177

White SS, Stanko JP, Kato K, Calafat AM, Hines EP, Fenton SE (2011) Gestational and chronic low-dose PFOA exposures and mammary gland growth and differentiation in three generations of CD-1 mice. Environmental Health Perspectives 119(8):1070-6 doi:10.1289/ehp.1002741

Wilhelm M, Bergmann S, Dieter HH (2010) Occurrence of perfluorinated compounds (PFCs) in drinking water of North Rhine-Westphalia, Germany and new approach to assess drinking water contamination by shorter-chained C4-C7 PFCs. International Journal of Hygiene and Environmental Health 213(3):224-32 doi:10.1016/j.ijheh.2010.05.004

Wolf CJ, Rider CV, Lau C, Abbott BD (2014) Evaluating the additivity of perfluoroalkyl acids in binary combinations on peroxisome proliferator-activated receptor-alpha activation. Toxicology 316:43-54 doi:10.1016/j.tox.2013.12.002

Wolf CJ, Takacs ML, Schmid JE, Lau C, Abbott BD (2008a) Activation of mouse and human peroxisome proliferator-activated receptor alpha by perfluoroalkyl acids of different functional groups and chain lengths. Toxicological Sciences 106(1):162-71 doi:10.1093/toxsci/kfn166

Wolf DC, Moore T, Abbott BD, Rosen MB, Das KP, Zehr RD, Lindstrom AB, Stynar MJ, Lau C. (2008b) Comparative hepatic effects of perfluorooctanoic acid and WY 14,643 in PPAR-alpha knockout and wild-type mice. Toxicologic Pathology 36(4):632-9 doi:10.1177/0192623308318216

Xiao F (2017) Emerging poly- and perfluoroalkyl substances in the aquatic environment: A review of current literature. Water Research 124:482-495 doi:10.1016/j.watres.2017.07.024

Xing C, Gong B, Xue Y, Han Y, Wang Y, Meng A, Jia S. (2015) TGFbeta1a regulates zebrafish posterior lateral line formation via Smad5 mediated pathway. Journal of Molecular and Cellular Biology 7(1):48-61 doi:10.1093/jmcb/mjv004

Yan C, Yang Q, Shen HM, Spitsbergen JM, Gong Z (2017) Chronically high level of tgfb1a induction causes both hepatocellular carcinoma and cholangiocarcinoma via a dominant Erk pathway in zebrafish. Oncotarget 8(44):77096-77109 doi:10.18632/oncotarget.20357

Yang CH, Glover KP, Han X (2010) Characterization of cellular uptake of perfluorooctanoate via organic anion-transporting polypeptide 1A2, organic anion transporter 4, and urate transporter 1 for their potential roles in mediating human renal reabsorption of perfluorocarboxylates. Toxicological Sciences 117(2):294-302 doi:10.1093/toxsci/kfq219

Yang Q, Xie Y, Alexson SE, Nelson BD, DePierre JW (2002) Involvement of the peroxisome proliferator-activated receptor alpha in the immunomodulation caused by peroxisome proliferators in mice. Biochemical Pharmacology 63(10):1893-900

Yen TT, Allan JA, Yu PL, Acton MA, Pearson DV (1976) Triacylglycerol contents and in vivo lipogenesis of ob/ob, db/db and Avy/a mice. Biochimica et Biophysica Acta 441(2):213-20

Yuan G, Peng H, Huang C, Hu J (2016) Ubiquitous occurrence of fluorotelomer alcohols in eco-friendly paper-made food-contact materials and their implication for human exposure. Environmental Science & Technology 50(2):942-50 doi:10.1021/acs.est.5b03806

Zeng XW, Qian Z, Emo B, et al. (2015) Association of polyfluoroalkyl chemical exposure with serum lipids in children. The Science of the Total Environment 512-513:364-370 doi:10.1016/j.scitotenv.2015.01.042

Zhang S, Merino N, Wang N, Ruan T, Lu X (2017) Impact of 6:2 fluorotelomer alcohol aerobic biotransformation on a sediment microbial community. The Science of the Total Environment 575:1361-1368 doi:10.1016/j.scitotenv.2016.09.214

Zhang W, Zhang Y, Zhang H, Wang J, Cui R, Dai J (2012) Sex differences in transcriptional expression of FABPs in zebrafish liver after chronic perfluorononanoic acid exposure. Environmental Science & Technology 46:5175-5182 doi:dx.doi.org/10.1021/es300147w

Zhang Y, Beesoon S, Zhu L, Martin JW (2013) Biomonitoring of perfluoroalkyl acids in human urine and estimates of biological half-life. Environmental Science & Technology 47(18):10619-27 doi:10.1021/es401905e

Zhao W, Zitzow JD, Weaver Y, Ehresman DJ, Chang SC, Butenhoff JL, Hagenbuch B. (2017) Organic anion transporting polypeptides contribute to the disposition of perfluoroalkyl acids in humans and rats. Toxicological Sciences 156(1):84-95 doi:10.1093/toxsci/kfw236

Zheng XM, Liu HL, Shi W, Wei S, Giesy JP, Yu HX (2011) Effects of perfluorinated compounds on development of zebrafish embryos. Environmental Science and Pollution Research International 19(7):2498-505 doi:10.1007/s11356-012-0977-y

Zhou Y, Hu LW, Qian ZM, Chang JJ, King C, Paul G, Lin S, Chen PC, Lee YL, Dong GH. (2016) Association of perfluoroalkyl substances exposure with reproductive hormone levels in adolescents: by sex status. Environment International 94:189-195 doi:10.1016/j.envint.2016.05.018

Zhu Y, Qin XD, Zeng XW, Paul G, Morawska L, Su MW, Tsai CH, Wang SQ, Lee YL, Dong GH. (2016) Associations of serum perfluoroalkyl acid levels with T-helper cell-specific cytokines in children: by gender and asthma status. The Science of the Total Environment 559:166-73 doi:10.1016/j.scitotenv.2016.03.187

Zizioli D, Forlanelli E, Guarienti M, Nicoli S, Fanzani A, Bresciani G, Borsani G, Preti A, Cotelli F, Schu P. (2010) Characterization of the AP-1 mu1A and mu1B adaptins in zebrafish (Danio rerio). Developmental Dynamics 239(9):2404-12 doi:10.1002/dvdy.22372

Zizioli D, Meyer C, Guhde G, Saftig P, von Figura K, Schu P (1999) Early embryonic death of mice deficient in gamma-adaptin. The Journal of Biological Chemistry 274(9):5385-90